A new class of feeds for offset reflectors

van 't Klooster, C.G.M.

Award date:
1978

TECHNISCHE HOGESCHOOL EINDHOVEN,

Afdeling der Elektrotechniek.

A new class of feeds for offset reflectors.

ET-13-78.

C.G.M. van 't Klooster.

Verslag van een afstudeeronderzoek
verricht in de vakgroep ET,
onder leiding van:

Dr. M. Jeuken.
Dr. V. Vokurka.

Eindhoven, augustus 1978.

Contents.

ABSTRACT

Application of frequency re-use by dual polarisation requires high-performance antennas and microwave components.
The separation between the two channels on the same frequency should be as good as possible.
In this study we confine ourselves to the investigations of the mutual influence of both channels in the antenna system; in particular the single off-set antenna system.

A general review in chapter I precedes a theoretical treatment with a definition of cross-polarisation in chapter II, while the description of an offset system is found in chapter III. In chapter IV we shall describe a feed which could eliminate the cross-polarisation of an off-set antenna. Since this feed supports propagation of only one mode, wideband operation may be expected.

We attain the special field configuration necessary for this elimination by means of a particular geometry,the so called coax-segmental structure.

Finally, in chapter V, we shall apply the same idea in a horn reflector paraboloid.
The difference between these two applications lies in the fact that in the lastnamed case the paraboloid is in the near-field region of the feed, whereas in the first case the paraboloid is positioned in the far-field region of the feed.

Chapter I

1. General Considerations.

The increase in international telephone and data traffic has been stimulated by the development of the communication satellite systems.

This increase has been so rapid, that a point has been reached where the available bandwidth in the existing frequency bands, 4 and 6 GHz, has become a problem. At present, 11 and 14 GHz bands are available for a new generation of satellites, while the 20 and 30 GHz bands could probably be used in the next decade.

Further, new techniques are being developed in order to utilise the available bands more efficiently. The most important technique is that of the reuse of frequency. Here one frequency is used to transfer two independent signals by exploiting the polarisation properties of a radio wave.

These signals are mostly transmitted in different beams to different locations on the earth by the use of highly directional antennas.

In the technique of frequency reuse, two waves, each with a different polarisation state, are used so that they can be received separately. If a signal interferes with another signal, we speak of crosspolarisation. As a matter of fact, this interference can take place everywhere along the radiolink, and the crosspolarisation of reflector antennas, the offset antenna in particular, will be discussed now.

The reason for this restriction is, that this type of antenna offers some important advantages compared to centrefed systems:
- the blockage due to the feed and its supports is avoided, so that unwanted diffraction effects do not occur.
- as the reflected field bypasses the feed, this antenna has a low V.S.W.R.

The result of these advantages is a higher overall efficiency and a better sidelobe envelope.

There is, however, a disadvantage which is very difficult to overcome: the offset antenna, if fed with a linearly polarised feed, has unsatisfactory crosspolarisation properties. The overall radiation field exhibits a pair of crosspolar lobes in the plane of asymmetry. In the other principal plane the crosspolar field vanishes.

If these disadvantages can be overcome, this type of antenna is specially suitable for satellites, due to its compactness and the advantages mentioned above.

Satellite antennas are generally designed to illuminate a large area on the earth's surface and they therefore need good polarisation characteristics over a large part of the mainbeam. Generally a level smaller than -30 dB is accepted for the crosspolarisation. The large earthstation antennas

are directed to the satellite and usually track it, which means that the polarisation properties are only important near the forward direction. Small low-gain terminals have a fixed position, so that a prescribed crosspolarisation performance should be satisfied within a cone (around the forward direction) in which the satellite is seen from the earth.

As an example of the high performance requirements for ground-station antennas, the CCIR reference patterns to be satisfied (Fig. 1.1) are given [27].

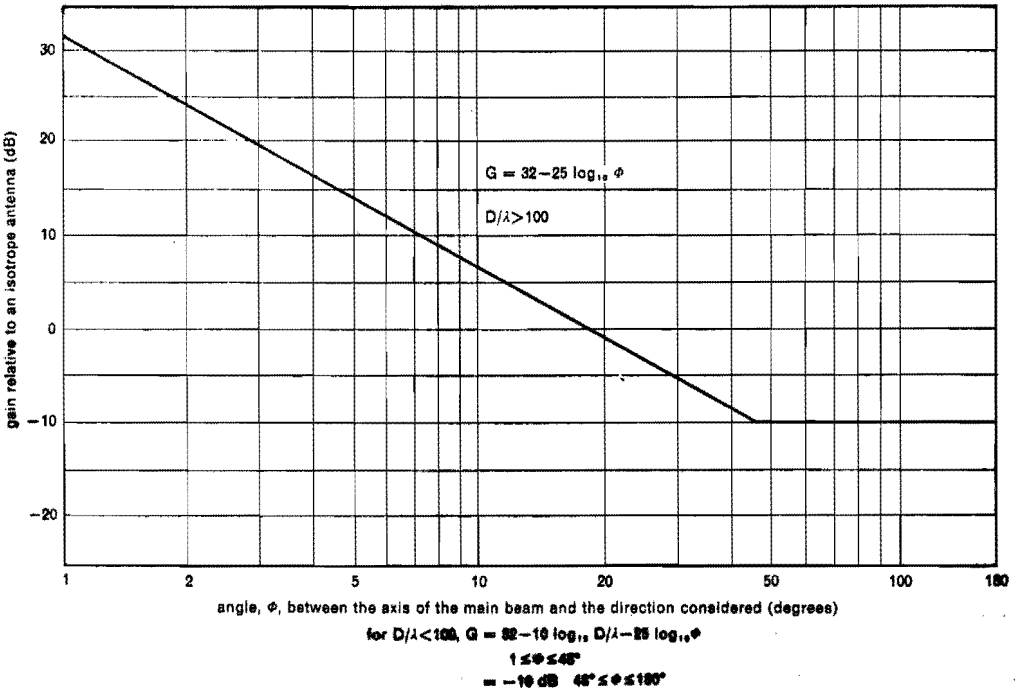

Fig.1.1 Reference radiation diagram of an earth station antenna.

These requirements become more and more stringent as shown in fig. (1.2) and fig.(1.3) which show, respectively, the reference patterns for a satellite transmitting antenna and an earth station low-gain antenna. [8].

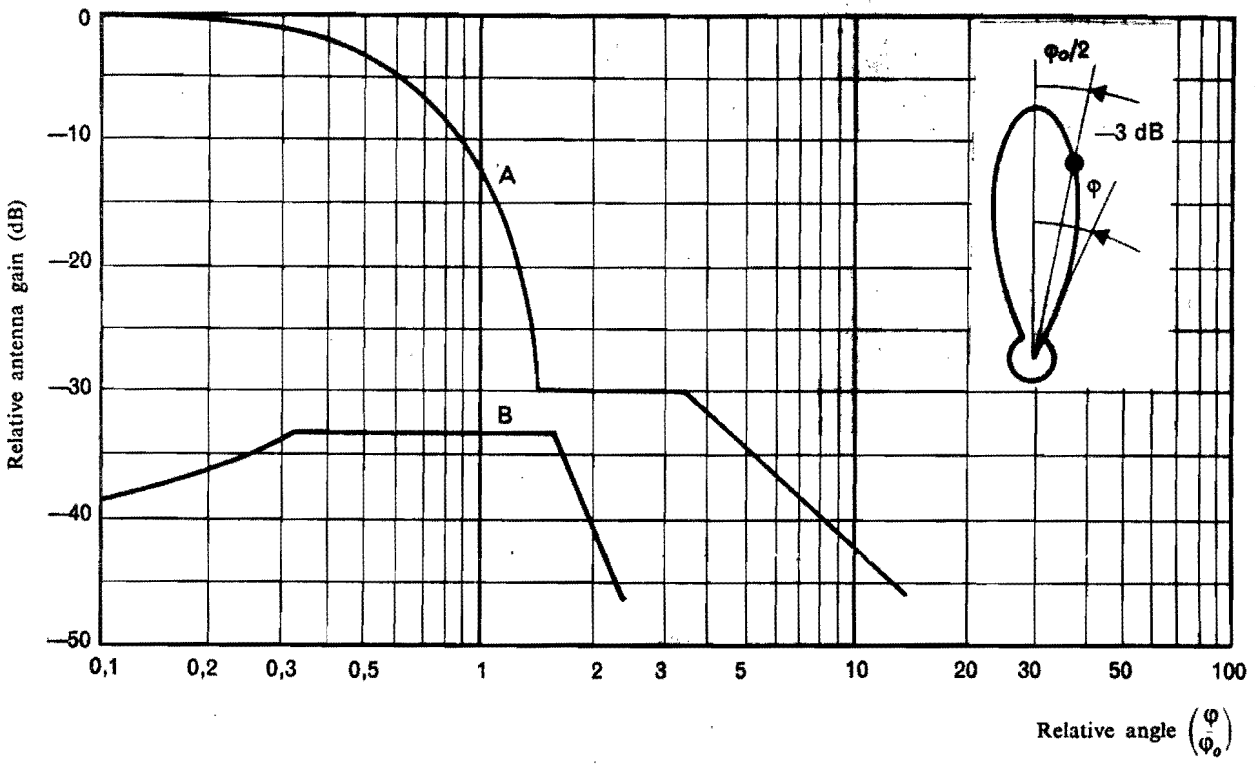

Fig. 1.2 Reference pattern for co- and cross-polar components for a satellite transmitting antenna.

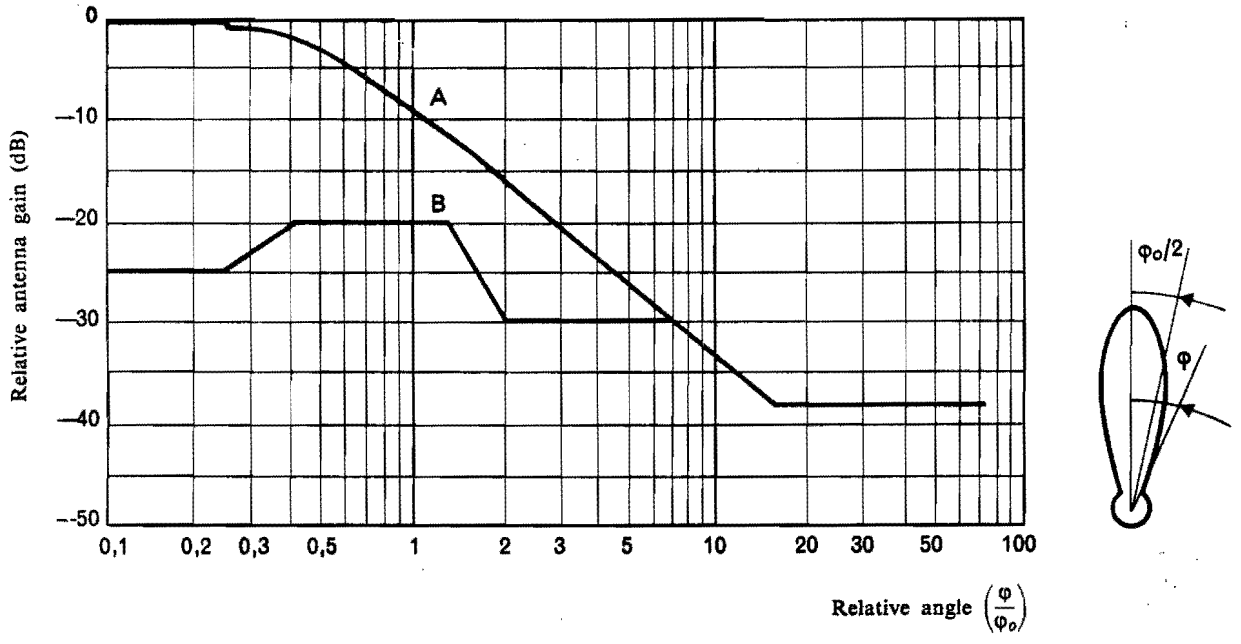

Fig. 1.3 Reference pattern for co- and cross-polar components for a receiving antenna on earth.

It is almost impossible to satisfy envelope B with an offset antenna, due to its unsatisfactory crosspolarisation properties (Fig.1.2).

In recent years many authors have investigated the possibility of improving the crosspolar characteristics of offset reflector antennas. Crosspolarisation analysis has been carried out and several definitions for this term are in circulation [4], [5], [13], [15].

It will be considered theoretically in the next chapter.

When discussing crosspolarisation in this paragraph the assumption of two spatially orthogonal directions allows one to understand the terms co- and crosspolar components, where we are dealing with linearly polarised fields. For circularly polarised fields, the co- and crosspolar components correspond to the opposite circular polarisation senses.

Using a linearly polarised feed in a centrefed paraboloid, the aperture field has parallel field lines, as stated by Koffman [26]. The simplest form of such a feed is a combination of an electric dipole in the x-direction and a magnetic dipole oriented in the y-direction. This configuration is called the Huygens source. We indicate its polarisation state as "p-polarised", whereas a source with the electric and magnetic dipole oriented respectively in the y- and -x-direction the polarisationstate is indicated as "q-polarised". Two Huygens sources with a "p"- and a "q-polarised" field, respectively will produce field patterns which are orthogonal everywhere in space. Due to this property, a Huygens' source is often taken as a reference to calculate the crosspolar component of the radiated field of an antenna.

Cook, Elam and Zucker [9], Chu and Turrin [7], Gans and Semplak [28] and Rudge [11], have given an extensive description of the offset antenna. Chu and Turrin use a balanced feed in their calculations. They show that the co- and crosspolar components are in phase in the aperture plane of the reflector. However, in the far field region of such an aperture, there is a phase difference of 90^{o}. The crosspolar component of the far field has a deep zero on the beam axis, and rises sharply off this axis to a level which depends on the value of the offset angle between the feed axis and paraboloid axis and the angle subtended reflector at the focus.

The characteristic crosspolarisation pattern of an offset antenna shows two lobes. A special class of offset antennas consists of the hornparaboloid antennas. A difference from the earlier described system is that the reflector is here positioned in the near field region of the feed. [24], [25].

Bem [12] has calculated the focal field of an offset antenna illuminated by a linearly polarised plane wave in the receiving mode. His calculations yield the fieldcomponents in a plane containing the focus and perpendicular to the feed axis.

These fieldcomponents differ in phase and in amplitude, and therefore the focal field is found to be elliptically polarised where the ellipticity depends on the offset angle.

Several methods used to eliminate the crosspolarisation of the offset antenna have been investigated. One of them is the mode-matching technique. Here one tries to match the field in the focal plane with a fitted aperture field of the feed. Rudge [10] tries to achieve matching by using the sum of three modes. Within a cylindrical smooth-walled waveguide the ground mode TE_{11} propagates. The TE_{21} and TM_{11} mode are generated at stepdiscontinuities.

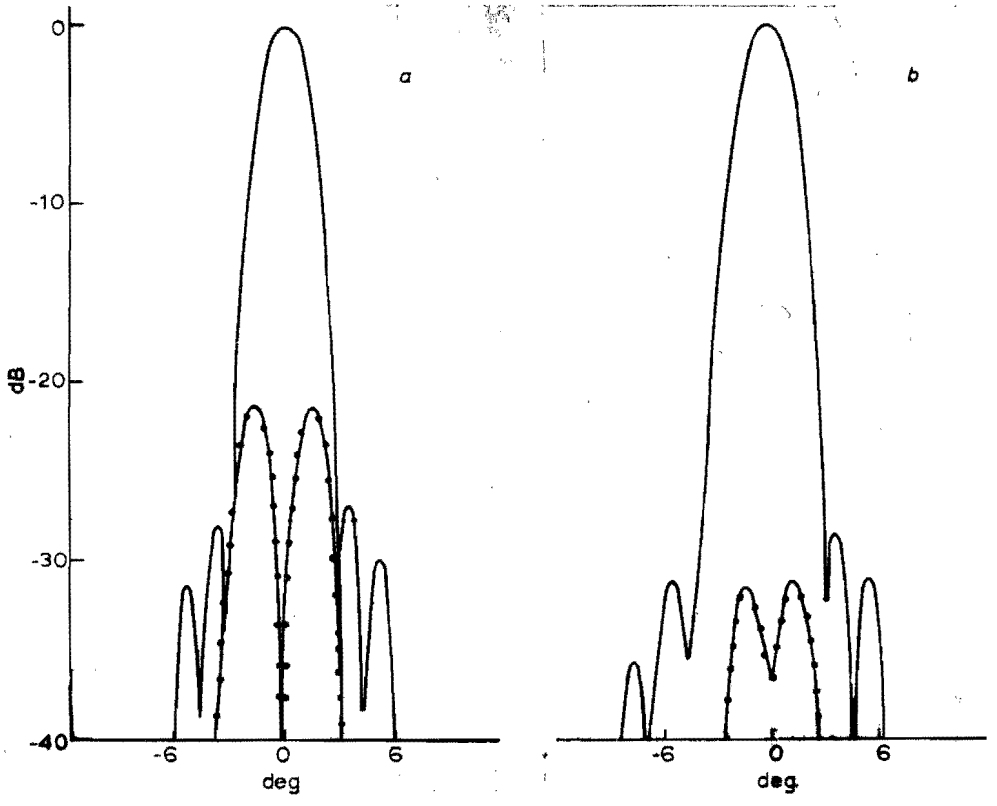

Fig. 1.4 Measured radiation pattern in the plane of asymmetry, a) conventional, b) trimode feed.

These modes are added to the ground mode, the correct phase difference and amplitude ratio being taken into account. Though this method of eliminating the crosspolar lobes has had a certain success, it has the disadvantage that the multimode horn is not a wideband device because of the discrete phase velocities of the various modes. The results of experiments with such a horn are given. (Fig.1.4) Note that Rudge only gives results for one plane. Crosspolarisation lobes possibly occur in the other plane, but he gives no information on that particular.

Jacobsen gives a suggestion for an offset feed in which two modes are used. [14] He uses a rectangular horn in which a TE_{20} mode is generated and added to the ground mode TE_{01}. Then he compares the p- and q-components for both modes. As already mentioned, a p- and a q-polarised Huygens' source

give rise to far field patterns which are orthogonal everywhere in space and define an orthogonal set of vectors p and q. When we resolve a field along p and q we talk about the p- and q-components. From pictures Jacobsen has observed a striking similarity between the q-components of the far field of a TE_{20} and the TE_{01} mode. As a matter of fact these pictures show only the absolute values of the q-components, no mention is made about the sign. Some properties of the Fouriertransform show that the TE_{01} mode has a far field which is completely real whereas the far field of the TE_{20} mode is completely imaginary. This can readily be indicated by representing the TE_{01} mode by an even and the TE_{20} mode by an odd function. The far field calculated by means of the Fouriertransform [17],[18] is completely real for even functions and completely imaginar for odd functions. Therefore the modes should be accurately added with the correct phase difference. Only if this difference is 90^{o} in the aperture will the far fields of both modes have a zero phase difference and only then does the total field have a linear polarisation state. A linearly polarised far field is necessary for compensating the crosspolarisation in an offset reflector. This can be concluded from the calculations of Chu and Turrin [7].

Jacobsen does not give any information at all about this phase matching, he only uses the word "proper matched" and is not very explicit in his article. It is also quite obvious that there is no possibility of creating an aperture field for the orthogonal polarisation so that crosspolarperformance is optimized. In other words, this system cannot be used for frequency re-use applications.

Multimode matching techniques are generally not wideband, owing to the discrete phase velocities of the modes within the waveguide. This is a great disadvantage.

We wish to deal with the problem of elimination of cross-polarisation rather differently. We shall consider a feed structure with a special geometrical configuration [21], where only one mode propagates. The geometry gives a special field distribution in the aperture of the feed from which the far field radiation pattern can be calculated. This feed structure has, like the offset reflector, one axis of symmetry in its aperture plane. The choice of the geometry should be such that the Maxwell equations can be solved within this structure. As a matter of fact the chosen configuration can be seen as part of a coaxial waveguide, and we shall find striking similarities between this structure and the coaxial system. The aperture field distribution shows a distinct curvature which leads us to expect a partial cancelling of the cross-polarisation.

In chapter IV a thorough calculation of this structure will be given for systems described in cylindrical coordinates. The same coax-segmental configuration forms the base of a feed used in a hornparaboloid antenna. Such an antenna has

the reflector positioned in the near field of the feed. In chapter V the calculations will be given for the special feed structure in spherical coordinates. Having calculated the aperture fields of the feed, a simple transform without difficult integrals gives the aperture field of the hornparaboloid.

It should be remarked that this method of exploiting geometrical structures has the great advantage of being wideband due to the single-mode excitation.

Chapter II

2.1. The general solution of the Maxwell equations.

For every problem dealing with electromagnetic radiation the Maxwell equations give the base of the treatment of the problem. We shall give here the general procedure for solving them.

We assume a time dependence according exp(jwt).
The Maxwell equations are given by:

$$\nabla \times \underline{E} + j\omega\mu \underline{H} = -\underline{M} , \tag{2.1}$$

$$\nabla \times \underline{H} - j\omega\varepsilon \underline{E} = \underline{J} . \tag{2.2}$$

With $\underline{M}$ and $\underline{J}$ describing the magnetic and electric sources respectively.
As equations (2.1) and (2.2) are linear, we may split $\underline{E}$ and $\underline{H}$:

$$\underline{E} = \underline{E}_1 + \underline{E}_2 \qquad \underline{H} = \underline{H}_1 + \underline{H}_2 . \tag{2.3}$$

$$\nabla \times \underline{E}_1 + j\omega\mu \underline{H}_1 = \underline{0} , \tag{2.4}$$

$$\nabla \times \underline{H}_1 - j\omega\varepsilon \underline{E}_1 = \underline{J} , \tag{2.5}$$

$$\nabla \times \underline{E}_2 + j\omega\mu \underline{H}_2 = -\underline{M} , \tag{2.6}$$

$$\nabla \times \underline{H}_2 - j\omega\varepsilon \underline{E}_2 = \underline{0} . \tag{2.7}$$

Equation (2.4) shows, since $\nabla . \nabla \times \underline{E} = 0$,

$$\nabla . \underline{H}_1 = 0 . \tag{2.8}$$

So we can write

$$\underline{H}_1 = \nabla \times \underline{A} , \tag{2.9}$$

which means with (2.3)

$$\nabla \times (\underline{E}_1 + j\omega\mu \underline{A}) = \underline{0} , \tag{2.10}$$

or, as $\nabla \times \nabla \Phi = 0$,

$$\underline{E}_1 + j\omega\mu\,\underline{A} = -\nabla\Phi \,. \tag{2.11}$$

With (2.5) we get

$$\nabla\times\nabla\times\underline{A} + j\omega\varepsilon\,\nabla\Phi - \omega^2\mu\varepsilon\,\underline{A} = \underline{J}, \tag{2.12}$$

or, using $\nabla\times\nabla\times\underline{A} = \nabla(\nabla.\underline{A}) - \nabla^2\underline{A}$ and the Lorentz-condition $\nabla.\underline{A}+j\omega\varepsilon\Phi=0$, the Helmholtz equation:

$$\nabla^2\underline{A} + \omega^2\mu\varepsilon\,\underline{A} = -\underline{J} \,. \tag{2.13}$$

Equation (2.13) has a general solution, which is the sum of a particular and a homogeneous solution:

$$\underline{A}(\underline{r}) = \underline{A}_p(\underline{r}) + \underline{A}_h(\underline{r}) \,. \tag{2.14}$$

The well-known solution $\underline{A}_p(\underline{r})$ is given by:

$$\underline{A}_p(\underline{r}) = \frac{1}{4\pi}\int_{V'} \underline{J}(\underline{r}')\,\frac{e^{-jkR}}{R}\,dV', \tag{2.15}$$

where $R = |\underline{r}-\underline{r}'|$ and $k = \omega\sqrt{\mu\varepsilon}$.

Just in the same way we obtain a solution for equations (2.6) and (2.7), where (2.6) leads to the defining of a vektor potential $\underline{F}$. This gives the Helmholtz equation for $\underline{F}$:

$$\nabla^2\underline{F} + k^2\underline{F} = -\underline{M} \,. \tag{2.16}$$

The particular solution reads

$$\underline{F}_p(\underline{r}) = \frac{1}{4\pi}\int_{V'} \underline{M}(\underline{r}')\,\frac{e^{-jkR}}{R}\,dV' \tag{2.17}$$

The homogeneous solution $\underline{A}_h(\underline{r})$ is gained from (2.13) with $\underline{J}=0$. The same procedure is followed to get the solution $\underline{F}_h(\underline{r})$ where $\underline{M}=0$ in (2.16).

Taking the sum of the particular and the homogeneous solution, we get, with the equations (2.4), (2.5), (2.6), and (2.7) the next expressions which can be used to derive the field:

$$\underline{E}_1 = \frac{1}{j\omega\varepsilon}\,(\nabla\times\nabla\times\underline{A} - \underline{J}), \tag{2.19}$$

$$\underline{H}_1 = \nabla\times\underline{A} \,, \tag{2.20}$$

$$\underline{E}_2 = -\nabla\times\underline{F} \,, \tag{2.21}$$

$$\underline{H}_2 = \frac{1}{j\omega\mu}\,(\nabla\times\nabla\times\underline{F} - \underline{M}). \tag{2.22}$$

By using (2.3) the total field is found.

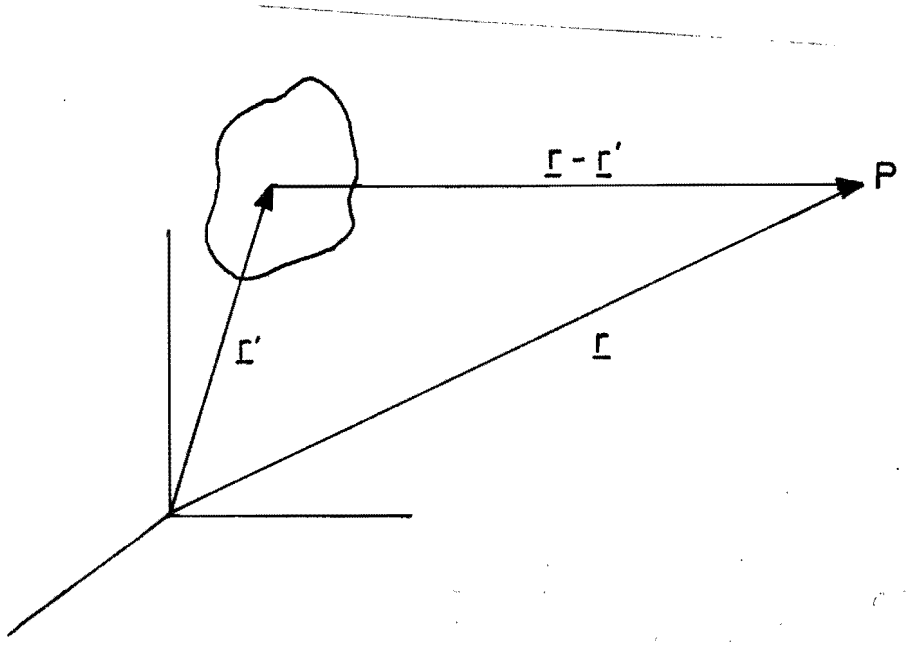

Fig. 2.1 Coordinate geometry.

2.2. A general definition of crosspolarisation.

We assume a plane wave of arbitrary polarisation travelling in the $\underline{u}_p$ direction (Fig 2.2) so that the phase fronts are all normal to $\underline{u}_p$ and therefore parallel with the $(\underline{u}_1, \underline{u}_2)$ plane.

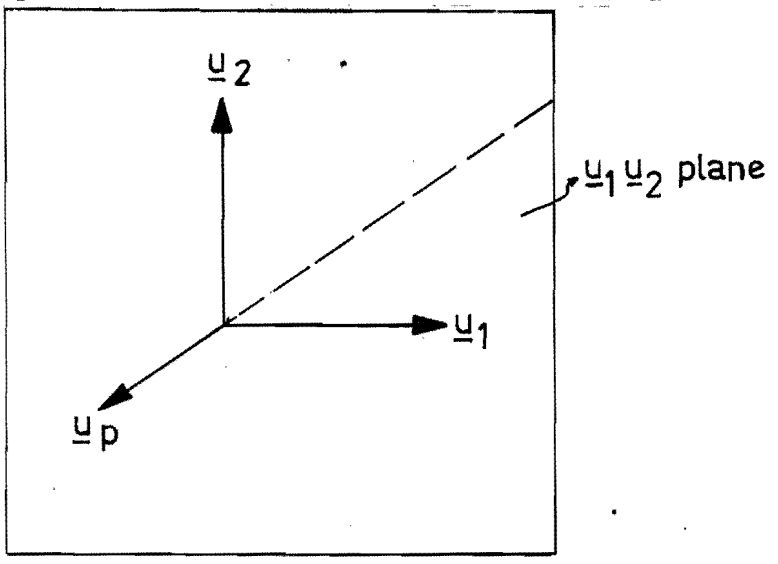

Fig 2.2 Geometry for a plane wave propagation in the $\underline{u}_p$ direction with $\underline{u}_1 \times \underline{u}_2 = \underline{u}_p$.

The electric field vector lies in the $(\underline{u}_1, \underline{u}_2)$ plane and can be resolved into components along $\underline{u}_1$ and $\underline{u}_2$ as follows:

$$\underline{E}(t) = E_{1m} \cos(\omega t)\, \underline{u}_1 + E_{2m} \cos(\omega t + \delta)\, \underline{u}_2 \qquad (2.23)$$

From expression (2.23) it is clear that the direction of the vector varies with time. The tip of the vector $\underline{E}(t)$ describes an elliptical locus, called the polarisation ellipse. The field and the wave producing the field are said to be elliptically polarised.
We can distinguish three cases, in which the polarisation ellipse becomes either a straight line or a circle:

(A) $\delta=0$ or $\delta=\pi$ yields a straight line

(B) $E_{1m}=0$ or $E_{2m}=0$ yields a straight line

(C) $E_{1m}=E_{2m}$ and $\delta=\pm\pi/2$ yields a circle, left-handed for $\delta=+\pi/2$ and right-handed for $\delta=-\pi/2$.

In (A) or (B) we have a linearly polarised wave, with (C) we have a circularly polarised wave.
The polarisation ellipse can be described by its axial ratio and its tilt-angle τ defined as the angle between the major axis of the ellipse and the vector u_1.

It can be shown that any field can be resolved into a left-circular and a right-circular component. Equation (2.23) can then be written as:

$$\underline{E}(t) = E_L\left[\cos(\omega t+\psi)\,\underline{u}_1 - \sin(\omega t+\psi)\,\underline{u}_2\right] + E_R\left[\cos(\omega t+\psi+\delta)\,\underline{u}_1 + \sin(\omega t+\psi+\delta)\,\underline{u}_2\right]. \quad (2.24)$$

Note that in (2.23) and (2.24) the coefficients of the goniometrical expressions are real and positive.
In order to maintain the original time reference used in (2.23), the angle ψ has been inserted in the four components of (2.24).
In (2.24) the phase difference between the left-circular and right-circular component is represented by δ_c.
The tilt angle τ is given as $\tau=\delta/2$, and another characteristic, the circular polarisation ratio, by $e = E_R/E_L$.
As shown in (2.23), a field can be resolved into two components along $\underline{u}_1$ and $\underline{u}_2$.
Equation (2.24) gives a resolvation into two circular components which are independent. We now want to generalize and we shall derive that it is possible to resolve a field into two components which are orthogonal in a special sense. These components will generally be elliptically polarised with the degenerated polarisation states, viz. linear and circular as two special cases. If detecting a signal use is made of a device which detects power. We therefore give a definition of orthogonality as follows:
Two component waves are defined as orthogonal in power if the sum of their time average power densities in the two component waves is equal to the total time average power density in the wave for any ratio of amplitudes and for any arbitrary relative phase of the component waves.

If this definition is satisfied, then a separation can be made between the two orthogonal component waves; then two signals can be transferred independentely (frequency re-use).

We have to show that for any amplitude ratio and any arbitrary phase difference between the components the following expression is valid:

$$\underline{E} \times \underline{H}^* = \underline{E}_M \times \underline{H}_M^* + \underline{E}_N \times \underline{H}_N^*. \quad (2.25)$$

where M and N indicate the two components. We have, with $\underline{E}=\underline{E}_M+\underline{E}_N$ and $\underline{H}=\underline{H}_M+\underline{H}_N$:

$$\underline{E} \times \underline{H}^* = (\underline{E}_M + \underline{E}_N) \times (\underline{H}_M^* + \underline{H}_N^*) \quad (2.26)$$

$$\underline{E} \times \underline{H}^* = (\underline{E}_M \times \underline{H}_M^*) + (\underline{E}_N \times \underline{H}_N^*) + (\underline{E}_M \times \underline{H}_N^*) + (\underline{E}_N \times \underline{H}_M^*). \quad (2.27)$$

Therefore, for orthogonality, as given above, it is necessary that:

$$\underline{E}_M \times \underline{H}_N^* + \underline{E}_N \times \underline{H}_M^* = \underline{0}. \qquad (2.28)$$

We assume the most general expressions, that is, elliptical, for the components:

$$\underline{E}_M = A\, e^{j\omega t}\, \underline{u}_1 + B\, e^{j(\omega t + \delta_M)}\, \underline{u}_2 , \qquad (2.29)$$

$$\underline{H}_M = -\frac{B}{Z_0} e^{j(\omega t + \delta_M)}\, \underline{u}_1 + \frac{A}{Z_0} e^{j\omega t}\, \underline{u}_2 , \qquad (2.30)$$

$$\underline{E}_N = C\, e^{j(\omega t + \varphi)}\, \underline{u}_1 + D\, e^{j(\omega t + \varphi + \delta_N)}\, \underline{u}_2 , \qquad (2.31)$$

$$\underline{H}_N = -\frac{D}{Z_0} e^{j(\omega t + \varphi + \delta_N)}\, \underline{u}_1 + \frac{C}{Z_0} e^{j(\omega t + \varphi)}\, \underline{u}_2 . \qquad (2.32)$$

Where A, B, C and D are real and positive and $Z_0 = \sqrt{\mu_0/\varepsilon_0}$. By substitution of (2.29), (2.30), (2.31) and (2.32) into (2.28) we get, with $\underline{u}_1 \times \underline{u}_2 = \underline{u}_p$:

$$\frac{AC}{Z_0} e^{-j\varphi}\, \underline{u}_p + \frac{BD}{Z_0} e^{j(\delta_M - \delta_N - \varphi)}\, \underline{u}_p + \frac{AC}{Z_0} e^{-j\varphi}\, \underline{u}_p + \frac{BD}{Z_0} e^{-j(\delta_M - \delta_N - \varphi)}\, \underline{u}_p , \qquad (2.33)$$

which reduces to:

$$AC \cos\varphi = -BD \cos(\delta_M - \delta_N - \varphi), \qquad (2.34)$$

$$\frac{A}{B} \cos\varphi = -\frac{D}{C}\left\{\cos\varphi \cos(\delta_M - \delta_N) + \sin\varphi \sin(\delta_M - \delta_N)\right\}. \qquad (2.35)$$

Expression (2.35) should be valid for any value of φ thus:

$$\frac{A}{B} = -\frac{D}{C} \cos(\delta_M - \delta_N) , \qquad (2.36)$$

$$0 = -\frac{D}{C} \sin(\delta_M - \delta_N) . \qquad (2.37)$$

As A, B, C and D are real and positive, we have from (2.36) and (2.37):

$$\frac{A}{B} = \frac{C}{D} \quad , \tag{2.38}$$

$$\delta_M - \delta_N = \pi \quad . \tag{2.39}$$

These are the conditions for orthogonality of the two elliptically polarised component waves $\underline{E}_M(t)$ and $\underline{E}_N(t)$.

Substitution of (2.38) and (2.39) in (2.29) and (2.31) with $A/B=\varepsilon$ yields after taken the real part.

$$\underline{E}_M(t) = B\left\{ \varepsilon \cos(\omega t)\, \underline{u}_1 + \cos(\omega t + \delta_M)\, \underline{u}_2 \right\}, \tag{2.40}$$

$$\underline{E}_N(t) = D\left\{ \varepsilon \cos(\omega t + \varphi)\, \underline{u}_1 - \cos(\omega t + \varphi + \delta_M)\, \underline{u}_2 \right\}. \tag{2.41}$$

Note that if $\underline{E}_M(t)$ is left-handed, $\underline{E}_N(t)$ is right-handed. After a straight-forward calculation it can be stated that the circular polarisation ratios of $\underline{E}_M(t)$ and $\underline{E}_N(t)$ are reciprocal. [3]. Furthermore, the tilt angles τ_M and τ_N differ ninety degrees.

Thus every plane wave, whatever its polarisation state may be, can be resolved into component waves which are elliptically polarised, and (2.38) and (2.39) should be valid for these component waves.

The special cases, circularly and linearly polarised component waves, are included. The problem can be approached somewhat differently. Assume we have an elliptically polarised plane wave W_1, then it is always possible to find another plane wave W_2 under the conditions of (2.38) and (2.39) which is orthogonal. These two waves W_1 and W_2 give rise to a resulting wave whose power density can be written as the sum of the power densities of W_1 and W_2 . Then these two waves W_1 and W_2 can transfer two signals independentely, provided that they are detected separately.

We shall now consider a transmitting system. There has to be a correct coupling between the transmitting antenna and the plane wave and between the plane wave and the receiving antenna. We can consider the field of a transmitting antenna as a local plane wave in the far-field region. This wave has a polarisation state which may depend on the spatial coordinates of the observation point. With the receiving antenna at this point there will be optimal reception if the polarisation of the receiving antenna is matched to the polarisation of the local plane wave.

Then, based on the preceding results a definition of cross-polarisation should be given as follows:

' Every field W_1 having a distinct polarisation state is related to another field W_2 which is orthogonal in power; the batter polarisation state is called cross-polarisation'.

With this definition it is possible to make calculations if we know the polarisation state of wave W_1.
For example, a transmitting antenna developed to radiate a wave W_1 will, for reasons of different kind, whatever they are, radiate a wave W_T which can be resolved in accordance with the forgoing into two components along W_1 and W_2. Then the component along W_2 is the cross-polar component.
In the receiving situation the same consideration is possible: an antenna designed to receive a wave W_R is not perfectly matched to wave W_R but, for instance matched to some other wave W_1, for whatever reasons. Then W_R has to be resolved along W_1 and W_2 orthogonal to W_1. Then the wave component along W_1 is the copolar component and the component along W_2 is cross-polar.

Practical problems arise, if the aim is to realize an antenna which can receive or transmit two orthogonal elliptically polarised waves simultaneously, because the condition (2.39) should be satisfied. This is very difficult and, therefore, a restriction is made in practice to the use of the degenerated cases, i.e. circularly or linearly polarised waves. It is then possible to use one antenna which can handle both orthogonal signals. Applying the definition of cross-polarisation to these two situations we get:

1) In the case of linear polarisation the direction of the cross-polar component is perpendicular to the copolar component. In this special case there is orthogonality in space in addition to the orthogonality in power, in other words, the co- and crosspolar components are perpendicular everywhere in space.

2) When circular polarisation is used the rotation sense of the crosspolar component is opposite to that of the copolar component: if the copolar component is left-handed, the cross-polar component is right-handed.

In both cases the cross-polar component can be very simply detected. Using linear polarisation, a rotation of the receiving antenna over ninety degrees around its axis, as spatial orthogonality exists between the co- and cross-polar components. Using circular polarisation, a detector detecting the opposite rotation sense yields the cross-polar component.

Conclusions

The definition of cross-polarisation given here is generally capable for the common polarisation-states and covers even orthogonal, elliptical polarisation-states.
It should be observed at this point that the definition given by IEEE [4] is the same as that given here provided that the word "orthogonal" is understood as orthogonality in power, and not as spatial orthogonality in their definition [4]. This is not explicity indicated.

Furthermore, the third definition given by Ludwig [5] is only applicable in the case of linear polarisation, as he assumes a spatially perpendicular set of components, or a spatial orthogonality.
As a matter of fact, Frijters [6] does the same with his definition based on a spatial in-product.
It is very important to realise that frequency re-use referred to orthogonality means orthogonality in power or the possibility of separating average powers and not spatial orthogonality.
Only if dealing with linear polarisation are the co- and cross-polar components orthogonal in power and orthogonal in space.

In appendix C we shall give a desription of a useful aid to describe polarisation states: the sphere of Poincaré.

Chapter III

The offset-reflector antenna

3.1 Introduction

An offset reflector antenna has the property that the reflector focus lies adjacent to the centre of the reflected main beam, so that a feed placed in the focus will not block the main beam.
If such a reflector is illuminated by a linearly polarised Huygens source, we find in the far-field region of the reflector a cross-polarisation pattern showing a pair of lobes on either side of the symmetry axis as shown in Fig. 3.1a.
When illuminated by a circularly polarised feed, the main beam will shift away from the axis in the plane of asymmetry, either to the left or to the right, depending on the rotation sense of the circularly polarised field.

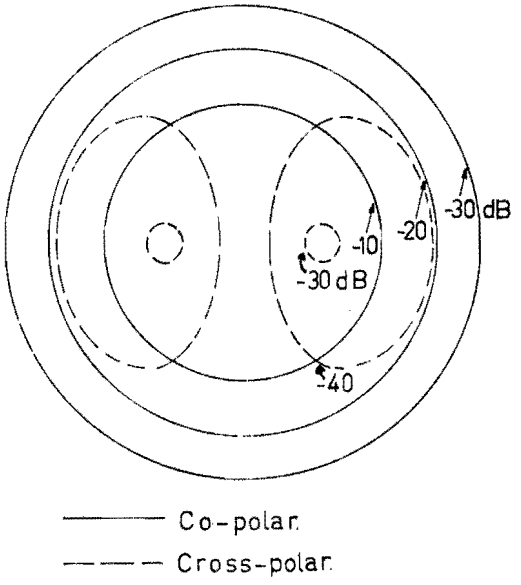

Fig 3.1a Contour lines of the far-field radiation of an off-set reflector fed by a linearly polarised Huygens source.

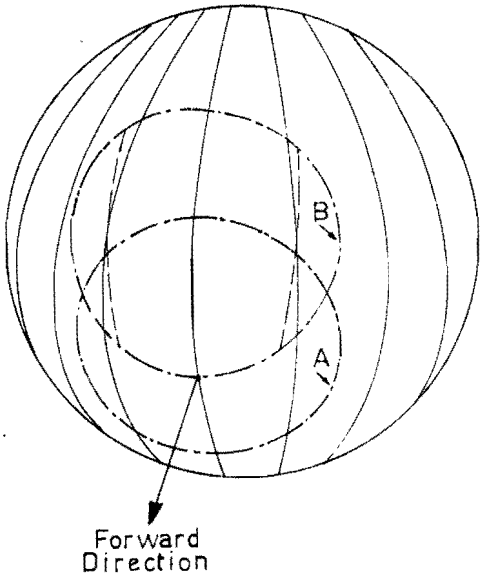

Fig 3.1b Field lines intercepted by a reflector fed by a linearly polarised Huygens source.

A simple explanation for the cause of the cross-polarisation can be given as follows:
Consider the Huygens source with field lines as shown in Fig. 3.1b. Then a symmetrical reflector intercepts part of the radiation pattern marked by circle A. An off-set reflector should intercept the part bounded by circle B. As the feed radiates most energy in the forward direction, it is tilted to illuminate the off-set reflector efficiently. Then the part bounded by circle A is intercepted by the off-set reflector. The field lines, dotted in Fig 3.1b do not coincide with the required field lines and a cross-polarisation results.

3.2 The geometry of an off-set reflector antenna.

A description has been given for instance by Cook, Elam and Zucker [9], Chu and Turrin [7], Rudge [11] and Semplak and Gaus [28]. A short summary of the main characteristics will be given here to elucidate the calculations made for this type of antenna.

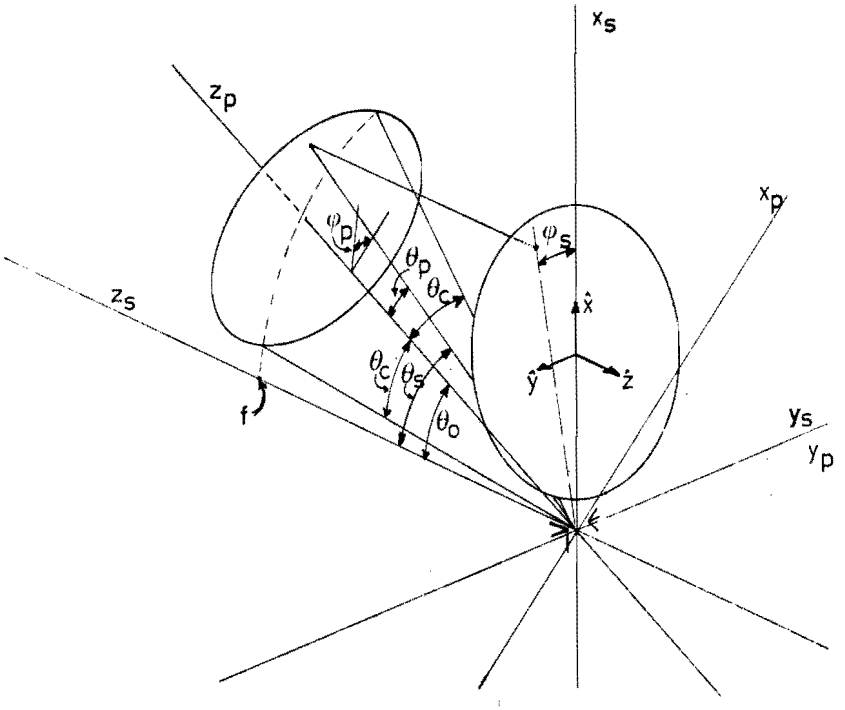

Fig 3.2 Geometry of an off-set antenna

Considering Fig 3.2, we have the following coordinate systems:

1) The primary system $(\hat{x}_p, \hat{y}_p, \hat{z}_p)$.
   The feed axis coincides with the z_p axis.
2) The secondary system $(\hat{x}_s, \hat{y}_s, \hat{z}_s)$.
   The paraboloid axis coincides with the z_s axis.
3) The coordinate system $(\hat{x}, \hat{y}, \hat{z})$ in which the far-field radiation pattern of the reflector will be expressed.

The origin of the (x,y,z) system is the centre of the aperture.
The relation between the primary and the secondary system is as follows:

$$\begin{aligned} \hat{x}_p &= \cos\vartheta_0\,\hat{x}_s - \sin\vartheta_0\,\hat{z}_s\,, \\ \hat{y}_p &= \hat{y}_s\,, \\ \hat{z}_p &= \sin\vartheta_0\,\hat{x}_s + \cos\vartheta_0\,\hat{z}_s\,, \end{aligned} \tag{3.1}$$

where ϑ_0 is the angle between the $\hat{z}_s$ - and the $\hat{z}_p$ axis.
Since $r_s = r_p$ we find, using (3.1) that:

$$\begin{aligned} \sin\vartheta_s\cos\varphi_s &= \sin\vartheta_p\cos\varphi_p\cos\vartheta_0 + \cos\vartheta_p\sin\vartheta_0\,, \\ \sin\vartheta_s\sin\varphi_s &= \sin\vartheta_p\sin\varphi_p\,, \\ \cos\vartheta_s &= -\sin\vartheta_p\cos\varphi_p\sin\vartheta_0 + \cos\vartheta_p\cos\vartheta_0\,. \end{aligned} \tag{3.2}$$

As $r_s = r_p$, we find for the equation of a paraboloid with the axis along the z_s axis that

$$e = \frac{2f}{t}\,, \tag{3.3}$$

where t is given by

$$t = 1 + \cos\vartheta_s = 1 + \cos\vartheta_p\cos\vartheta_0 - \sin\vartheta_p\cos\varphi_p\sin\vartheta_0\,. \tag{3.4}$$

The angle ϑ_c in Fig (3.2) is subtended by the reflector at the focus.
If we project the intersections of cones described by $\vartheta_p = \vartheta_c$ with the paraboloid on the $x_s y_s$ plane, we find circles given by

$$(x_s - x_c)^2 - y_s^2 = (D/2)^2\,, \tag{3.5}$$

where x_c and D are given respectively by:

$$x_c = \frac{2f \sin\vartheta_o}{\cos\vartheta_o + \cos\vartheta_c}, \tag{3.6}$$

$$D = \frac{4f \sin\vartheta_c}{\cos\vartheta_o + \cos\vartheta_c}. \tag{3.7}$$

Equation (3.6) shows that x_c has different values for different angles ϑ_c. Thus the circles in the aperture are not concentric The relation between the (xyz) system and the secondary coordinates is given by:

$$\begin{aligned} x &= x_s - x_c, \\ y &= -y_s, \\ z &= -z_s. \end{aligned} \tag{3.8}$$

3.3 The aperture field.

Assuming a geometrical optical reflection, the aperture field can be calculated with:

$$\underline{E}_{as} = 2(\underline{E}_f \cdot \hat{n})\hat{n} - \underline{E}_f. \tag{3.9}$$

Here E_{as} denotes the aperture field and E_f the far-field of the source, $\hat{n}$ is the normal to the paraboloid.
A general expression for the far-field of the feed is

$$\underline{E}_f = E_{f\vartheta}\,\hat{\vartheta}_p + E_{f\varphi}\,\hat{\varphi}_p. \tag{3.10}$$

The normal $\hat{n}$ is given by

$$\hat{n} = \frac{-(\hat{r}+\hat{z})}{\sqrt{2t}}. \tag{3.11}$$

Here t is given by (3.4)
If we then substitute (3.10) and (3.11) in (3.9) when we take $\underline{E}_{as} = E_{axs}\hat{x}_s + E_{ays}\hat{y}_s$, we get:

$$E_{axs} = \frac{1}{t}\Big\{\Big[\sin\vartheta_p \sin\vartheta_o - \cos\varphi_p(1+\cos\vartheta_p\cos\vartheta_o)\Big]E_{f\vartheta} + \Big[\sin\varphi_p(\cos\vartheta_o + \cos\vartheta_p)\Big]E_{f\varphi}\Big\}, \tag{3.12}$$

$$E_{ays} = \frac{1}{t}\Big\{\Big[-\sin\varphi_p(\cos\vartheta_o + \cos\vartheta_p)\Big]E_{f\vartheta} + \Big[\sin\vartheta_p \sin\vartheta_o - \cos\varphi_p(1+\cos\vartheta_p\cos\vartheta_o)\Big]E_{f\varphi}\Big\}. \tag{3.13}$$

Denoting f_1 and f_2 as the geometrical coefficients, including $\frac{1}{r}$, we get:

$$E_{axs} = f_1 E_{f\vartheta} + f_2 E_{f\varphi} , \qquad (3.14)$$

$$E_{ays} = -f_2 E_{f\vartheta} + f_1 E_{f\varphi} . \qquad (3.15)$$

We shall now investigate how the aperture field behaves if we use a **primary** feed with a far-field having respectively

a) a **linear** polarisation state,

b) a circular polarisation state,

c) an elliptical polarisation state.

a) Equation (3.10) can be written as follows for a linearly polarised feed:

$$\underline{E}_f = A\, \hat{\vartheta}_p + c\, A\, \hat{\varphi}_p , \qquad (3.16)$$

where A is a function of ϑ_p and φ_p multiplied by $\frac{e^{-jkr}}{r}$, furthermore, c is a real constant.

Substitution of (3.16) in (3.14) and (3.15) yields

$$E_{axs} = (f_1 + c f_2)\, A , \qquad (3.17)$$

$$E_{ays} = (-f_2 + c f_1)\, A . \qquad (3.18)$$

The angle τ between the polarisation direction of the $\underline{E}_{as}$-field and the $\hat{x}_s$ direction is given by

$$\tau = \arctan\left[\frac{c f_1 - f_2}{f_1 + c f_2}\right] . \qquad (3.19)$$

The result is that the aperture field, given by (3.17) and (3.18) is linearly polarised. The direction of the $\underline{E}$-vector changes over the aperture, as f_1 and f_2 depend on the primary coordinates and thus τ, given by (3.19), changes.

b) Equation (3.10) can be written for a circularly polarised feed as follows:

$$\underline{E}_f = A\,\hat{\vartheta}_p + jA\,\hat{\varphi}_p, \qquad (3.20)$$

where A is defined as mentioned above.

Substitution of (3.20) in (3.14) and (3.15) yields

$$E_{axs} = (f_1 + jf_2)A, \qquad (3.21)$$

$$E_{ays} = (-f_2 + jf_1)A. \qquad (3.22)$$

The result is a circularly polarised aperture field, for (3.21) and (3.22) show that

$$E_{axs} = -j\,E_{ays}. \qquad (3.23)$$

c) An elliptically polarised source can be described by (3.10) as follows:

$$\underline{E}_f = A\,\hat{\vartheta}_p + jcA\,\hat{\varphi}_p. \qquad (3.24)$$

Again A and C are defined as for a linearly polarised feed. The substitution of (3.24) in (3.14) and (3.15) yields:

$$E_{axs} = (f_1 + jcf_2)A, \qquad (3.25)$$

$$E_{ays} = (-f_2 + jcf_1)A. \qquad (3.26)$$

The relationship between the components given by (3.25) and (3.26) is not a simple one. The aperture field remains elliptical; moreover, due to the variations of f_1 and f_2 over the aperture, the ellipticity of the aperture field varies over the aperture.

A balanced feed has a far-field radiation which can be written as

$$\underline{E}_f = F(\vartheta_p, \varphi_p)\left\{\cos\varphi_p\,\hat{\vartheta}_p - \sin\varphi_p\,\hat{\varphi}_p\right\}\frac{e^{-jkr}}{r} \qquad (3.27)$$

corresponding to a principal linear polarisation along the x_s axis.

Using such a feed in an off-set antenna, we get the aperture field components by the substitution of (3.27) into (3.12) and (3.13):

$$E_{axs} = \frac{F(\vartheta_p,\varphi_p)}{te}\Big\{\sin\vartheta_p\cos\varphi_p\sin\vartheta_o - \sin^2\varphi_p(\cos\vartheta_p+\cos\vartheta_o)+ - \cos^2\varphi_p(1+\cos\vartheta_o\cos\vartheta_p)\Big\}, \qquad (3.28)$$

$$E_{ays} = \frac{F(\vartheta_p,\varphi_p)}{te}\Big\{-\sin\vartheta_p\sin\varphi_p\sin\vartheta_o + + \sin\varphi_p\cos\varphi_p(1-\cos\vartheta_p)(1-\cos\vartheta_o)\Big\}. \qquad (3.29)$$

From the expressions (3.28) and (3.29) it can be seen that a centre-fed paraboloid with such a feed has only a component E_{axs}, as $\vartheta_0=0$.
For such a case the field lines will be parallel in the aperture.
Note that for small angles ϑ_p the cross-polarisation decreases too.
Rotation of the feed around the z_p axis over 90° implies a rotation of the aperture field over 90° around the z_s axis.

According to (3.28) and (3.29) the aperture field has a x_s component and a small y_s component if the feed is x_p-polarised as given by (3.27). The component along $\hat{y}_s$ gives rise to the cross-polar component in the far-field and in absent when we are dealing with centre-fed paraboloids.

Investigation of (3.28) and (3.29), after evaluation with the formulas:

$$\sin^2\varphi = \tfrac{1}{2}(1-\cos 2\varphi), \qquad (3.30)$$

$$\cos^2\varphi = \tfrac{1}{2}(1+\cos 2\varphi), \qquad (3.31)$$

shows that the aperture components can be written as:

$$E_{axs} = \frac{F(\vartheta_p,\varphi_p)}{te}\Big\{-\tfrac{1}{2}(1+\cos\vartheta_p)(1+\cos\vartheta_o) + \sin\vartheta_p\sin\vartheta_o\cos\varphi_p + - \tfrac{1}{2}(1-\cos\vartheta_p)(1-\cos\vartheta_o)\cos 2\varphi_p\Big\}, \qquad (3.32)$$

$$E_{ays} = \frac{F(\vartheta_p,\varphi_p)}{te}\Big\{-\sin\vartheta_p\sin\vartheta_o\sin\varphi_p + + \tfrac{1}{2}(1-\cos\vartheta_p)(1-\cos\vartheta_o)\sin 2\varphi_p\Big\}. \qquad (3.33)$$

Substitution of the following coefficients

$$\begin{aligned} d &= \tfrac{1}{2}(1+\cos\vartheta_o)(1+\cos\vartheta_p), \\ e &= \sin\vartheta_p\sin\vartheta_o, \\ f &= \tfrac{1}{2}(1-\cos\vartheta_o)(1-\cos\vartheta_p), \end{aligned} \qquad (3.34)$$

in (3.32) and (3.33) yields

$$E_{axs} = \frac{F(\vartheta_p,\varphi_p)}{et}\left\{-d + e\cos\varphi_p - f\cos 2\varphi_p\right\}, \quad (3.35)$$

$$E_{ays} = \frac{F(\vartheta_p,\varphi_p)}{et}\left\{ - e\sin\varphi_p + f\cos 2\varphi_p\right\}. \quad (3.36)$$

Expressions (3.35) and (3.36) show a decomposition into components with a different ϑ_p dependence. We can calculate the amplitude ratio given by e/d and f/d and we get:

$$e/d = \frac{2\sin\vartheta_p \sin\vartheta_o}{(1+\cos\vartheta_p)(1+\cos\vartheta_o)} = 2\tan\frac{\vartheta_o}{2}\tan\frac{\vartheta_p}{2} \quad (3.37)$$

$$f/d = \frac{(1-\cos\vartheta_p)(1-\cos\vartheta_o)}{(1+\cos\vartheta_p)(1+\cos\vartheta_o)} = \tan^2\frac{\vartheta_o}{2}\tan^2\frac{\vartheta_p}{2} \quad (3.38)$$

If we have a centre-fed paraboloid, e and f vanish as $V_o=0$.
We can see the E_{axs} component as having a ground component, denoted by d, with two higher-order components, denoted by e and f, respectively.
In the E_{ays} component, only these higher-order components occur.

3.4 The far field radiation

With the Lorentz Lamor theorem we can calculate the far-field of a radiating aperture S_A with a given field distribution.

This theorem reads as follows:

$$\underline{E}(\underline{r}) = \nabla_r \times \int_{S_A}\left\{\hat{n}\times\underline{E}(\underline{r}')\right\}\psi(\underline{r},\underline{r}')\,dS + \\ + \frac{1}{j\omega\varepsilon_o}\nabla_r\times\nabla_r\times\int_{S_A}\left\{\hat{n}\times\underline{H}(\underline{r}')\right\}\psi(\underline{r},\underline{r}')\,dS, \quad (3.39)$$

$$\underline{H}(\underline{r}) = \nabla_r \times \int_{S_A}\left\{\hat{n}\times\underline{H}(\underline{r}')\right\}\psi(\underline{r},\underline{r}')\,dS + \\ - \frac{1}{j\omega\mu_o}\nabla_r\times\nabla_r\times\int_{S_A}\left\{\hat{n}\times\underline{E}(\underline{r}')\right\}\psi(\underline{r},\underline{r}')\,dS. \quad (3.40)$$

Here the function $\Psi(\underline{r},\underline{r}')$ is given as

$$\Psi(\underline{r},\underline{r}') = \frac{e^{-jk|\underline{r}-\underline{r}'|}}{|\underline{r}-\underline{r}'|} . \qquad (3.41)$$

Furthermore, $\hat{n}$ denotes the normal to S_A and the prime indicates coordinates describing the aperture. (Fig 3.3)

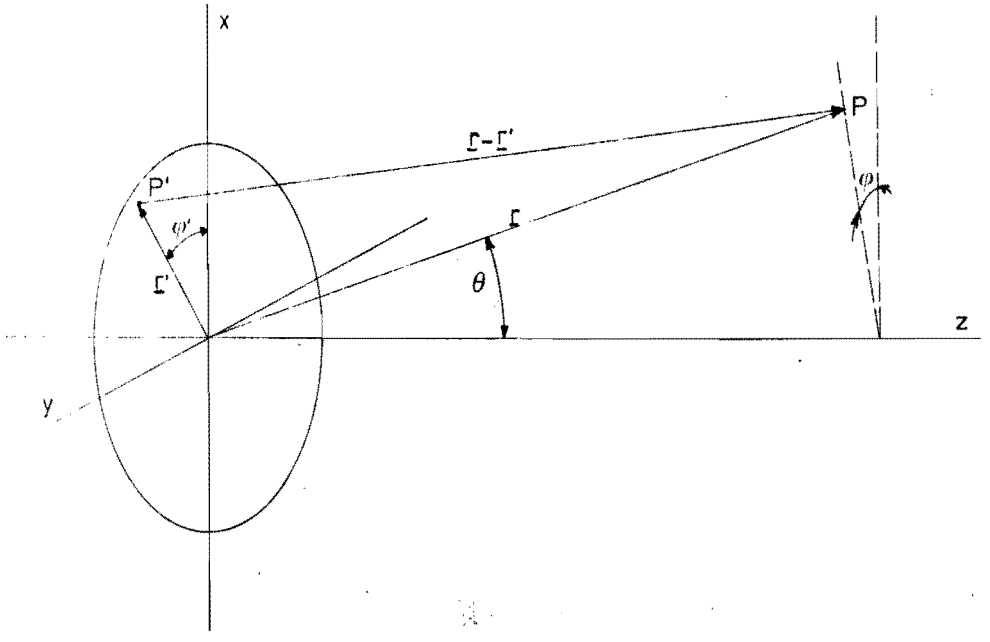

Fig 3.3 Coordinates for a radiating aperture in the xy plane.

The approximation for the far-field [23] gives:

$$\underline{E}(\underline{r}) = -jk\, \frac{e^{-jkr}}{4\pi r}\, \hat{r} \times \int_{S_A} \left\{ \left[\hat{n} \times \underline{E}(\underline{r}') \right] - \hat{r} \times \left[\hat{n} \times Z_0\, \underline{H}(\underline{r}') \right] \right\} e^{jk(\hat{r}\cdot\underline{r}')}\, dS, \qquad (3.42)$$

$$Z_0\, \underline{H}(\underline{r}) = \hat{r} \times \underline{E}(\underline{r}) . \qquad (3.43)$$

where $\hat{r}$ denotes the unit vector from the origin directed to P the fieldpoint.

Introducing polar coordinates for the description of an aperture, we obtain from formulas (3.39) and (3.40) the following expressions [22] after some calculation.

$$E_\vartheta(r) = jk\,\frac{e^{-jkr}}{4\pi r}\int_{S_A}\Big\{(E_r' + Z_0 H_\varphi'\cos\vartheta)\cos(\varphi-\varphi') + (E_\varphi' - Z_0 H_r'\cos\vartheta)\sin(\varphi-\varphi')\Big\}e^{jkr'\sin\vartheta\cos(\varphi-\varphi')}\,dS, \tag{3.44}$$

$$E_\varphi(r) = jk\,\frac{e^{-jkr}}{4\pi r}\int_{S_A}\Big\{(E_\varphi'\cos\vartheta - Z_0 H_r')\cos(\varphi-\varphi') - (E_r'\cos\vartheta + Z_0 H_\varphi')\sin(\varphi-\varphi')\Big\}e^{jkr'\sin\vartheta\cos(\varphi-\varphi')}\,dS. \tag{3.45}$$

If the aperture field is given by components in a rectangular system (xyz) and are indicated by E_{ax} and E_{ay}, we use the following procedure [23], [6].

An aperture field given by $\underline{E}_a = E_{ax}\hat{x}$ gives rise to a far-field $\underline{E}_1(r)$, so that

$$\underline{E}_1(\underline{r}) = -jk\,\frac{e^{-jkr}}{4\pi r}(1+\cos\vartheta)\Big\{-\cos\varphi\,\hat{\vartheta} + \sin\varphi\,\hat{\varphi}\Big\}\int_{S_A} E_{ax}\,e^{jk(\hat{r}.\underline{r}')}\,dS. \tag{3.46}$$

An aperture field given by $E_a = E_{ay}\hat{y}$ gives rise to a far-field $\underline{E}_2(r)$, so that

$$\underline{E}_2(\underline{r}) = -jk\,\frac{e^{-jkr}}{4\pi r}(1+\cos\vartheta)\Big\{\sin\varphi\,\hat{\vartheta} + \cos\varphi\,\hat{\varphi}\Big\}\int_{S_A} E_{ay}\,e^{jk(\hat{r}.\underline{r}')}\,dS. \tag{3.47}$$

It should be noted that $\underline{E}_1(\underline{r})$ and $\underline{E}_2(\underline{r})$ are perpendicular as $(\underline{E}_1.\underline{E}_2)=0$ everywhere in space.
Furthermore, the coordinate system in which the far-field is calculated is the (xyz) system.

If we have an off-set antenna fed by a balanced feed, polarised in the $\hat{x}_p$ direction, the aperture field is described by the expressions (3.28) and (3.29). It should be noted that this field is given in the (x_s,y_s,z_s) system. Thus a transformation to the (xyz) system is necessary, using (3.8).

Then, with (3.46) and (3.47) we obtain the far-field components of this aperture.
The E_{ax} component gives rise to a field $\underline{E}_1$, the copolar field.
The small E_{ay} component gives rise to a field $\underline{E}_2$, the cross-polar field.
This for the case that the feed is linearly polarised in the $\hat{x}_p$ direction, and thus the aperture field has an E_{ax} component and a small E_{ay} component.

Chapter IV

The waveguide with the coax-segmental cross-section.

4.1. Introduction.

In this chapter we shall investigate the waveguide with a coax segmental cross-section. Formulas for the field within the waveguide will be derived [21] and the far field radiated from its aperture will be computed.

Experimental investigations have been carried out to verify these calculations for two feeds, the A-132 and A-133.
The A-132 is a waveguide feed with an aperture equal to its cross-section.
The A-133 is a horn with a small flare angle. The aperture plane of this horn has the same geometry as a cross-section of the coax-segmental waveguide, the flare angle is 10^{o}.

The calculations for the far field radiation of the A-133 are based on the principle that the aperture field of a horn with a small flare angle can be approximated by the aperture field of a waveguide having the same aperture as the horn. This approximation is valid for flare angles up to about 15^{o}. We shall give a prediction over the usefulness of these feed structures, when used as offset feeds with the reflector positioned in the far field region of the feed.

4.2. The modes within the waveguide.

The cylindrical structure of the waveguide involves the use of cylindrical coordinates related to the (xyz)system. (Fig. 4.1) Note that the xz plane ($\phi = 0$) coincides with the symmetry plane of the waveguide.

As we are dealing with a source-free region within the waveguide, we have to solve (2.13) and (2.16) with $\underline{J} = 0$ and $\underline{M} = 0$, respectively. We assume that $\underline{A}$ and $\underline{F}$ only have z-components and denote, neglecting the time dependence $e^{j\omega t}$:

$$\underline{A} = \Psi_1(r,\varphi,z)\,\hat{z}, \tag{4.1}$$

$$\underline{F} = \Psi_2(r,\varphi,z)\,\hat{z}. \tag{4.2}$$

Both Ψ_1 and Ψ_2 have to satisfy the Helmholtz equation in free space, viz. $(\nabla^2 + k^2)\Psi = 0$, or in cylindrical coordinates:

$$\frac{1}{r}\frac{\partial}{\partial r}\left\{r\frac{\partial \Psi}{\partial r}\right\} + \frac{1}{r^2}\frac{\partial^2 \Psi}{\partial \varphi^2} + \frac{\partial^2 \Psi}{\partial z^2} + k^2\Psi = 0. \tag{4.3}$$

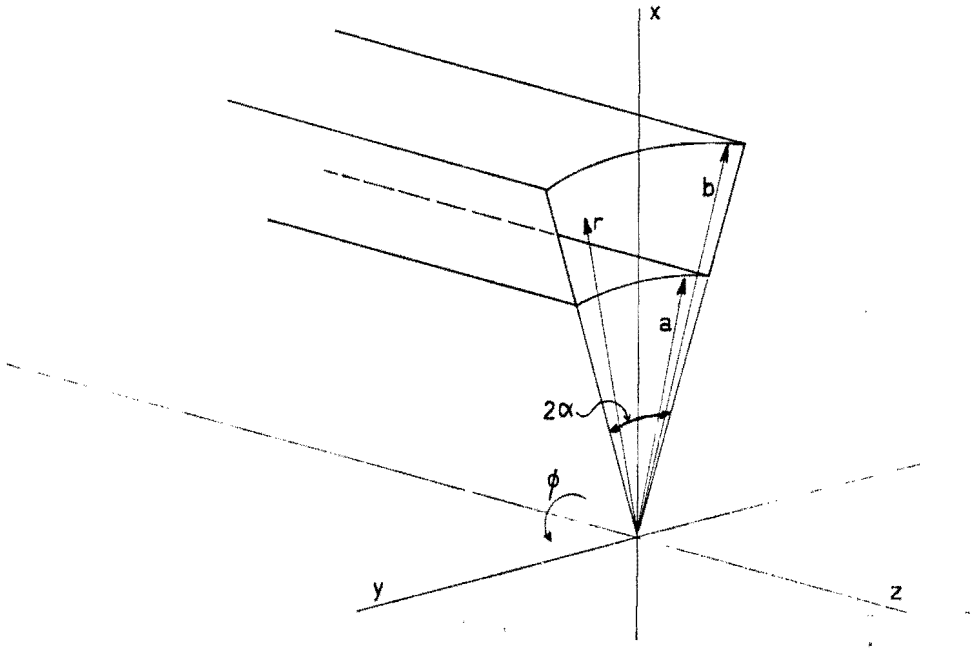

Fig.4.1 Geometry of the coax-segmental waveguide.

Using the method of separation of variables we get the general solution for Ψ_1 and Ψ_2 :

$$\Psi_1(r,\varphi,z) = \Psi_2(r,\varphi,z) = R(r)\,\Phi(\varphi)\,Z(z), \qquad (4.4)$$

where

$$R(r) = C_1 J_\mu(k_c r) + C_2 Y_\mu(k_c r),$$
$$\Phi(\varphi) = C_3 \cos(\mu\varphi) + C_4 \sin(\mu\varphi),$$
$$Z(z) = C_5 e^{-\gamma z} + C_6 e^{+\gamma z},$$

with $k_c = k^2 + \gamma^2$, $k = \omega^2\mu\varepsilon$, $\gamma = j\beta$.
The constants $C_1 \ldots\ldots C_6$ are to be determined by applying the boundary conditions. J_μ and Y_μ are Besselfunctions, of the first and the second kind respectively, and both of order μ.

Propagation of a wave only in the positive z-direction requires: $C_6 = 0$. The choice of the coordinate system is such that $\Phi = 0$ along the symmetry axis. This implies that in (4.5) either C_3 or C_4 is equal to zero. We shall apply this after a general derivation of values for μ and k_c.

The components of the TE field are derived [19] from:

$$\left.\begin{aligned} E_r &= -\frac{1}{r}\frac{\partial \Psi_1}{\partial \varphi}, & H_r &= \frac{1}{j\omega\mu_0}\frac{\partial^2 \Psi_1}{\partial r\,\partial z}, \\ E_\varphi &= \frac{\partial \Psi_1}{\partial r}, & H_\varphi &= \frac{1}{j\omega\mu_0}\frac{\partial^2 \Psi_1}{\partial \varphi\,\partial z}, \\ E_z &= 0, & H_z &= \frac{1}{j\omega\mu_0}\left(k^2\Psi_1 + \frac{\partial^2 \Psi_1}{\partial z^2}\right). \end{aligned}\right\} \quad (4.5)$$

Substituting (4.4) into (4.5) with a new notation for the constants we obtain:

$$\left.\begin{aligned} E_r &= -\frac{1}{r}\left\{A_1 J_\mu(k_c r) + B_1 Y_\mu(k_c r)\right\}\left\{-C_1 \mu \sin(\mu\varphi) + D_1 \mu \cos(\mu\varphi)\right\} e^{-j\beta z} \\ E_\varphi &= k_c\left\{A_1 \frac{dJ_\mu(k_c r)}{dr} + B_1 \frac{dY_\mu(k_c r)}{dr}\right\}\left\{C_1 \cos(\mu\varphi) + D_1 \sin(\mu\varphi)\right\} e^{-j\beta z} \\ E_z &= 0. \end{aligned}\right\} \quad (4.6)$$

$$\left.\begin{aligned} H_r &= \frac{-\beta}{\omega\mu_0} k_c \left\{A_1 \frac{dJ_\mu(k_c r)}{dr} + B_1 \frac{dY_\mu(k_c r)}{dr}\right\}\left\{C_1 \cos(\mu\varphi) + D_1 \sin(\mu\varphi)\right\} e^{-j\beta z} \\ H_\varphi &= \frac{-\beta}{\omega\mu_0}\frac{1}{r}\left\{A_1 J_\mu(k_c r) + B_1 Y_\mu(k_c r)\right\}\left\{-C_1 \mu \sin(\mu\varphi) + D_1 \mu \cos(\mu\varphi)\right\} e^{-j\beta z} \\ H_z &= \frac{1}{j\omega\mu_0} k_c^2 \left\{A_1 J_\mu(k_c r) + B_1 Y_\mu(k_c r)\right\}\left\{C_1 \cos(\mu\varphi) + D_1 \sin(\mu\varphi)\right\} e^{-j\beta z} \end{aligned}\right\}$$

The components of the TM field are derived from the following expressions [19]:

$$\left.\begin{aligned} E_r &= \frac{1}{j\omega\varepsilon_0}\frac{\partial^2 \Psi_2}{\partial r\,\partial z}, & H_r &= \frac{1}{r}\frac{\partial \Psi_2}{\partial \varphi}, \\ E_\varphi &= \frac{1}{j\omega\varepsilon_0}\frac{\partial^2 \Psi_2}{\partial \varphi\,\partial z}, & H_\varphi &= \frac{\partial^2 \Psi_2}{\partial r}, \\ E_z &= \frac{1}{j\omega\varepsilon_0}\left[k^2\Psi_2 + \frac{\partial^2 \Psi_2}{\partial z^2}\right], & H_z &= 0. \end{aligned}\right\} \quad (4.7)$$

$$\left.\begin{aligned} E_r &= \frac{-\beta}{\omega\varepsilon_0} k_c \left\{A_2 \frac{dJ_\mu(k_c r)}{dr} + B_2 \frac{dY_\mu(k_c r)}{dr}\right\}\left\{C_2 \cos(\mu\varphi) + D_2 \sin(\mu\varphi)\right\} e^{-j\beta z} \\ E_\varphi &= \frac{-\beta}{\omega\varepsilon_0}\frac{1}{r}\left\{A_2 J_\mu(k_c r) + B_2 Y_\mu(k_c r)\right\}\left\{-C_2 \mu \sin(\mu\varphi) + D_2 \mu \cos(\mu\varphi)\right\} e^{-j\beta z} \\ E_z &= \frac{1}{j\omega\varepsilon_0} k_c^2 \left\{A_2 J_\mu(k_c r) + B_2 Y_\mu(k_c r)\right\}\left\{C_2 \cos(\mu\varphi) + D_2 \sin(\mu\varphi)\right\} e^{-j\beta z} \end{aligned}\right\} \quad (4.8)$$

$$
\left.
\begin{aligned}
H_r &= \frac{1}{r}\left\{A_2 J_\mu(k_c r) + B_2 Y_\mu(k_c r)\right\}\left\{-C_2/\mu \sin(\mu\varphi) + D_2/\mu \cos(\mu\varphi)\right\} e^{-j\beta z} \\
H_\varphi &= -k_c\left\{A_2 \frac{dJ_\mu(k_c r)}{dr} + B_2 \frac{dY_\mu(k_c r)}{dr}\right\}\left\{C_2 \cos(\mu\varphi) + D_2 \sin(\mu\varphi)\right\} e^{-j\beta z} \\
H_z &= 0.
\end{aligned}
\right\} \quad (4.8)
$$

Expressions (4.6) and (4.8) give the fieldcomponents in as general terms as possible. By applying the boundary conditions, we find distinct values for the constants. This will be examined in the following paragraph.

4.3. The Boundary Conditions.

For both the TE and the TM field the following boundary conditions are valid at $\varphi = +\alpha$ and $\varphi = -\alpha$:

$$
\left.
\begin{aligned}
E_r(\varphi=\alpha) &= E_r(\varphi=-\alpha) = 0, \\
E_z(\varphi=\alpha) &= E_z(\varphi=-\alpha) = 0.
\end{aligned}
\right\} \quad (4.9)
$$

and at r = a and r = b:

$$
\left.
\begin{aligned}
E_\varphi(r=a) &= E_\varphi(r=b) = 0, \\
E_z(r=a) &= E_z(r=b) = 0.
\end{aligned}
\right\} \quad (4.10)
$$

The propagating mode, TE or TM, is characterised by two integers m and n. As will be described below, m labels the denumerable roots μ of (4.9), n does the same with the denumerable roots k_c of (4.10). It should be noted that μ is not restricted to integer values.

In the case of a TE field, substitution of (4.6) in (4.9) yields:

$$
\left.
\begin{aligned}
-C_1 \mu \sin(\mu\alpha) + D_1 \mu \cos(\mu\alpha) &= 0, \\
C_1 \mu \sin(\mu\alpha) + D_1 \mu \cos(\mu\alpha) &= 0,
\end{aligned}
\right\} \quad (4.11)
$$

with a non-trivial solution where the determinant is equal to zero:

$$2\cos(\mu\alpha)\sin(\mu\alpha) = 0 \qquad (4.12)$$

Thus $$\mu = m\frac{\pi}{2\alpha} \quad \text{with } m = 0, 1, 2, 3\ldots. \qquad (4.13)$$

A special case m = 0 needs to be considered apart. In that particular case there is only an E_ϕ component. The H_ϕ component vanishes too, as is seen from (4.6).

Having determined μ by (4.13), the order of the Bessel-functions is fixed.
Substituting (4.6) into (4.10) we then get:

$$\left.\begin{aligned} A_1 \frac{dJ_\mu(k_c a)}{dr} + B_1 \frac{dY_\mu(k_c a)}{dr} &= 0 , \\ A_1 \frac{dJ_\mu(k_c b)}{dr} + B_1 \frac{dY_\mu(k_c b)}{dr} &= 0 , \end{aligned}\right\} (4.14)$$

with a non-trivial solution when

$$\frac{dJ_\mu(k_c a)}{dr}\frac{dY_\mu(k_c b)}{dr} - \frac{dJ_\mu(k_c b)}{dr}\frac{dY_\mu(k_c a)}{dr} = 0 \qquad (4.15)$$

Note that this last expression is identical to the dispersion equation for TE modes in a coaxial waveguide if μ is an integer. For fixed values of a and b it has an infinite number of denumerable roots k_c. They are labeled by n in accordance with the increasing value of k_c.
The expressions from (4.14) also give a relation between A_1 and B_1:

$$B_1/A_1 = -\frac{dJ_\mu(k_c a)}{dr} \Big/ \frac{dY_\mu(k_c a)}{dr} = -\frac{dJ_\mu(k_c b)}{dr} \Big/ \frac{dY_\mu(k_c b)}{dr} , \qquad (4.16)$$

Having determined the TE_{mn} modes, the same procedure can be followed for the TM_{mn} modes. Then substitution of (4.8) into (4.9) yields:

$$\left.\begin{aligned} C_2\cos(\mu\alpha) + D_2\sin(\mu\alpha) &= 0 , \\ C_2\cos(\mu\alpha) - D_2\sin(\mu\alpha) &= 0 , \end{aligned}\right\} \qquad (4.17)$$

with a non-trivial solution for μ where

$$2 \cos(\mu\alpha) \sin(\mu\alpha) = 0 \quad . \tag{4.18}$$

Thus $$\mu = m \frac{\pi}{2\alpha} \quad , \quad m = 0, 1, 2, 3 \ldots \tag{4.19}$$

It is of interest that m = 0 is allowed here, as opposed to the TE case, where m = 0 should be considered apart.

Again m fixes the order μ of the Besselfunctions and hence by substitution of (4.8) into (4.10) we get:

$$\left.\begin{aligned} A_2 J_\mu(k_c a) + B_2 Y_\mu(k_c a) &= 0 , \\ A_2 J_\mu(k_c b) + B_2 Y_\mu(k_c b) &= 0 , \end{aligned}\right\} \tag{4.20}$$

with the necessary condition for non-trivial solutions:

$$J_\mu(k_c a)\, Y_\mu(k_c b) - J_\mu(k_c b)\, Y_\mu(k_c a) = 0 . \tag{4.21}$$

This is the dispersion equation for the TM case; for integer values of μ this equation is the same as the dispersion equation for the TM modes in a coaxial waveguide.

From (4.21) the solutions for k_c are obtained, labeled with n according to the increasing value of k_c.

Expressions (4.20) also define a relation between A_2 and B_2 as follows:

$$B_2/A_2 = - \frac{J_\mu(k_c a)}{Y_\mu(k_c a)} = - \frac{J_\mu(k_c b)}{Y_\mu(k_c b)} \quad . \tag{4.22}$$

With the above procedure a complete calculation of a TE_{mn} or TM_{mn} field is possible.

Two important linear polarisation directions in the waveguide can be distinguished, a tangential and a radial direction, related to the cylindrical coordinates which describe the fields. (Fig. 4.1)

The mode with the lowest cut-off frequency in both directions is a TE mode, with m = 0 and m = 1 for the tangential and radial direction, respectively. [20]. According to the classification used by Marcuvitz, they are denoted as TE_{02} and TE_{11} modes.

4.4 The dispersion equation.

We have solved the transcendental equation (4.15) numerically, and for the lowest values of k_c we have plotted β/k as a function of $2a/\lambda$.
Here a is the innerradius of the coax-segmental waveguide; a and the other dimensions of the feeds, applied in the experiments, are given in the table in Fig. 4.4.
With

$$\beta/k = \sqrt{1 - \left(\frac{k_c a}{\pi}\right)^2 \left(\frac{\lambda}{2a}\right)^2} \quad , \qquad (4.23)$$

for different values of k_c we get two sets of branches, namely for m=0 and m=1. These sets are shown in Figs. 4.2 and 4.3, respectively. Each curve in Fig. 4.2 corresponds to a TE_{0n}mode. The first non-vanishing solution (lowest value of $k_c a$) is designated as the TE_{02}mode rather than the TE_{01}mode.[20].
In Fig. 4.3 the lowest value of $k_c a$ corresponds to the TE_{11}mode It is of interest to note,that the startingvalue and the progress of the β/k curves are roughly the same for the TE_{02} and the TE_{11}modes.

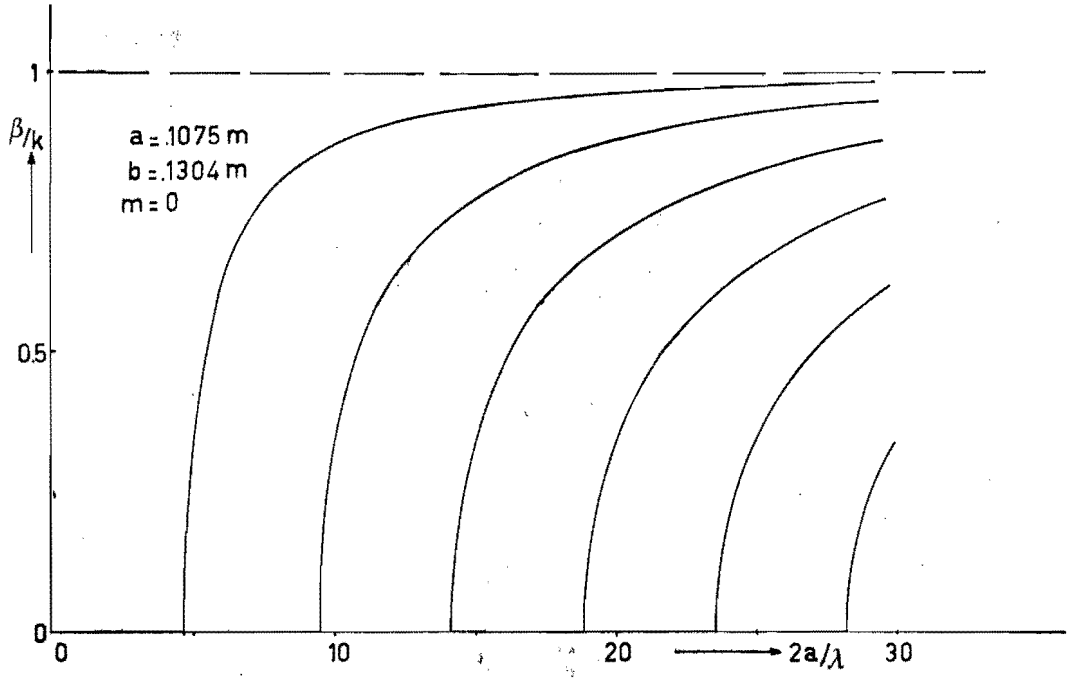

Fig. 4.2 β/k versus $2a/\lambda$ in the case m=0.

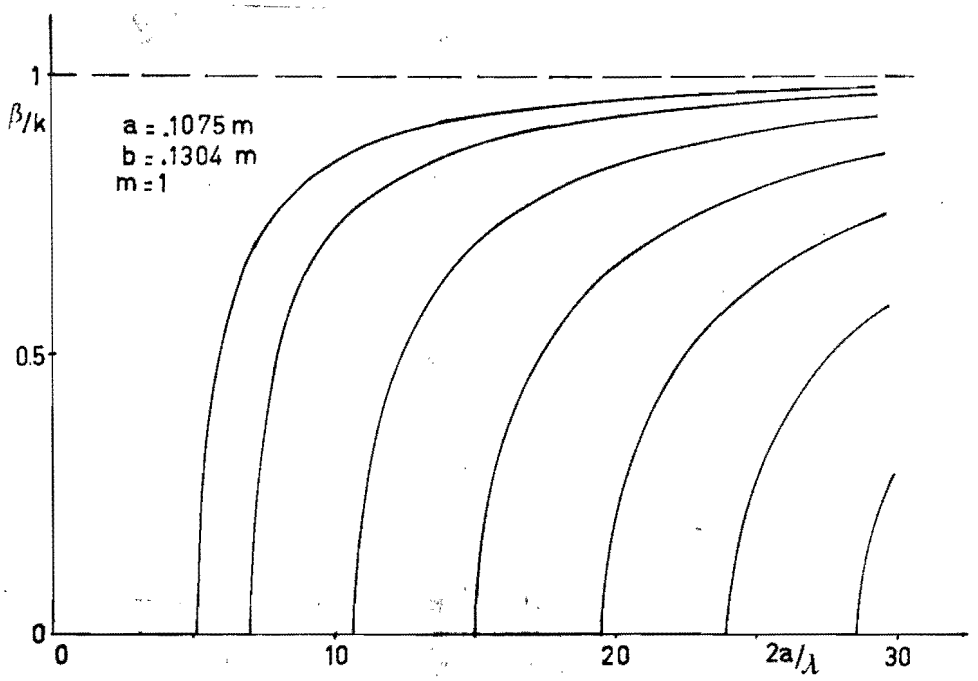

Fig. 4.3 β/k versus $2a/\lambda$ in the case m=1.

The phase difference in the aperture of a coaxsegmental waveguide between the TE_{02} and the TE_{11} modes is given by

$$\Delta\phi(k) = kL\left(\beta_{02}/k - \beta_{11}/k\right), \qquad (4.24)$$

where L is the length of the waveguide and β_{02} and β_{11} the wave numbers of the TE_{02} and the TE_{11} mode, respectively. For short lengths L and with β_{02} and β_{11}, almost the same values the phase difference, given by (4.24) will be nearly zero.

From this we may conclude that a coax-segmental feed, under the conditions mentioned above has an aperture field with no phase shift worth mentioning. Thus an excitation with TE_{02} and TE_{11} in phase yields an aperture field with the modes in phase, and circular excitation of the feed gives rise to a circularly polarised aperture field.

4.5 The aperture fields of the coax-segmental waveguide.

After having solved the dispersion equation for k_c we are able to give the fields for the TE_{02} and TE_{11} modes, respectively. If the waveguide has perfectly conducting walls and there is no current flowing on the outside, and if the waveguide is well matched to the space (there are no reflections), these fields may be taken as aperture fields.
For m = 0 we get the following TE_{02} components.

$$E_r = 0, \tag{4.25}$$

$$E_\varphi = -E_0 \cdot k_c \left\{ J_1(k_c r) - K_0 Y_1(k_c r) \right\}, \tag{4.26}$$

$$E_z = 0, \tag{4.27}$$

$$H_r = E_0 \frac{\beta}{\omega \mu_0} \cdot k_c \left\{ J_1(k_c r) - K_0 Y_1(k_c r) \right\}, \tag{4.28}$$

$$H_\varphi = 0, \tag{4.29}$$

$$H_z = -E_0 \frac{k_c^2}{\omega \mu_0} \left\{ J_1(k_c r) - K_0 Y_1(k_c r) \right\}, \tag{4.30}$$

where $K_0 = \left\{ J_1(k_c a) / Y_1(k_c a) \right\}$. (4.31)

For m = 1 we get the following TE_{11} components

$$E_r = -E_1 \frac{1}{r} \left\{ J_{18}(k_c r) - K_1 Y_{18}(k_c r) \right\} 18 \cos(18\varphi), \tag{4.32}$$

$$E_\varphi = E_1 k_c \left\{ \frac{dJ_{18}(k_c r)}{dr} - K_1 \frac{dY_{18}(k_c r)}{dr} \right\} \sin(18\varphi), \tag{4.33}$$

$$E_z = 0,$$

$$H_r = -E_1 \frac{\beta}{\omega \mu_0} k_c \left\{ \frac{dJ_{18}(k_c r)}{dr} - K_1 \frac{dY_{18}(k_c r)}{dr} \right\} \sin(18\varphi), \tag{4.35}$$

$$H_\varphi = -E_1 \frac{\beta}{\omega \mu_0} \frac{1}{r} \left\{ J_{18}(k_c r) - K_1 Y_{18}(k_c r) \right\} 18 \cos(18\varphi), \tag{4.36}$$

$$H_z = E_1 \frac{k_c^2}{j\omega \mu_0} \left\{ J_{18}(k_c r) - K_1 Y_{18}(k_c r) \right\} \sin(18\varphi). \tag{4.37}$$

where $K_1 = \left\{ \frac{dJ_{18}(k_c r)}{dr} \Big/ \frac{dY_{18}(k_c r)}{dr} \right\}_{r=a}$. (4.38)

It should be noted that, for small values of α, the behaviour of the TE_{02} mode is very similar to that of the TE_{01} mode in a rectangular waveguide. From (4.26) we see that the TE_{02} mode has a uniform progress in the φ-direction; its r-dependency approaches a cosine. The TE_{11} mode, however, does not have a uniform progress in the r-direction; it only uniform when α is large and there is a slight difference between a and b. (Fig.4.4)

4.6 The radiation pattern.

If we substitute the expressions for the components of the TE_{02} and TE_{11} mode derived in the previous paragraph in the formulas (3.44) and (3.45), we get the **expressions** for the calculation of the electromagnetic field at a point P far from the aperture. (Fig. 4.4).

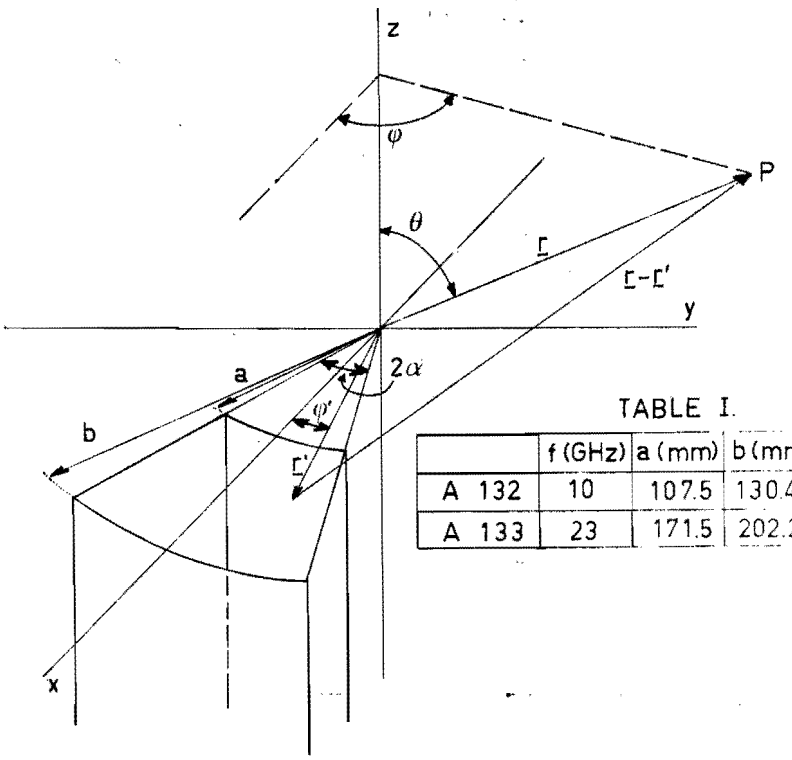

TABLE I.

	f (GHz)	a (mm)	b (mm)	α (degr.)
A 132	10	107.5	130.4	5
A 133	23	171.5	202.2	5

Fig. 4.4 Coax-segmental waveguide .

Table I antenna dimensions.

For m=0 this substitution yields:

$$E_\vartheta(r) = -jk\frac{e^{-jkr}}{4\pi r} E_0 k_c \left(1+\frac{\beta}{k}\cos\vartheta\right) x$$
$$x \int_a^b\int_{-\alpha}^{\alpha}\left\{J_1(k_c r') - k_0 Y_1(k_c r')\right\} \sin(\varphi-\varphi')\, e^{jkr'\sin\vartheta\cos(\varphi-\varphi')}\, r'dr'd\varphi', \qquad (4.39)$$

$$E_\varphi(r) = -jk\frac{e^{-jkr}}{4\pi r} E_0 k_c \left(\cos\vartheta+\frac{\beta}{k}\right) x$$
$$x \int_a^b\int_{-\alpha}^{\alpha}\left\{J_1(k_c r') - k_0 Y_1(k_c r')\right\} \cos(\varphi-\varphi')\, e^{jkr'\sin\vartheta\cos(\varphi-\varphi')}\, r'dr'd\varphi' \qquad (4.40)$$

For m=1 we get:

$$E_\vartheta(r) = -jk\frac{e^{-jkr}}{4\pi r} E_1 \left(1+\frac{\beta}{k}\cos\vartheta\right) x$$
$$x \int_a^b\int_{-\alpha}^{\alpha}\left[\frac{1}{r'}\left\{J_{18}(k_c r') - K_1 Y_{18}(k_c r')\right\} 18\cos(18\varphi')\cos(\varphi-\varphi') + \right.$$
$$\left. - k_c\left\{\frac{dJ_{18}(k_c r')}{dr'} - K_1\frac{dY_{18}(k_c r')}{dr'}\right\} \sin(18\varphi')\sin(\varphi-\varphi')\right] x$$
$$x\, e^{jkr'\sin\vartheta\cos(\varphi-\varphi')}\, r'dr'd\varphi', \qquad (4.41)$$

$$E_\varphi(r) = jk\frac{e^{-jkr}}{4\pi r} E_1 \left(\cos\vartheta+\frac{\beta}{k}\right) x$$
$$x \int_a^b\int_{-\alpha}^{\alpha}\left[\frac{1}{r'}\left\{J_{18}(k_c r') - K_1 Y_{18}(k_c r')\right\} 18\cos(18\varphi')\sin(\varphi-\varphi') + \right.$$
$$\left. - k_c\left\{\frac{dJ_{18}(k_c r')}{dr'} - K_1\frac{dY_{18}(k_c r')}{dr'}\right\} \sin(18\varphi')\cos(\varphi-\varphi')\right] x$$
$$x\, e^{jkr'\sin\vartheta\cos(\varphi-\varphi')}\, r'dr'd\varphi'. \qquad (4.42)$$

4.7 Experimental Investigation

We have computed numerically the far-field patterns of the waveguide feed A 132 and the horn with a small flare angle A 133. The dimensions of both antennas are given in Fig. 4.4.
The co- and cross-polar components are also recorded for both polarisations. (Figs. 4.6 and 4.7).
Comparison of measured values with the calculated ones demonstrates a difference for the co-polar component, that becomes larger with increasing θ. The reason is that the aperture is small in terms of wave-lengths. In that case the formulas (4.39), (4.40), (4.41) and (4.42) do not describe the field accurately for large values of θ.

If we take into account that measurements below -30 dB are quite inaccurate due to the unpredictable reflections and disturbances in the anechoic chamber, it has to be noted that the measured cross-polar components at such low levels agrees very well with the computed one.

The reflected power is below -20 dB for both polarisations, as is found from Fig. 4.7.

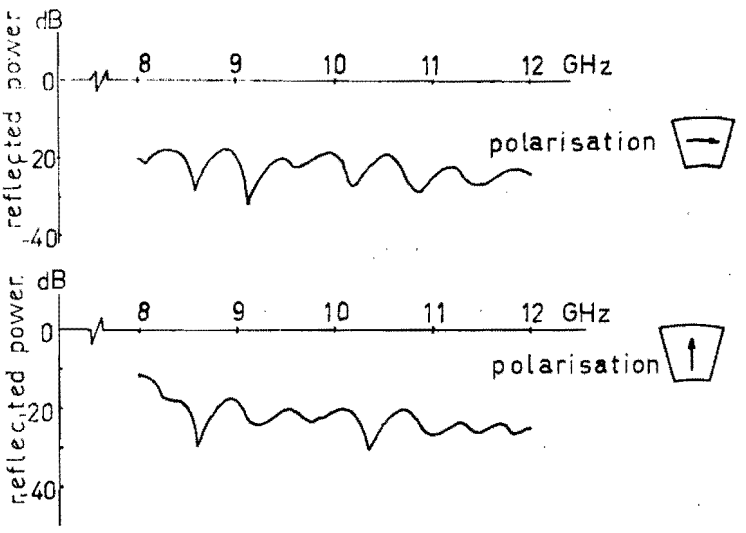

Fig. 4.5. Reflected power, A 132.

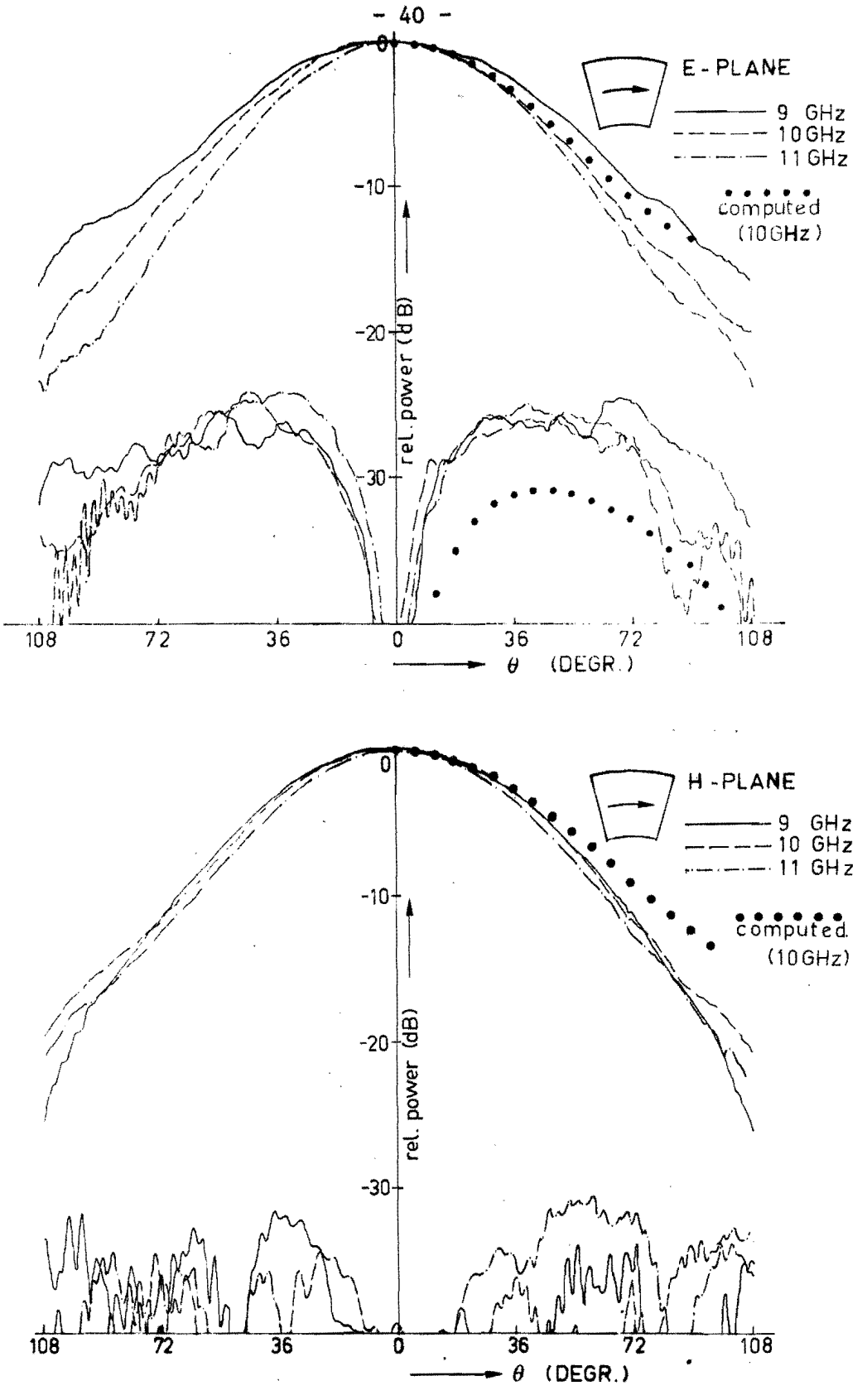

Fig. 4.6 Far field radiation pattern of the antenna A 132, horizontal polarisation.

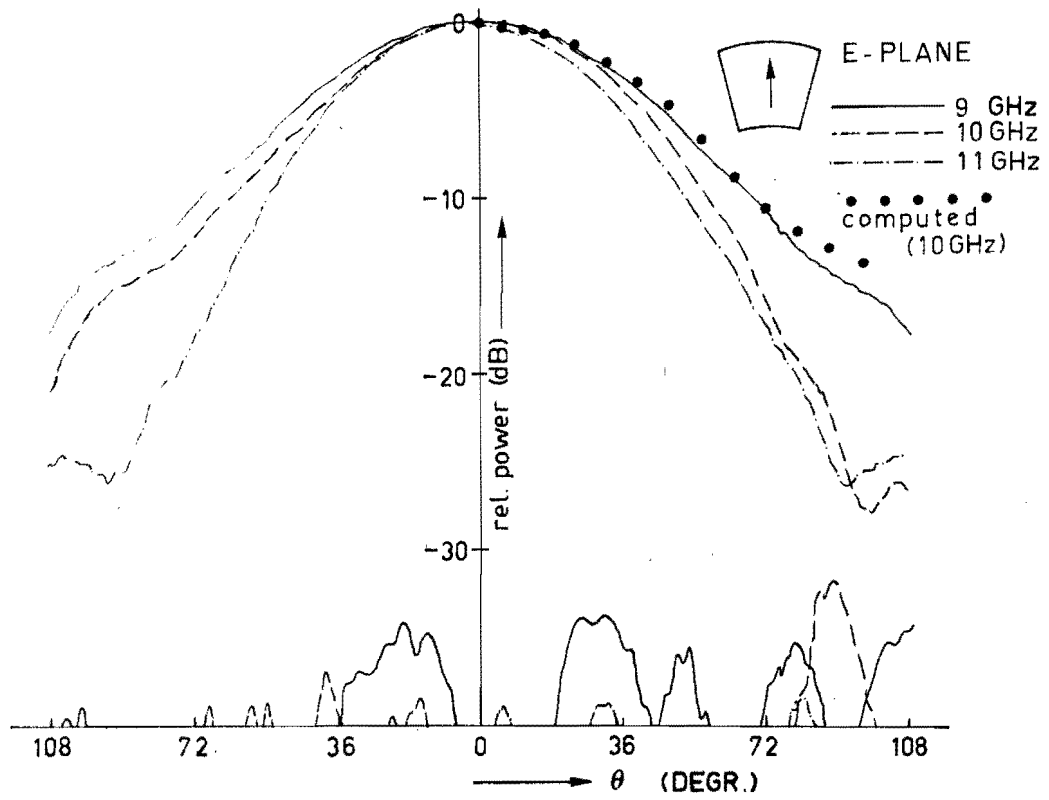

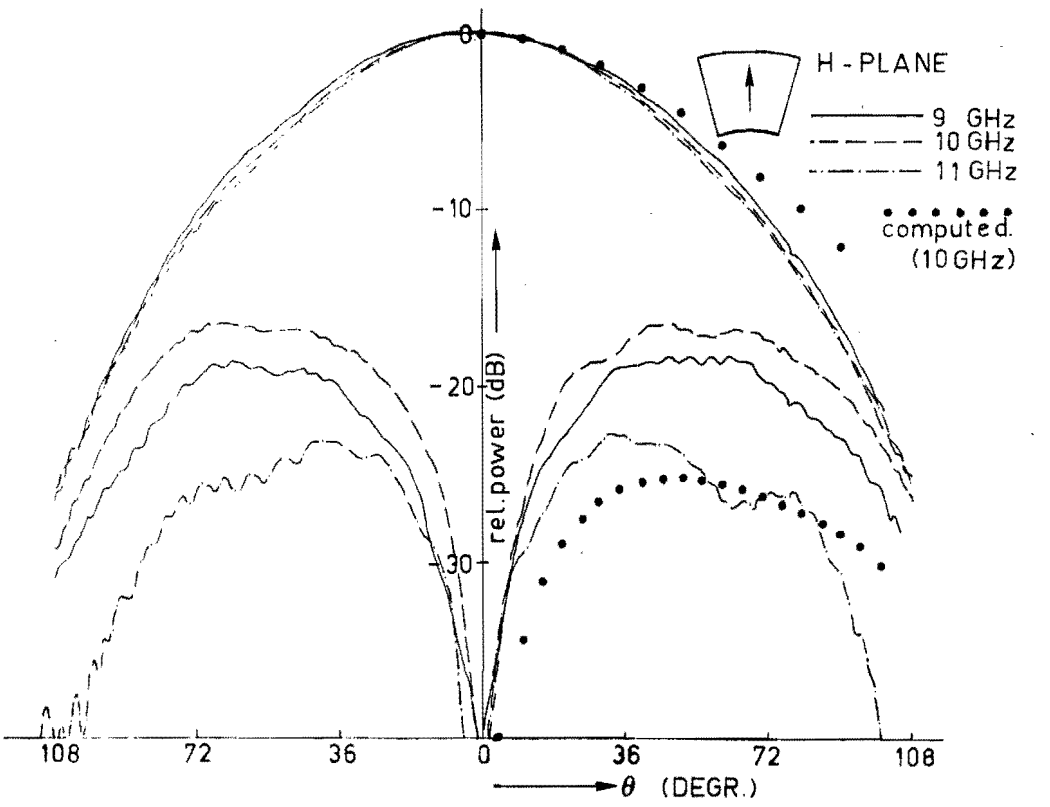

Fig. 4.7 Far field radiation pattern of the antenna A 132, vertical polarisation.

We have also recorded the phase of the cross-polar component relative to the co-polar component in the plane of asymmetry (Fig. 4.8). The phase difference is about 90°.
This results in a far field radiation which is elliptically polarised.

As shown in (3.25) and (3.26), an off-set reflector, illuminated by an elliptically polarised primary field has an aperture field which is still elliptically polarised
Since we need a linearly polarised primary field for the elimination of the cross-polarisation, the waveguide feed with a coax-segmental cross-section cannot be used for this purpose.

In Appendix B we have derived that there is a phase difference of 90° between the E_ϑ and E_φ components in the plane of asymmetry, thus an elliptically polarised far field.

The antenna A 133 shows better agreement between measured and computed co-polar components, as the aperture dimension is somewhat larger in wavelength compared to A 132.
(Figs. 4.9 and 4.10) We have used the same formulas for the calculation of the far field patterns as for the A 132. This is permitted if the horn flare angle is small.

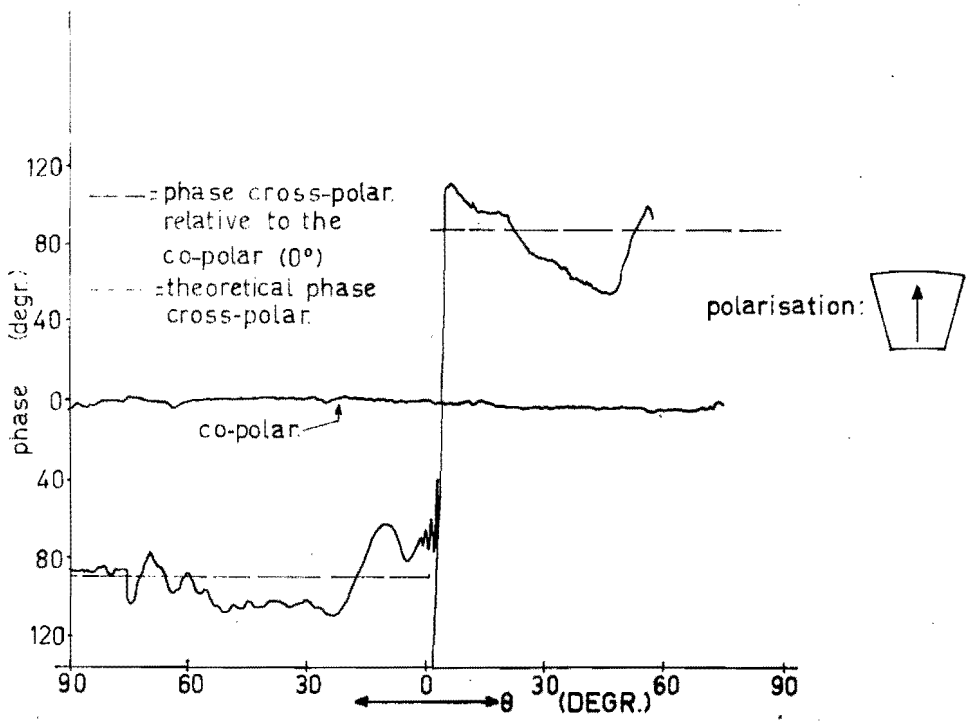

Fig. 4.8 Measured phase difference between the co- and cross-polar components of the A 132.

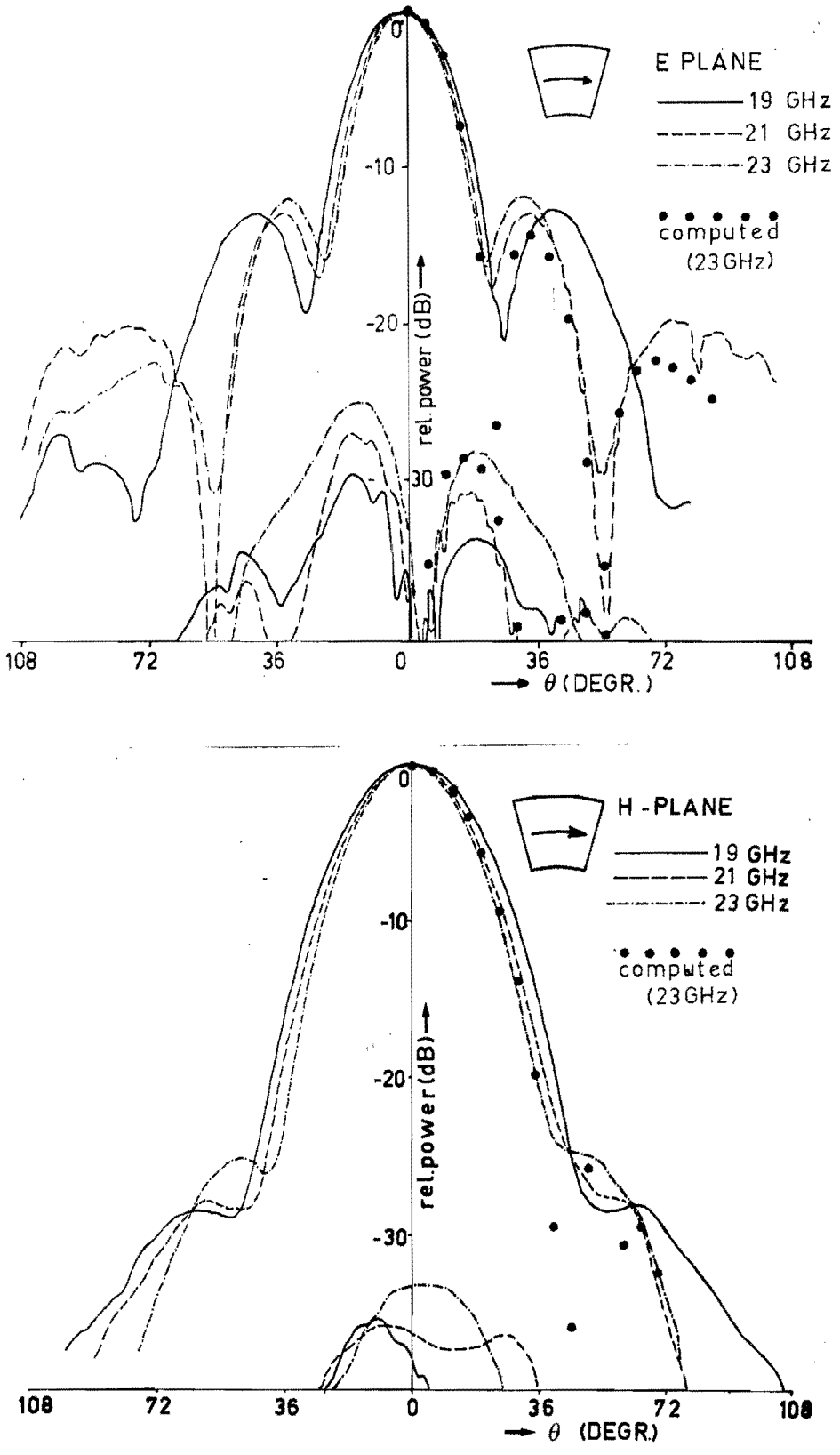

Fig. 4.9. Far field radiation patterns of the antenna A 133, horizontal polarisation.

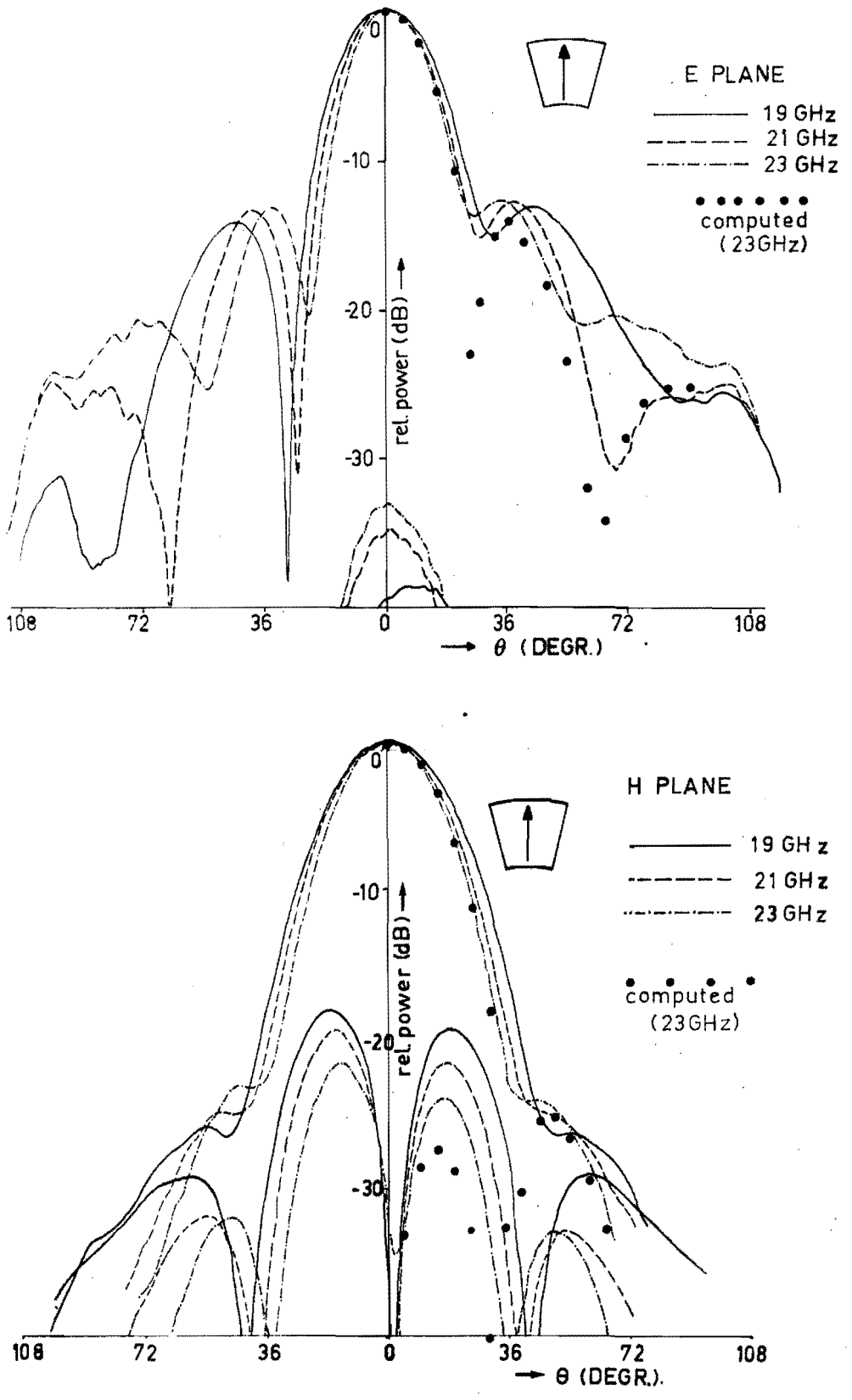

Fig. 4.10. Far field radiation patterns for the antenna A 133, vertical polarisation.

Again, taking into account the inaccuracy in measurements below -30 dB, we find that the measured cross-polarcomponent agrees well with the computed one.

The approximation of the horn aperture fields by waveguide aperture fields implies in the calculation an elliptically polarised far field radiation in the plane of asymmetry (appendix B).
An error has been made since the phase and amplitude distribution over the horn aperture is not the same as that over the waveguide aperture.
Therefore we cannot assume at once that the phasedifference between the components in the plane of asymmetry is exactly 90^0 as it was for the A 132.

The reflected power has been measured (Fig. 4.11) and a good matching of the horn found.

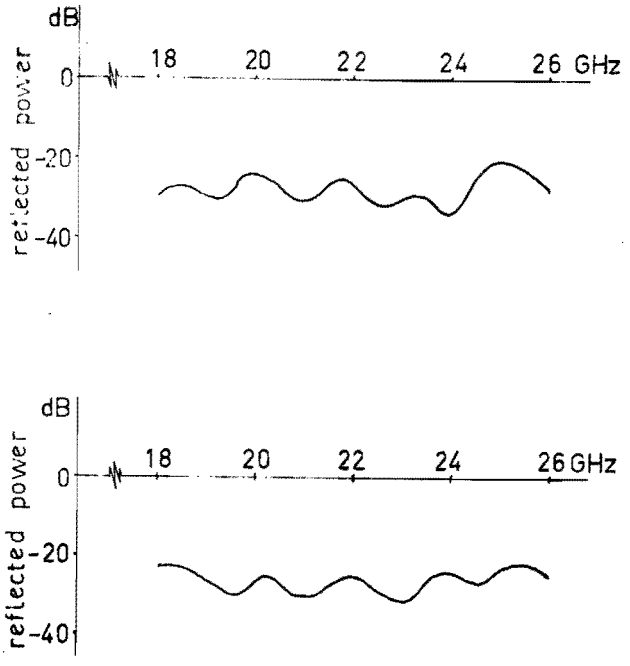

Fig 4.11. Reflected power, A 133.

Chapter V

The biconical segment horn.

In the preceding chapter we discussed the waveguide feed having a coax-segmental geometry. The far-field radiation of this feed was found to be elliptically polarised and hence that the cross-polar lobes of the classical off-set antenna cannot be eliminated. In the present chapter we shall first calculate the electro-magnetic field components in a biconical-segment horn (BSH) and follow that by discussing its applicability in horn paraboloids.
This particular arrangement is called the biconical-segment horn paraboloid (BSHP).
It is the aim of this study to determine the radiation properties of this last named antenna.

5.1 Introduction

There are at present two main types of horn paraboloids, one with a conical horn and one with a pyramidal horn (Figs. 5.1a and 5.1b).
The apex of the horn in this case coincides with the focus of the paraboloid.

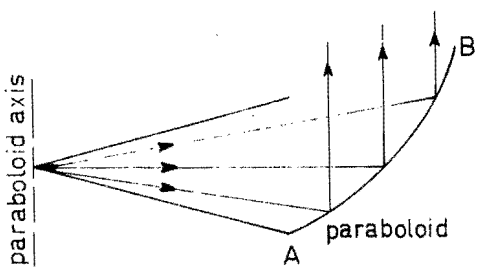

Fig. 5.1a Conical hornreflector.

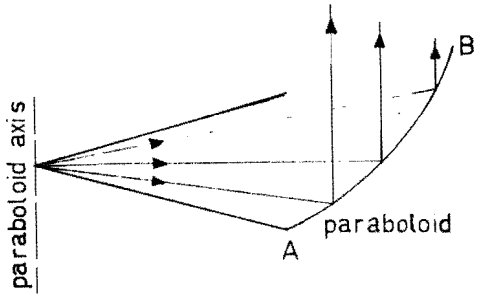

Fig. 5.1b Pyramidal horn-reflector.

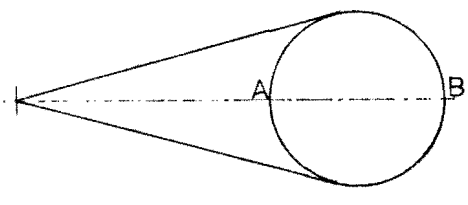

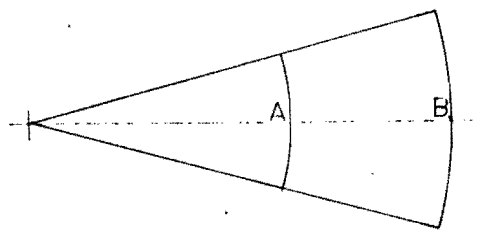

An excellent review of the state of the art is given by Hines, Tingue Li and Turrin [24] and by Crawford, Hogg and Hunt [25]. These antennas are widely used in microwave links. As ground station antennas for satellite communication they are not very suitable, because of the constructional difficulties which arise when such antennas with large apertures are needed.

A horn paraboloid can be considered as an off-set reflector with a large off-set angle $\varphi_0 = 90^\circ$.
It has the advantages of off-set antennas, i.e. no blockage and low V.S.W.R.
Moreover, due to the shielding effect of the horn, the wide-angle sidelobes are at very low levels.
Another advantage is encountered when calculating the aperture fields of a horn paraboloid.
The reflector is positioned in the near field of the spherical horn aperture. We may assume that the field distribution does not change much over the distance between aperture and reflector, and that propagation is along straight lines from the focus to the reflector (geometrical optics). Then the aperture fields are obtained by a simple transformation, as opposed to the classical off-set antenna, where integrals have to be computed (sometimes difficult) in order to obtain the aperture field.

A disadvantage is the high cross-polarisation in the reflector field due to the transformation of the field.
This is shown in Fig. 5.2.

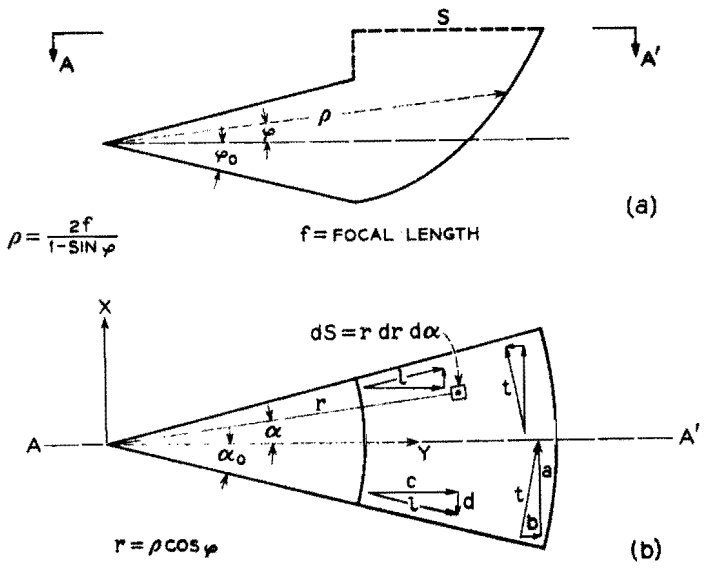

Fig. 5.2 Coordinate system and projected aperture.

The propagating mode is assumed to have a uniform distribution along one coordinate and a cosine distribution along the orthogonal coordinate in the pyramidal horn, just as in a rectangular waveguide. The fields of both polarisation directions can be resolved into components [25] indicated by a,b,c and d. Each of these components can be expressed as follows:

$$E_a = E_o \frac{\rho_o}{\rho} \cos\left(\frac{\pi\varphi}{2\varphi_o}\right) \cos\alpha \,, \qquad (5.1)$$

$$E_b = E_o \frac{\rho_o}{\rho} \cos\left(\frac{\pi\varphi}{2\varphi_o}\right) \sin\alpha \,, \qquad (5.2)$$

$$E_c = E_o \frac{\rho_o}{\rho} \cos\left(\frac{\pi\alpha}{2\alpha_o}\right) \cos\alpha \,, \qquad (5.3)$$

$$E_d = E_o \frac{\rho_o}{\rho} \cos\left(\frac{\pi\alpha}{2\alpha_o}\right) \sin\alpha \,. \qquad (5.4)$$

The components are normalised to E_o, the value of the field at $\rho=\rho_o= 2f$. The flare angles of the horn are indicated by α_o and ϕ_o.
For transversal polarisation E_a and E_b are the respective co-polar and cross-polar components; for longitude polarisation these components are respectively E_c and E_d.
The component E is not equal to zero and has a maximum value for $\alpha=\alpha_o$.
For the far-field radiation pattern of this aperture this implies a cross-polar component, and this can be calculated with (3.47).
For the other polarisation direction the component E_d gives rise to a cross-polar component in the far-field of the aperture.
The radiation patterns of the far-field of such a horn paraboloid [25] are given in Fig. 5.3.
Note the cross-polarisation lobes at a level of -20dB.

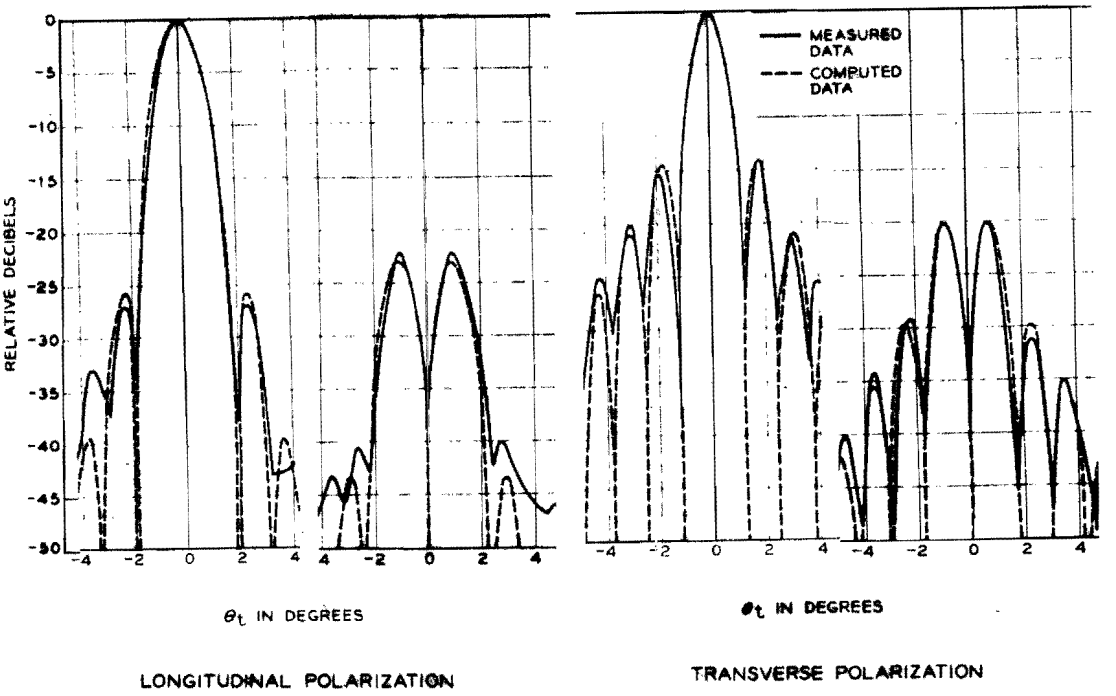

Fig. 5.3 Radiation patterns of a conventional horn reflector plane of asymmetry [25].

We may expect that this cross-polarisation can be eliminated by using a modified horn with aperture-field components which are curved in such a way that, after reflection an aperture field results having parallel field lines. Then the cross-polarisation will be zero in the far-field region.

We try to achieve this by choosing the biconical-segment horn with single-mode excitation.

5.2 The fields in the biconical-segment horn.

The general procedure for obtaining the fields is as follows: we solve the Helmholtz equations (2.13) and (2.16) and, with the solutions for the vector potentials $\underline{A}$ and $\underline{F}$, we can derive the TE and TM modes from [19] the following expressions which are the spherical components of (2.19), (2.20), (2.21) and (2.22) where (2.3) is used, with $\underline{J}=\underline{M}=\underline{o}$.

$$
\begin{aligned}
E_r &= \frac{1}{j\omega\varepsilon_o}\left\{\frac{\partial^2}{\partial r^2}+k^2\right\}A_r \quad , & H_r &= \frac{1}{j\omega\mu_o}\left\{\frac{\partial^2}{\partial r^2}+k^2\right\}F_r \quad , \\
E_\vartheta &= \frac{1}{j\omega\varepsilon_o}\frac{1}{r}\frac{\partial^2 A_r}{\partial r\,\partial\vartheta} - \frac{1}{r\sin\vartheta}\frac{\partial F_r}{\partial\varphi} \quad , & H_\vartheta &= \frac{1}{j\omega\mu_o}\frac{1}{r}\frac{\partial^2 F_r}{\partial r\,\partial\vartheta} + \frac{1}{r\sin\vartheta}\frac{\partial A_r}{\partial\varphi} \quad , \\
E_\varphi &= \frac{1}{j\omega\varepsilon_o}\frac{1}{r\sin\vartheta}\frac{\partial^2 A_r}{\partial r\,\partial\varphi} + \frac{1}{r}\frac{\partial F_r}{\partial\vartheta} \quad , & H_\varphi &= \frac{1}{j\omega\mu_o}\frac{1}{r\sin\vartheta}\frac{\partial^2 F_r}{\partial r\,\partial\varphi} - \frac{1}{r}\frac{\partial A_r}{\partial\vartheta} \quad . \qquad (5.1)
\end{aligned}
$$

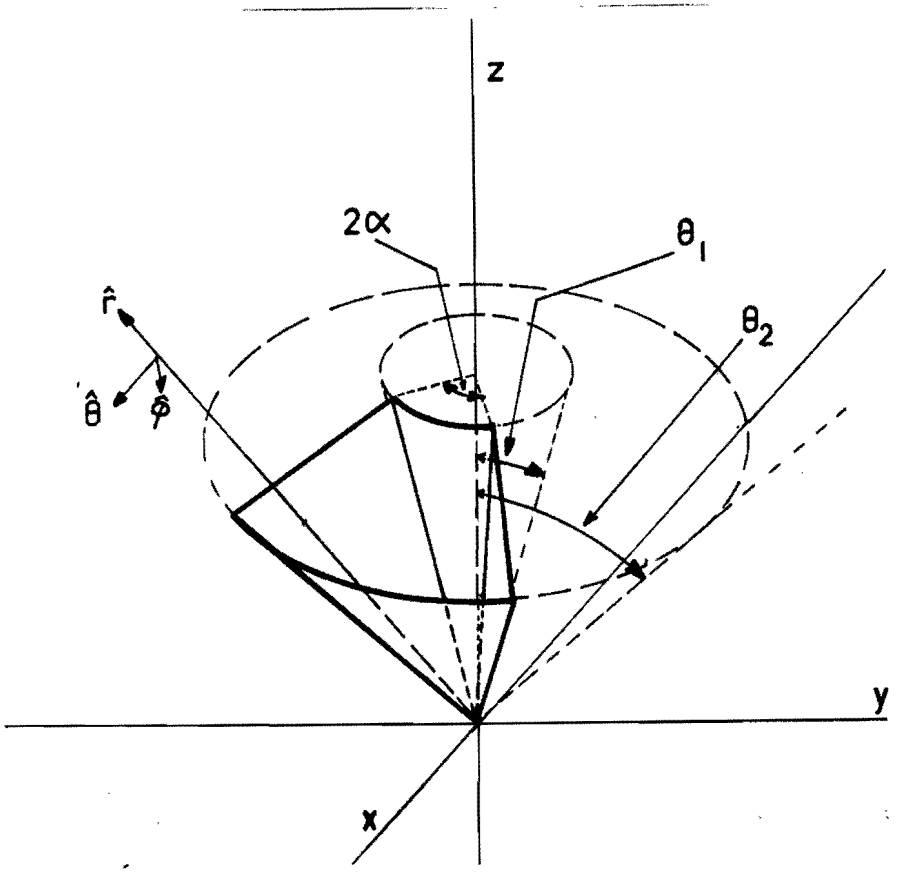

Fig. 5.4 Geometry of the biconical-segment horn (BSH).

The vector potentials $\underline{A}$ and $\underline{F}$ have only radial components, thus $\underline{A}=A_r\hat{r}$ and $\underline{F}=F_r\hat{r}$.
Next, we shall consider only TE modes so that we only need $\underline{F}$, the magnetic vector potential.

The solution of F_r is [19]

$$(F_r)_{\mu\nu} = \left\{A_1 P_\nu^\mu(\cos\vartheta) + B_1 Q_\nu^\mu(\cos\vartheta)\right\} \hat{H}_\nu^{(2)}(kr)\left\{C_1\cos(\mu\varphi) + D_1\sin(\mu\varphi)\right\}. \qquad (5.2)$$

As $\vartheta=0$ and $\vartheta=\pi$ are excluded from the field region, we need both the legendre functions $P_\nu^\mu(\cos\vartheta)$ and $Q_\nu^\mu(\cos\vartheta)$.
$\hat{H}_\nu^{(2)}(kr)$ is the spherical Hankel function of the second kind and order ν, and represents an outward travelling wave.
In general, μ is not restricted to integer values; however, in the following calculations we have only used integer values for μ.

Substituting (5.2) in (5.1) we obtain the following expressions for the TE-mode:

$$\left.\begin{aligned}
E_r &= 0\\
E_\vartheta &= \frac{-1}{r\sin\vartheta}\left\{A_1 P_\nu^\mu(\cos\vartheta) + B_1 Q_\nu^\mu(\cos\vartheta)\right\}\hat{H}_\nu^{(2)}(kr)\left\{-\mu C_1\sin(\mu\varphi) + \mu D_1\cos(\mu\varphi)\right\}\\
E_\varphi &= \frac{1}{r}\left\{A_1\frac{dP_\nu^\mu(\cos\vartheta)}{d\vartheta} + B_1\frac{dQ_\nu^\mu(\cos\vartheta)}{d\vartheta}\right\}\hat{H}_\nu^{(2)}(kr)\left\{C_1\cos(\mu\varphi) + D_1\sin(\mu\varphi)\right\}
\end{aligned}\right\} \qquad (5.3)$$

$$
\begin{aligned}
Z_0 H_r &= \frac{\nu(\nu+1)}{jkr^2}\left\{ A_1 P_\nu^\mu(\cos\vartheta) + B_1 Q_\nu^\mu(\cos\vartheta) \right\} \hat{H}_\nu^{(2)}(kr)\left\{ C_1\cos(\mu\varphi) + D_1\sin(\mu\varphi)\right\}, \\
Z_0 H_\vartheta &= \frac{1}{jk\mu_0}\frac{1}{r}\left\{ A_1 \frac{dP_\nu^\mu(\cos\vartheta)}{d\vartheta} + B_1 \frac{dQ_\nu^\mu(\cos\vartheta)}{d\vartheta}\right\} \hat{H}_\nu^{(2)}(kr)\left\{ C_1\cos(\mu\varphi) + D_1\sin(\mu\varphi)\right\}, \\
Z_0 H_\varphi &= \frac{1}{jk\mu_0}\frac{1}{r\sin\vartheta}\left\{ A_1 P_\nu^\mu(\cos\vartheta) + B\, Q_\nu^\mu(\cos\vartheta)\right\} \hat{H}_\nu^{(2)}(kr)\left\{ -\mu C_1\sin(\mu\varphi) + \mu D_1\cos(\mu\varphi)\right\}.
\end{aligned}
\tag{5.3}
$$

5.3 The boundary conditions, the dispersion relation

The boundaries of the BSH are an inner- and outer-cone at $\vartheta=\vartheta_1$ and $\vartheta=\vartheta_2$ respectively, and two planes, viz. $\phi=\alpha$ and $\phi=-\alpha$.

Applying the boundary conditions:

$$E_\vartheta(\varphi=\alpha) = E_\vartheta(\varphi=-\alpha) = 0, \tag{5.4}$$

$$E_\varphi(\vartheta=\vartheta_1) = E_\varphi(\vartheta=\vartheta_2) = 0, \tag{5.5}$$

we are able to determine μ and ν.

Substitution of $\phi=\alpha$ and $\phi=-\alpha$ in (5.3) yields:

$$-\mu C_1\sin(\mu\alpha) + \mu D_1\cos(\mu\alpha) = 0, \tag{5.6}$$

$$\mu C_1\sin(\mu\alpha) + \mu D_1\cos(\mu\alpha) = 0, \tag{5.7}$$

with a non-trivial solution if the determinant is equal to zero. We get:

$$2\sin(\mu\alpha)\cos(\mu\alpha) = 0, \tag{5.8}$$

or

$$\mu = m\frac{\pi}{2\alpha} \quad \text{with} \quad m = 0, 1, 2, 3\ldots \tag{5.9}$$

The solution for which m=0 needs to be considered separately; for the latter there is only an E_ϕ component, the E_ϑ component vanishes as can be seen from (5.3).
In that case, we have a field which is ϕ-independent and the choice of α can be arbitrary. Here the indicator m labels the values of μ in ascending value.
Since we have chosen our coordinate system such that the x-axis is a symmetry axis, we have either $C_1=0$ or $D_1=0$ owing to symmetric properties and depending on the value of μ. For instance

m=odd implies $C_1=0$ and m=even implies $D_1=0$.
If we apply (5.5) we obtain from (5.3):

$$\left\{ A_1 \frac{d P_\nu^\mu(\cos\vartheta)}{d\vartheta} + B_1 \frac{d Q_\nu^\mu(\cos\vartheta)}{d\vartheta} \right\}_{\vartheta=\vartheta_1} = 0, \qquad (5.10)$$

$$\left\{ A_1 \frac{d P_\nu^\mu(\cos\vartheta)}{d\vartheta} + B_1 \frac{d Q_\nu^\mu(\cos\vartheta)}{d\vartheta} \right\}_{\vartheta=\vartheta_2} = 0, \qquad (5.11)$$

With a non-trivial solution when the determinant is equal to zero,

$$\left[\frac{d P_\nu^\mu(\cos\vartheta)}{d\vartheta}\right]_{\vartheta=\vartheta_1}\left[\frac{d Q_\nu^\mu(\cos\vartheta)}{d\vartheta}\right]_{\vartheta=\vartheta_2} - \left[\frac{d P_\nu^\mu(\cos\vartheta)}{d\vartheta}\right]_{\vartheta=\vartheta_2}\left[\frac{d Q_\nu^\mu(\cos\vartheta)}{d\vartheta}\right]_{\vartheta=\vartheta_1} = 0 \qquad (5.12)$$

For given values of ϑ_1 and ϑ_2 the dispersion equation (5.12) has an infinite number of solutions for ν. They are labeled with integer n according to their increasing value.

Now we characterise the TE_{mn} mode in a BSH with its two integers m and n.
We have solved equation (5.12) numerically for several combinations of ϑ_1 and ϑ_2. As we are only interested in the lowest possible TE modes we have calculated the smallest ν-values for m=0 and the smallest-but-one ν values for m=1. For α we have to choose particular values to obtain μ as an integer. We have chosen $\alpha=30^\circ$ and $22^\circ30'$ corresponding to $\mu=3$ and $\mu=4$ respectively.
The results are given in tables:

- Table 5.1 The ν-values for the TE_{01} mode.
- Table 5.2 The ν-values for the TE_{11}- and TE_{12}-mode in a BSH with $\alpha=30^\circ$
- Table 5.3 The ν-values for the TE_{11}-and TE_{12}-mode in a BSH with $\alpha=22^\circ30'$.

From (5.10) we obtain the following relation between the constants A_1 and B_1.

$$B_1/A_1 = -\left[\frac{d P_\nu^\mu(\cos\vartheta)}{d\vartheta} \Big/ \frac{d Q_\nu^\mu(\cos\vartheta)}{d\vartheta}\right]_{\vartheta=\vartheta_1 \text{ or } \vartheta=\vartheta_2} = -L_\mu. \qquad (5.13)$$

		θ_1				
		25^o	30^o	35^o	40^o	45^o
θ_2	30^o	.....	.....	.....	.....	.....
		.....	.....	.....	.....	.....
	35^o	16.7147	.....	.....	.....	.....
		.....	.....	.....	.....	.....
	40^o	11.6099	.....	16.9447	.....	.....
		.....	.....	.....	.....	.....
	45^o	8.6294	11.5851	14.9927	17.0617	.....
		.....	.....	.....	.....	.....
	50^o	6.8447	8.6024	11.5689	16.0525	16.0100
		.....	.....	.....	.....	.....
	55^o	5.6568	6.8165	8.5842	11.5576	14.9931
		.....	.....	.....	.....	.....
	60^o	4.8094	5.6283	6.7973	8.5716	8.5626
		.....	.....	.....	.....	.....
	70^o	3.8617	4.1471	4.7641	5.5945	6.7739
		.....	.....	.....	.....	.....
	75^o	3.2878	3.6549	4.1275	4.7472	5.5843
		.....	.....	.....	.....	.....
	80^o	3.0001	3.2620	3.6358	4.1134	4.7368
		.....	.....	.....	.....	.....

Table 5.1 The ν values for μ=0.

θ_2	θ_1 25°	30°	35°	40°	45°
30°	1.9844	.....	.....	.....	.....
	6.0250	.....	.....	.....	.....
35°	1.9794	1.9771	.....	.....	.....
	5.5412	5.1116	.....	.....	.....
40°	1.9727	1.9708	1.9675	.....	.....
	5.1275	4.7699	4.4573	.....	.....
45°	1.9639	1.9623	1.9594	1.9548	.....
	4.7625	4.4754	4.2060	3.9716	.....
50°	1.9523	1.9510	1.9485	1.9444	1.9378
	4.4371	4.2153	3.9882	3.7816	3.6019
55°	1.9374	1.9363	1.9340	1.9301	1.9241
	4.1479	3.9825	3.7961	3.6166	3.4558
60°	1.9176	1.9166	1.9146	1.9110	1.9053
	3.8934	3.7736	3.6245	3.4714	3.3289
65°	1.8908	1.8899	1.8881	1.8847	1.8792
	3.6726	3.5871	3.4708	3.3426	3.2180
70°	1.8533	1.8524	1.8507	1.8475	1.8423
	3.4833	3.4229	3.3336	3.2281	3.1206
75°	1.7972	1.7965	1.7948	1.7918	1.7867
	3.3230	3.2801	3.2123	3.1268	3.0352
80°	1.7035	1.7028	1.7013	1.6983	1.6932
	3.1890	3.1583	3.1069	3.0384	2.9610

Table 5.2 The ν-values for $\mu=3$.

θ_2	θ_1 25°	30°	35°	40°	45°
30°	2.9881	.....	.....	.....	.....
	8.1877	.....	.....	.....	.....
35°	2.9840	2.9825	.....	.....	.....
	7.5325	6.9686	.....	.....	.....
40°	2.9738	2.9773	2.9750	.....	.....
	6.9555	6.5080	6.0949	.....	.....
45°	2.9708	2.9701	2.9684	2.9652	.....
	6.4324	6.1025	5.7569	5.4457	.....
50°	2.9609	2.9604	2.9591	2.9565	2.9519
	5.9603	5.7350	5.5595	5.1905	4.9514
55°	2.9480	2.9475	2.9466	2.9444	2.9404
	5.5439	5.3994	5.1914	4.9664	4.7557
60°	2.9067	2.9065	2.9057	2.9041	2.9008
	5.1851	5.0960	4.9469	4.7657	4.5835
65°	2.9067	2.9065	2.9057	2.9041	2.9008
	4.8814	4.8273	4.7247	4.5844	4.4313
70°	2.8726	2.8724	2.8718	2.8703	2.8673
	4.5944	4.5944	4.4205	4.4205	4.2956
75°	2.8209	2.8207	2.8201	2.8188	2.9160
	4.4170	4.3966	4.3508	4.2741	4.1747
80°	2.7330	2,7329	2.7324	2.7331	2.7285
	4.2429	4.2320	4.2013	4.1461	4.0686

Table 5.3 The ν-values for $\mu=4$.

5.4 The aperture fields.

Substituting the results of the preceding paragraph in the expression (5.3) we obtain the TE modes in a BSH.
We distinguish two cases, relevant for us, with m=0 and m=1 respectively.
For m=0 we obtain:

$$
\begin{aligned}
&E_r = E_\vartheta = 0, \\
&E_\varphi = E_0 \frac{1}{r}\left\{\frac{dP_\nu^0(\cos\vartheta)}{d\vartheta} - L_0 \frac{dQ_\nu^0(\cos\vartheta)}{d\vartheta}\right\} \hat{H}_\nu^{(2)}(kr), \\
&Z_0 H_r = \frac{\nu(\nu+1)}{jkr^2} E_0 \left\{P_\nu^0(\cos\vartheta) - L_0 Q_\nu^0(\cos\vartheta)\right\} \hat{H}_\nu^{(2)}(kr), \\
&Z_0 H_\vartheta = \frac{1}{j\omega\mu_0}\frac{1}{r} E_0 \left\{\frac{dP_\nu^0(\cos\vartheta)}{d\vartheta} - L_0 \frac{dQ_\nu^0(\cos\vartheta)}{d\vartheta}\right\} \frac{d\hat{H}_\nu^{(2)}(kr)}{dr}, \\
&Z_0 H_\varphi = 0.
\end{aligned}
\qquad (5.14)
$$

Here L_0 denotes the constant given by (5.13) for m=0.
For m=1 we obtain the following expressions:

$$
\begin{aligned}
&E_r = 0, \\
&E_\vartheta = \frac{-1}{r\sin\vartheta} E_1 \left\{P_\nu^\mu(\cos\vartheta) - L_\mu Q_\nu^\mu(\cos\vartheta)\right\} \hat{H}_\nu^{(2)}(kr)\, \mu \cos(\mu\varphi), \\
&E_\varphi = \frac{1}{r} E_1 \left\{\frac{dP_\nu^\mu(\cos\vartheta)}{d\vartheta} - L_\mu \frac{dQ_\nu^\mu(\cos\vartheta)}{d\vartheta}\right\} \hat{H}_\nu^{(2)}(kr) \sin(\mu\varphi), \\
&Z_0 H_r = \frac{\nu(\nu+1)}{jkr^2} E_1 \left\{P_\nu^\mu(\cos\vartheta) - L_\mu Q_\nu^\mu(\cos\vartheta)\right\} \hat{H}_\nu^{(2)}(kr) \sin(\mu\varphi), \\
&Z_0 H_\varphi = \frac{1}{j\omega\mu_0}\frac{1}{r} E_1 \left\{\frac{dP_\nu^\mu(\cos\vartheta)}{d\vartheta} - L_\mu \frac{dQ_\nu^\mu(\cos\vartheta)}{d\vartheta}\right\} \frac{d\hat{H}_\nu^{(2)}(kr)}{dr} \sin(\mu\varphi), \\
&Z_0 H_\vartheta = \frac{1}{j\omega\mu_0}\frac{1}{r\sin\vartheta} E_1 \left\{P_\nu^\mu(\cos\vartheta) - L_\mu Q_\nu^\mu(\cos\vartheta)\right\} \frac{d\hat{H}_\nu^{(2)}(kr)}{dr}\, \mu \cos(\mu\varphi).
\end{aligned}
\qquad (5.15)
$$

In the expression (5.15) L_1 denotes a constant given by (5.13) for m=1.
The value of μ depends on the value of the angle α.
For m=1 we find that $\mu=3$ for $\alpha=30^\circ$ while $\mu=4$ for $\alpha=22^\circ 30'$.

The expressions (5.14) indicate that the TE_{on} modes have only an E_ϕ component.
Owing to this property the choice of α has no influence on the field configuration of these modes.

We have made calculations for the amplitude of the E_ϕ component of the TE_{01} mode in a BSH.
This has been done as shown for different values of ϑ_1 and ϑ_2 (Fig. 5.5). We remark that only the dependence in the ϑ-direction is represented, since the amplitude shows no variation in the ϕ direction.
For a small value of the difference between ϑ_1 and ϑ_2 the curvature becomes almost that of a cosine.

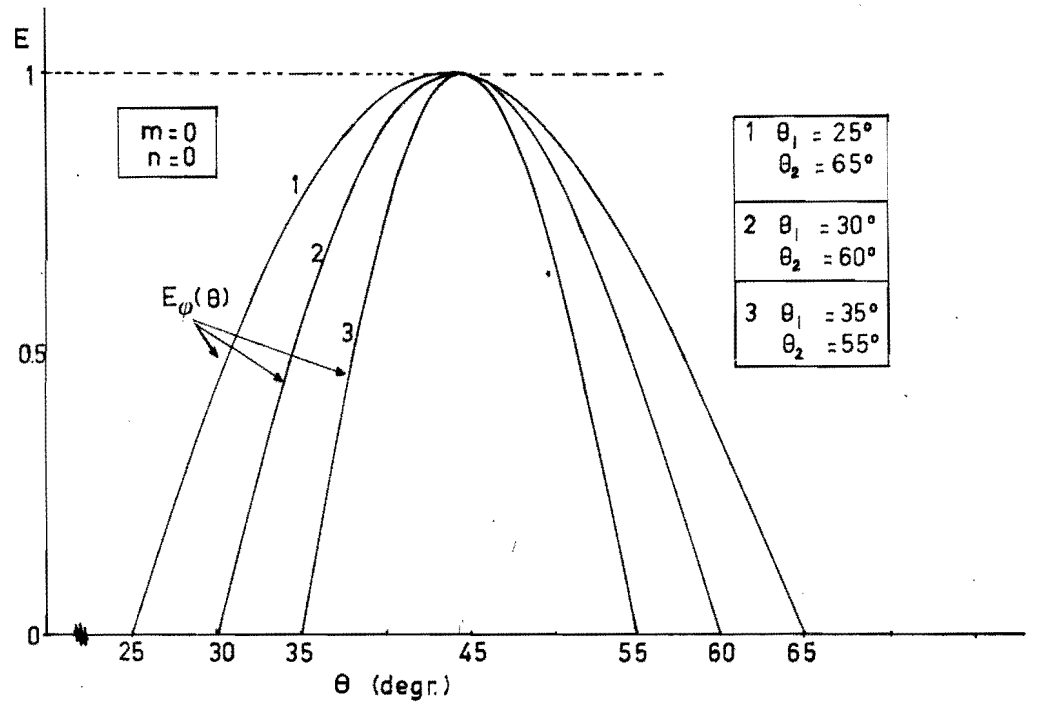

Fig. 5.5 The amplitude of the TE_{01} mode normalised at its maximal value.

The expressions in (5.15) are more complex.
It cannot be seen directly from the formulas that the E_ϑ component is large compared with the E_ϕ component.

We have therefore computed the components of the TE_{11} and the TE_{12} mode numerically for two values of α, viz $\alpha=30$ and $\alpha=22\ 30'$. For $\alpha=30$, thus $\mu=3$, the amplitude of the TE_{11} components normalised to their max. is represented in Fig. 5.6.
Here E_ϑ is given as a function of ϑ for $\phi=0$ and E_ϕ as a function of ϑ for $\phi=\alpha$. Both components are thus calculated for those values of ϕ where they are maximum.
We observe a rather steep envelope of $E_\vartheta(\vartheta)$. This will give rise to a great difference between this E_ϑ progression and the uniform distribution of the field which excites the BSH.

(The TE_{11} in a circular or TE_{01} mode in a rectangular waveguide). A more uniform field distribution as a function of ϑ has the TE_{12} mode. The amplitude diagrams of the components normalised to the maximum value of E_ϑ are shown in Fig. 5.7.

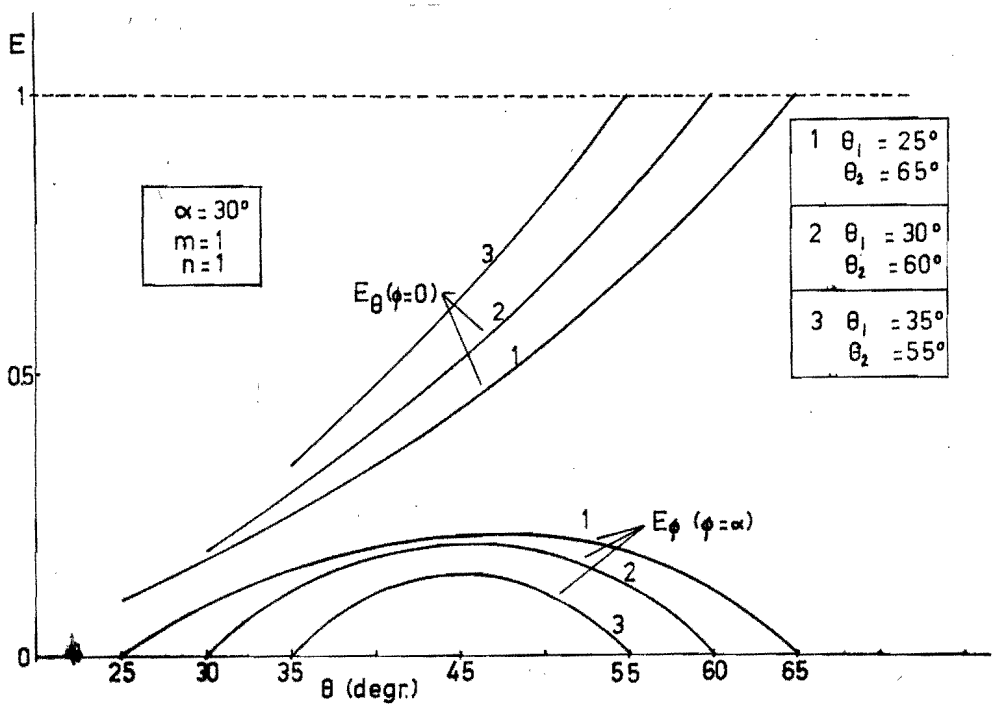

Fig. 5.6 Aperture fields TE_{11} mode, $\alpha = 30^o$

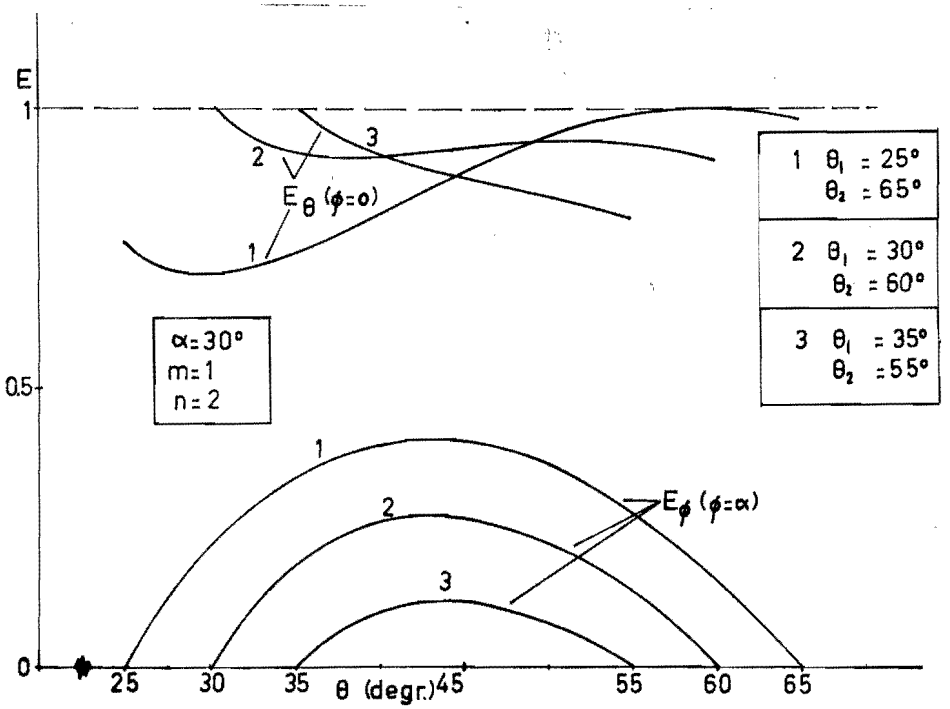

Fig. 5.7 Aperture fields TE_{12} mode, $\alpha = 30^\circ$.

The same calculations have been carried out for an angle $\alpha = 22^\circ 30'$ thus $\mu = 4$, another BSH. The results are given in Fig. 5.8 and 5.9 for the TE_{11}- and TE_{12} mode, respectively.

From the calculations can be concluded that, for a small difference between ϑ_1 and ϑ_2, the E_ϑ component of the TE_{12} mode has a nearly uniform envelope whereas the E_ϕ component has an amplitude which is much smaller than that of the corresponding E_ϑ component.

As is found by comparison of Fig 5.6 with Fig. 5.8, the E component of the TE_{12} mode becomes smaller if α is large. Then the E component becomes more uniform.

For large values of α and a small difference between ϑ_1 and ϑ_2 it is thus possible to create two aperture fields for two different polarisations which are nearly orthogonal in the horn aperture. One field has only an E_ϕ component (TE_{01} mode) and the other has an E_ϑ component and only a very small E_ϕ component.

In the next paragraph we shall discuss the design of horn paraboloids with the BSH as a feed.

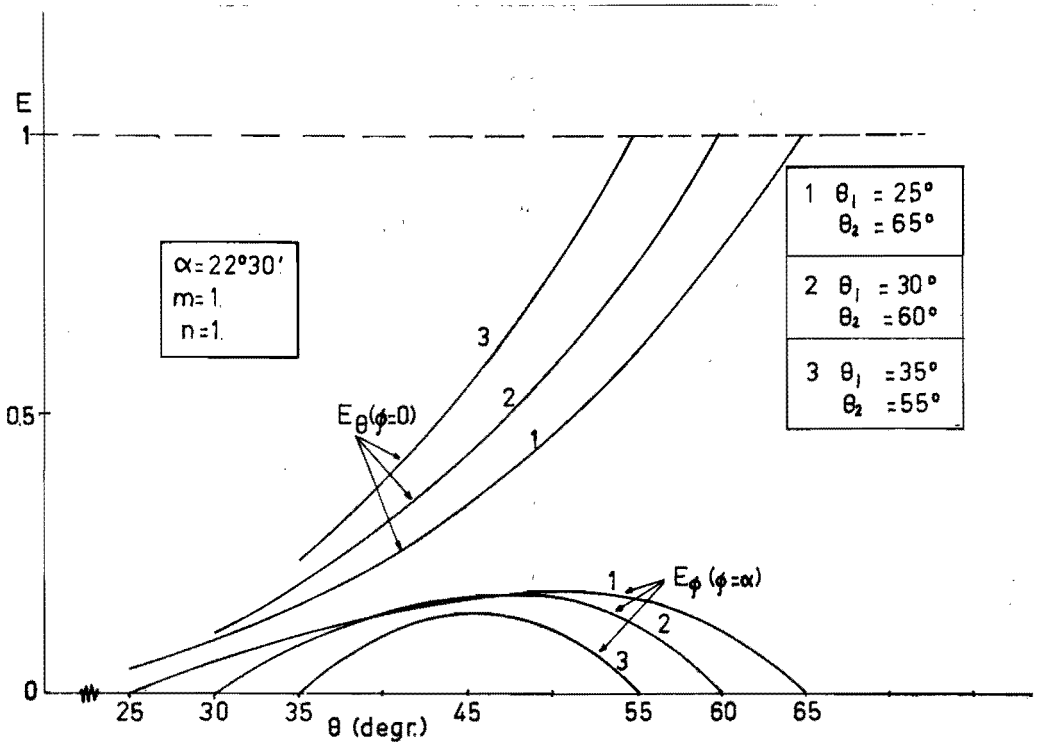

Fig. 5.8 Aperture field TE_{11} mode, $\alpha = 22^{\circ}30'$.

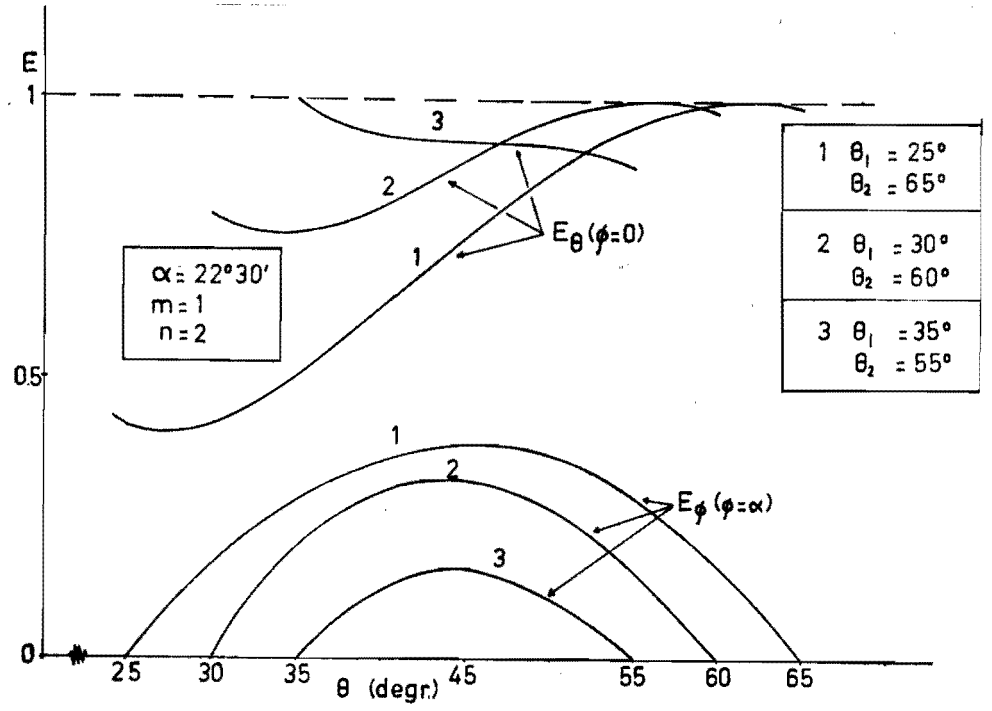

Fig. 5.9 Aperture field TE_{12} mode, $\alpha = 22^{\circ}30'$.

5.5 The biconical-segment horn paraboloid.

By using the biconical-segment horn as a feed in a horn paraboloid, we get the biconical-segment horn paraboloid. (= BSHP),(Fig. 5.10)

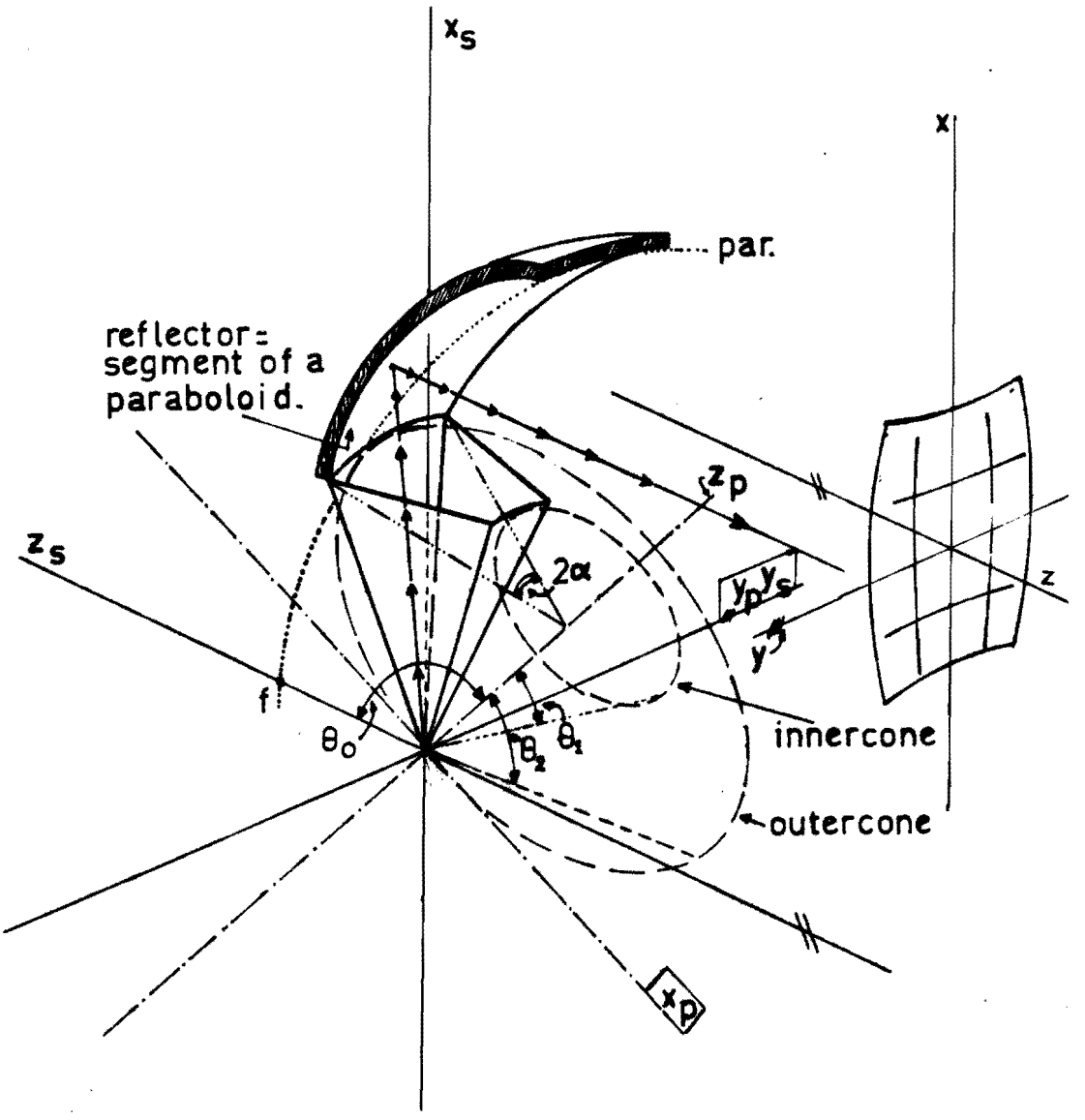

Fig. 5.10 Geometry of the biconical segment horn paraboloid.

The coordinate systems for the description of the BSHP are the same as those used for the classical off-set reflector antenna. (see chapter III).

Thus we have an $(x_p y_p z_p)$ system for the feed description, an $(x_s y_s z_s)$ system for the paraboloid of revolution with the apex in $z_s = f$, and an $(x\ y\ z)$ system for the far-field radiation of the BSHP.

The coordinate transformations are given in chapter III. The off-set angle is defined as the angle θ_0 between the z_p and the z_s axis.

Normally, the horn paraboloids have an off-set angle $\theta_0 = 90^0$. Since the BSH radiates maximally in a direction described by θ_{mp}, where θ_{mp} is about $(\theta_1 + \theta_2)/2$, the off-set angle of a BSHP will have a value $\theta_0 = 90^0 + \theta_{mp}$.

If we project the intersections of the boundary surfaces of the BSH with the paraboloid on the $x_s y_s$ plane we get the contourline of the aperture of the BSHP.

These surfaces are the cones $\theta_p = \theta_1$ and $\theta_p = \theta_2$ and the planes $\phi_p = +\alpha$ and $\phi_p = -\alpha$.

Generally, cones and planes described by $\theta_p = \theta_c$ and $\phi_p = \phi_c$, respectively yield projections of such intersections on the $x_s y_s$ plane which are given by the following formulas. (see appendix A).

For a cone described by $\theta_p = \theta_c$ we get

$$\left(x_s - 2f\frac{\sin\vartheta_0}{\cos\vartheta_0+\cos\vartheta_c}\right)^2 + y_s^2 = 4f^2\frac{\sin^2\vartheta_c}{(\cos\vartheta_0+\cos\vartheta_c)^2}. \qquad (5.16)$$

and for a plane $\phi_p = \phi_c$ we have

$$\left(x_s + 2f\frac{1}{\tan\vartheta_0}\right)^2 + \left(y_s - 2f\frac{1}{\sin\vartheta_0\tan\varphi_c}\right)^2 = 4f^2\left(\frac{1}{\sin\vartheta_0\sin\varphi_c}\right)^2. \qquad (5.17)$$

Substitution of $\theta_c = \theta_1$ and $\theta_c = \theta_2$ in (5.16) and $\phi_c = +\alpha$ and $\phi_c = -\alpha$ in (5.17) gives the contour line of the aperture; note that the $x_s y_s$ plane is parallel to the aperture plane as can be seen from Fig. 5.10

Substitution of $\theta_c = \theta_p$ and $\phi_c = \phi_p$ in (5.16) and (5.17) respectively, makes it possible to calculate projections of various cones and planes.

The images of $E\phi_p$ components on the aperture plane are directed along the projections given by (5.16).

The images of $E_{\theta p}$ components on the aperture plane are directed along the projections given by (5.17).

Considering (5.16), we note that this projection becomes a straight line if

$$\cos \vartheta_c = -\cos \vartheta_o . \qquad (5.18)$$

It is found from 5.17 that a straight line occurs for $\phi_c = 0^0$ or 180^0. This is the symmetry plane of the off-set system.

We should now recall formulas (3.12) and (3.13) which, in the secondary system $(x_s y_s z_s)$ describe the aperture field components. These formulas are:

$$E_{axs} = \frac{1}{t}\left\{\left[\sin\vartheta_p \sin\vartheta_o - \cos\varphi_p (1+\cos\vartheta_p \cos\vartheta_o)\right] E_{f\vartheta} + \right.$$
$$\left. + \left[\sin\varphi_p (\cos\vartheta_o + \cos\vartheta_p)\right] E_{f\varphi}\right\}, \qquad (3.12)$$

$$E_{ays} = \frac{1}{t}\left\{\left[-\sin\varphi_p (\cos\vartheta_o + \cos\vartheta_p)\right] E_{f\vartheta} + \right.$$
$$\left. + \left[\sin\vartheta_p \sin\vartheta_o - \cos\varphi_p (1+\cos\vartheta_p \cos\vartheta_o)\right] E_{f\varphi}\right\}. \qquad (3.13)$$

The above formulas can also be used to calculate the aperture field of the horn reflector.

We read the formulas with $\theta_p = \theta_c$ and $\phi_p = \phi_c$.

The primary field components $E_{f\theta}$ and $E_{f\phi}$ lie respectively in planes $\phi_p = \phi_c$ or on cones $\theta_p = \theta_c$.

If we have a feed with an aperture distribution with only an $E_{f\phi}$ component then from (3.12) and (3.13) we get an aperture field with only an E_{ays} component if equation 5.18 is satisfied.
This is the case for $\theta_c = 180^0 - \theta_0$.

A feed with only an $E_{f\theta}$ component in its aperture only yields an E_{axs} component with (3.12) and (3.13), if (5.18) is satisfied.

For both cases this implies a zero cross-polarisation in the plane of asymmetry of the reflector.

Our biconical-segment horn only has an $E_{f\phi}$ component for a particular polarisation (TE_{0n}).

For another polarisation there is an $E_{f\theta}$ component and a small $E_{f\phi}$ component (relative to $E_{f\theta}$). The condition (5.18) is satisfied for $\theta_c = \theta_{mp} = \frac{\theta_1+\theta_1}{2}$ in our model.

For the BSHP the result is that in the aperture the cross-polar component is zero along the y_s axis, if a TE_{0n} mode is used.
If a feed with only an $E_{f\theta}$ component is used (the BSH approximates this case if a sum of two modes is used to create such an aperture field) the cross-polarisation will also be zero along the y_s axis in the aperture (plane of asymmetry). Along the negative x_s axis (image of $\phi_c = 180^0$) the cross-polar component is equal to zero too (for both such polarisations) owing to the symmetry of the system.

We have calculated (5.16) and (5.17) for such a model with the following data:

$$\theta_1 = 25^0 , \qquad f = 100 \text{ mm},$$

$$\theta_2 = 65^0 , \qquad \theta_0 = 135^0.$$

$$\alpha = 30^0 ,$$

In Fig. 5.11 the images of ϕ_c = constant and θ_c = constant on the $x_s y_s$-plane are represented. The values of θ_c and ϕ_c are taken in the $(x_D y_D z_D)$ system.

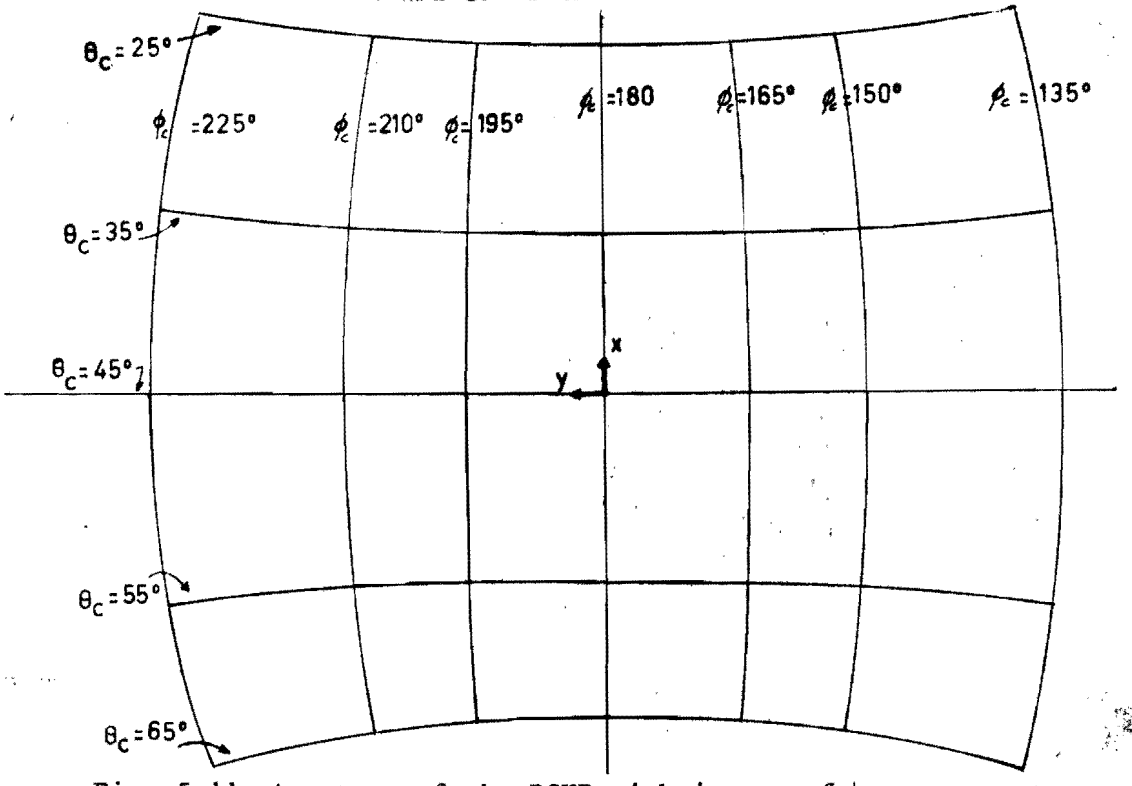

Fig. 5.11 Aperture of the BSHP with images of ϕ_c = constant and θ_c = constant.

Note that only the planes given by $180^0 - \alpha < \phi_c < 180^0 + \alpha$ are of interest; the symmetry-plane is given by $\phi_c = 180^0$. (See Fig. 5.10).

The aperture fields can be calculated from (3.12) and (3.13) with the proviso the spatial attenuation should be taken into account.
This attenuation goes inversely with the distance from the focus to the paraboloid.

From the formulas (3.12) and (3.13) we have derived how the cross-polar component behaves if we only take into account the depolarisation due to the curvature of the reflector. Then we get a depolarisation factor D given by

$$D = 20\,{}^{10}\log \left| \frac{\sin\varphi_p (\cos\vartheta_p + \cos\vartheta_0)}{\sin\vartheta_p \sin\vartheta_0 - \cos\varphi_p (1 + \cos\vartheta_p \cos\vartheta_0)} \right| . \qquad (5.19)$$

We have calculated (5.19) for several values of θ_p, (Fig. 5.12) with $\theta_0 = 135^0$.

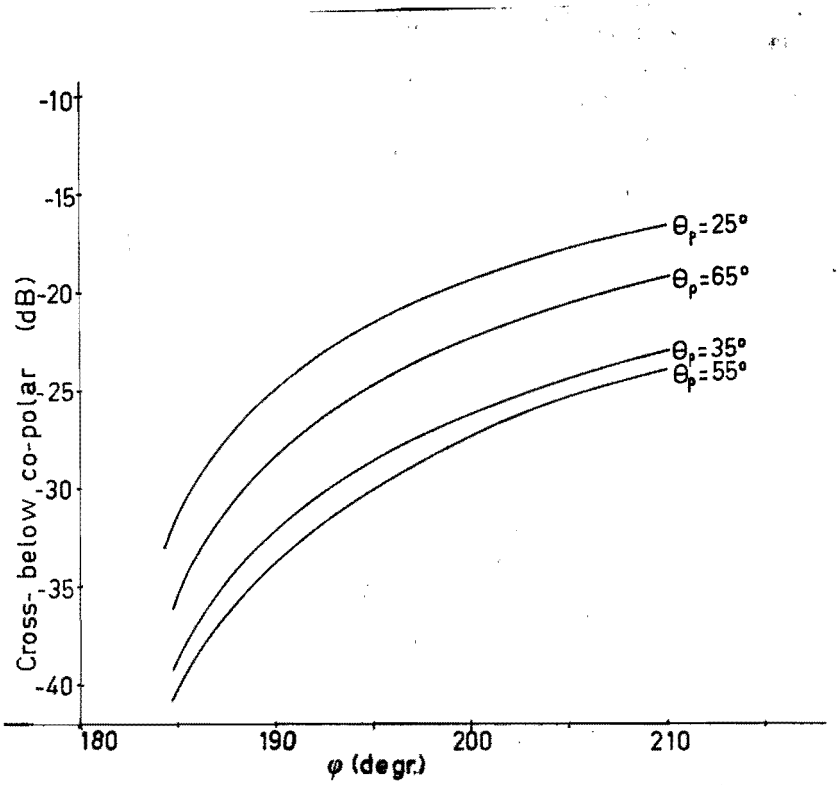

Fig. 5.12 The cross-polarisation below co-polarisation.

The far field radiation pattern can be calculated with the formulas (3.46) and (3.47) from the aperture distribution of the biconical segment horn paraboloid. These formulas are recalled here:

$$\underline{E}_1(\underline{r}) = -jk\,\frac{e^{-jkr}}{4\pi r}\,(1+\cos\vartheta)\left\{-\cos\varphi\,\hat{\vartheta} + \sin\varphi\,\hat{\varphi}\right\}\int_{S_A} E_{ax}\,e^{jk(\underline{r}'\cdot\hat{r})}\,dS', \tag{3.46}$$

$$\underline{E}_2(\underline{r}) = -jk\,\frac{e^{-jkr}}{4\pi r}\,(1+\cos\vartheta)\left\{\sin\varphi\,\hat{\vartheta} + \cos\varphi\,\hat{\varphi}\right\}\int_{S_A} E_{ay}\,e^{jk(\underline{r}'\cdot\hat{r})}\,dS', \tag{3.47}$$

where S_A should be taken as shown in Fig. 5.10, with the boundaries $\theta_p = \theta_1$, $\theta_p = \theta_2$ and $\phi_p = 180^0 - \alpha$, $\phi_p = 180^0 + \alpha$.

5.6. Experimental investigation of the far field radiation characteristics of a biconical segment horn paraboloid.

We have investigated a model of the BSHP with the following dimensions.

Antenna

reg. nr.	θ_1	θ_2	α	focal length
A 134	25^0	65^0	30^0	f = 100 mm.

Table 5.4.

The dimensions are chosen in such a way that measurements can be carried out in the anechoic chamber. The aperture of the BSHP has almost a square cross-section; the maximum dimension is about 10λ.

The co- and cross-polar components in both principal planes are recorded for both polarisation directions. This has been done for four frequencies in the K-band; the patterns are shown in Figs. 5.12, 5.13, 5.14 and 5.15.

We shall refer to the polarisation directions as "horizontal" and "vertical".
"Horizontal" corresponds to the TE_{01} mode and "vertical" to the TE_{12} mode.
From Figs 5.12 and 5.13 it is found that the cross-polar component is below -30 dB for the horizontal polarisation. This low level can easily be achieved even with reflectors small in terms of wavelength.

In Fig. 5.13. one example is given of the spill-over lobe. This lobe is a typical property of a horn reflector. [25]. The worst case, at 19 GHz, is represented.

In Figs 5.14. and 5.15 the patterns are shown for vertical polarisation.
In the plane of symmetry, the cross-polarisation should be equal to zero. Measurements shown that very low level.
Again one example of a spill-over lobe is represented, at 19 GHz, the worst case.
However, in the plane of asymmetry, the H-plane we note two cross-polar lobes at the unsatisfactory high level of -9 dB.

The reason for this is that there is still an $E\phi$ component in the aperture of the BSHP. Thus, after reflection there is a field which has not the desired pattern with nearly parallel field lines.
Apparently the mode used in the biconical segment horn is not very suitable for creating a linearly polarised aperture field.

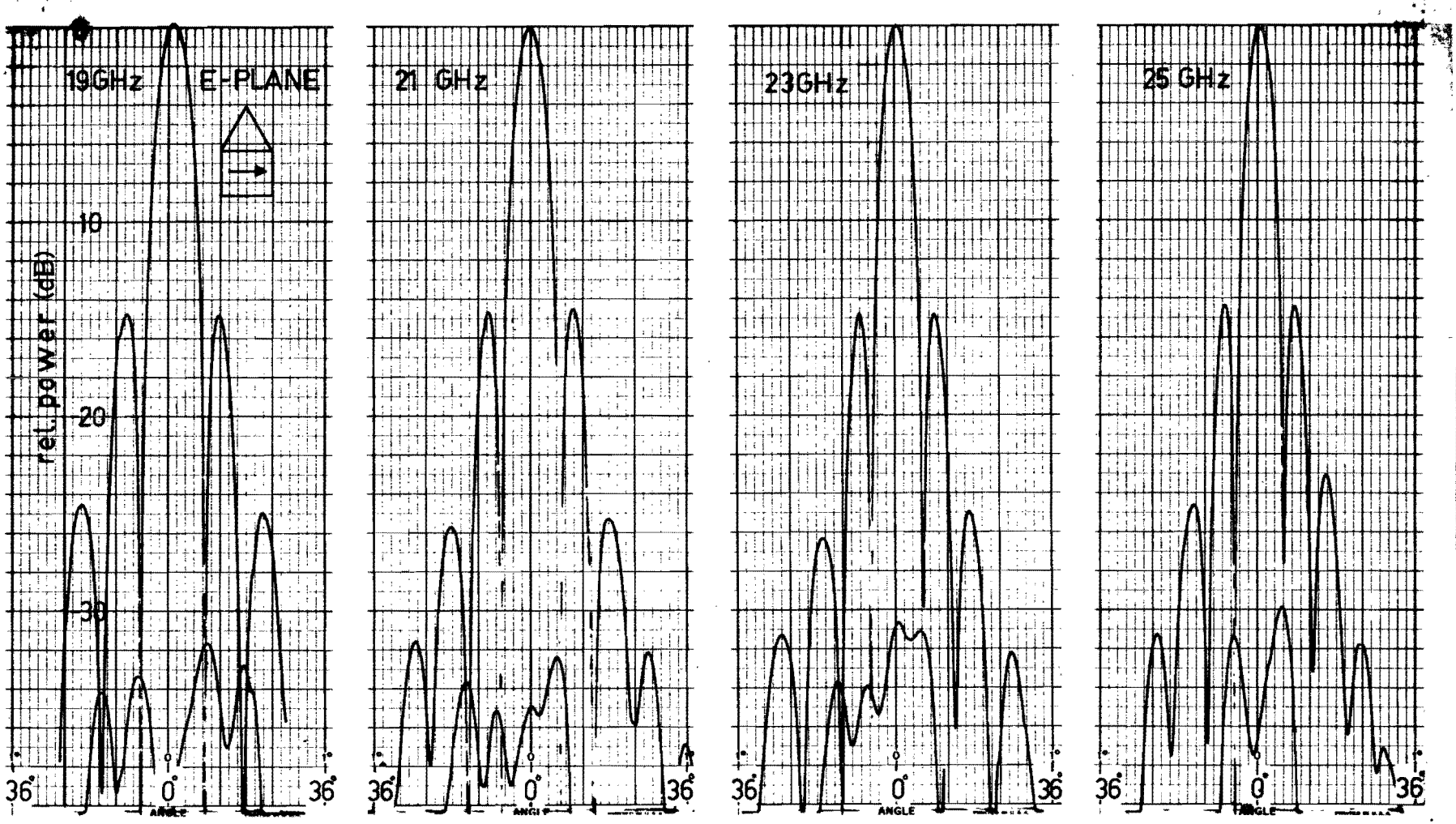

Fig. 5.12 E plane, far field radiation patterns, horizontal polarisation.

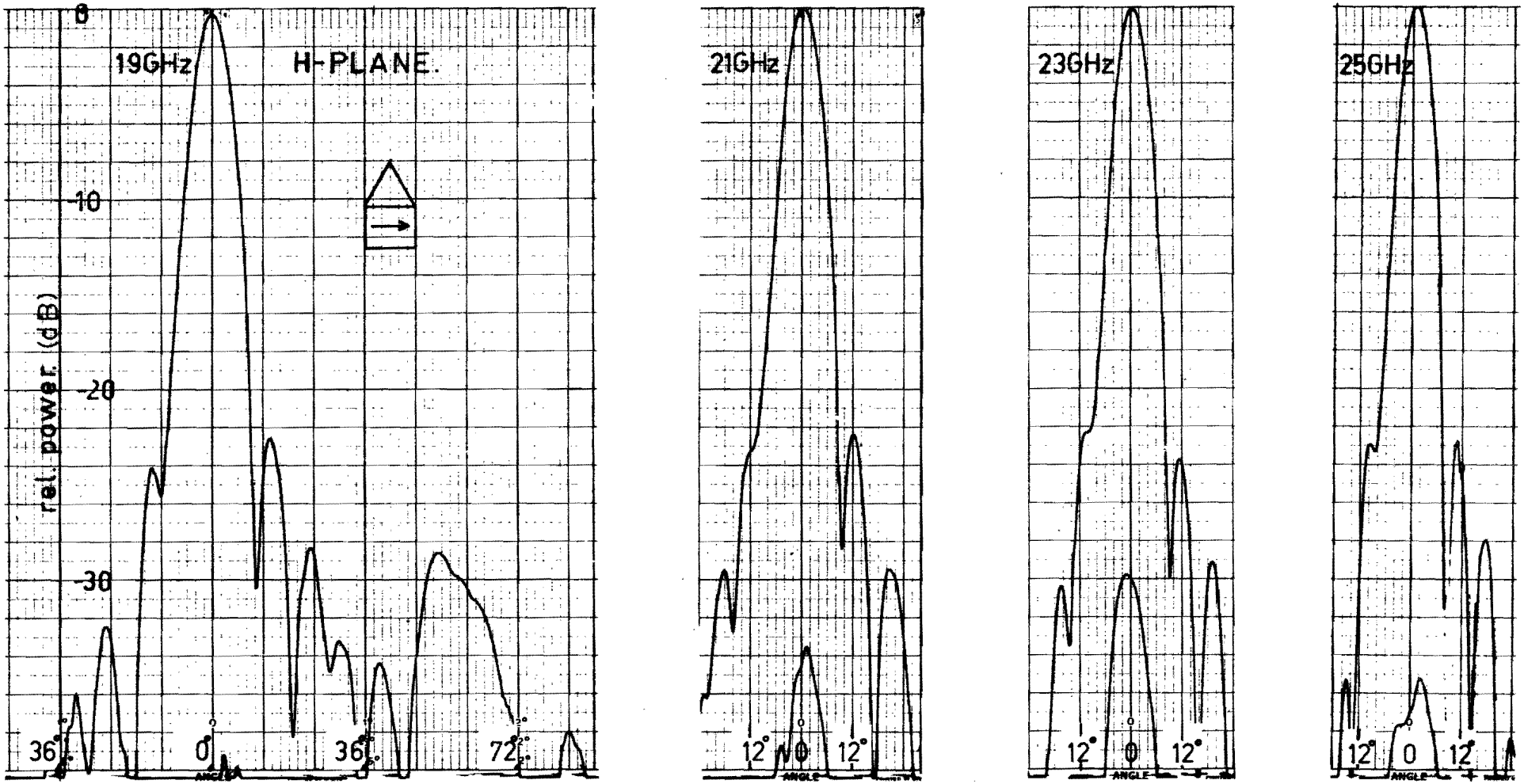

Fig. 5.13 H plane, far field radiation patterns, horizontal polarisation.

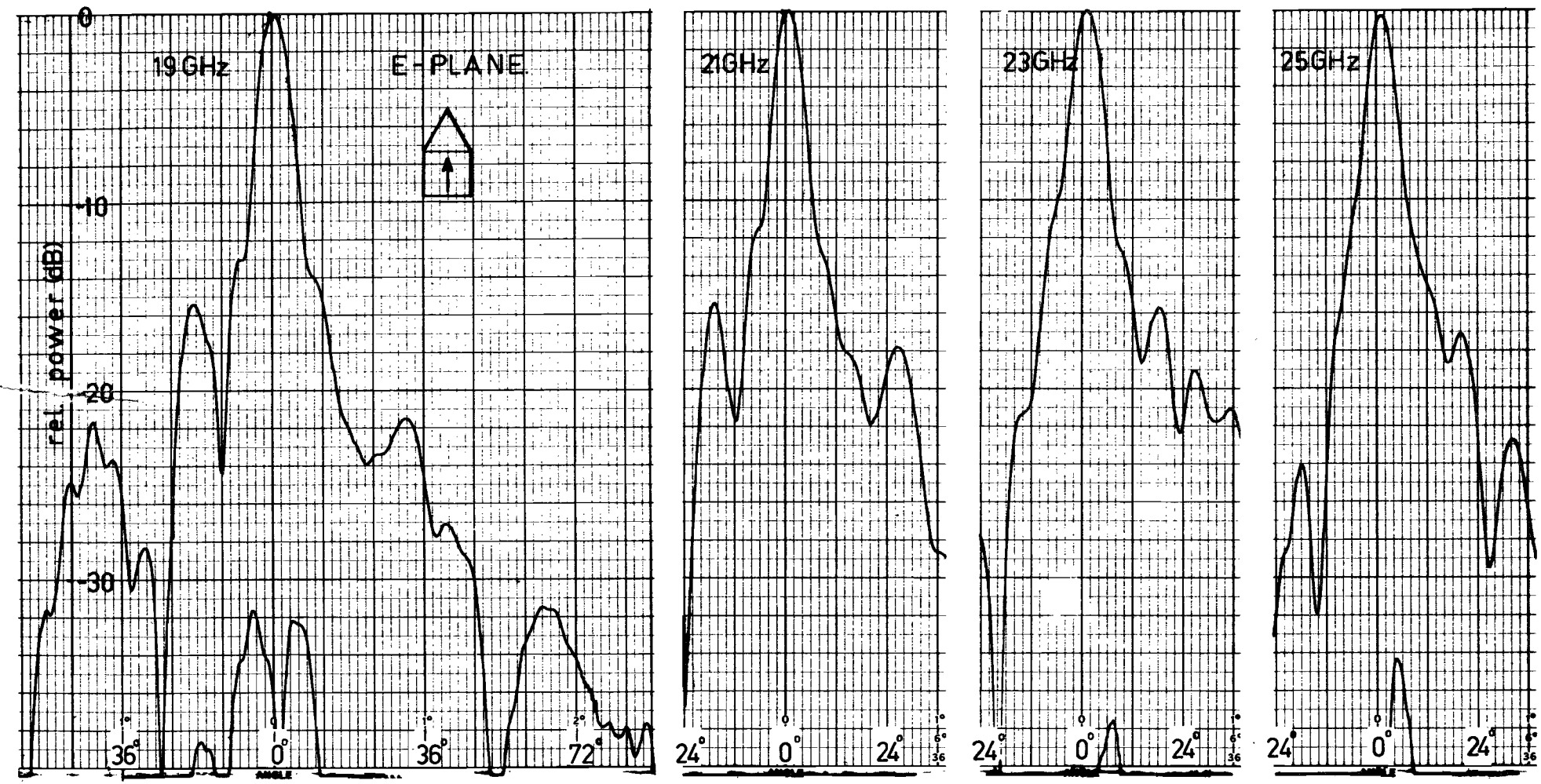

Fig. 5.14 E plane, far field radiation patterns, vertical polarisation

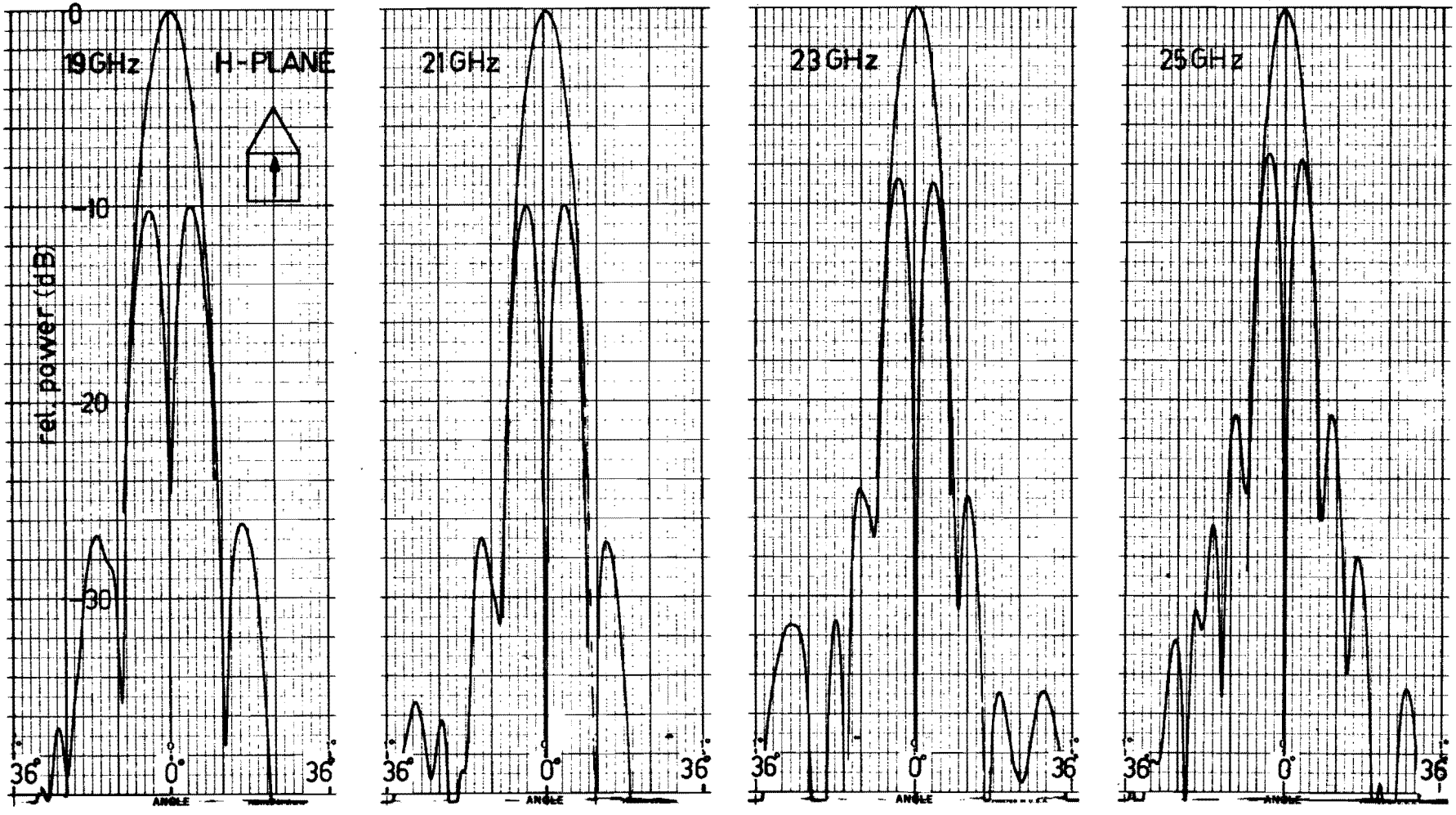

Fig. 5.15 H plane, far field radiation patterns, vertical polarisation.

As is found in paragraph 5.4, the aperture fields of TE_{mn} modes with m= 1 all have E_ϕ components.
A possibility for creating an aperture field with only an E_ϑ component is to choose a large value α, and a small value for the difference $(\vartheta_2 - \vartheta_1)$.
We have tried to create a field with only an E_ϑ component, by adding a higher mode to the TE_{12} mode in the BSH.
The latter is excited by a TE_{11} mode in a circular waveguide.
By means of a discontinuity the TE_{21} mode is excited and added to this TE_{11} mode.
This sum of two modes, with the correct relationship between phase and amplitude, excites the biconical horn. The result is a far-field radiation with a very low cross-polarisation.
In Fig. 5.16 the results of experiments are given.

The level of the cross-polar component is below -28 dB.
Note that this is some 10 dB lower than the conventional design.
Since the discontinuity influences only the vertical polarisation, the horizontal polarisation keeps its properties as before, i.e. low cross-polarisation in both principal planes.
The disadvantage of the solution with dual-mode excitation is the relative narrow bandwidth.
As shown in Fig 5.17, the reflected power is below -20 db over a great part of the K band, for both polarisations.
If we carry out the same measurements with the discontinuity in the waveguide, thus dual-mode operation, we get the results given in Fig. 5.18.
As shown, the power reflection is rather high, about -5dB at 19 GHz for vertical polarisation and -15 dB for horizontal polarisation.
The latter measurement has been carried out in a frequency band from 18.8 to 19.2 GHz.

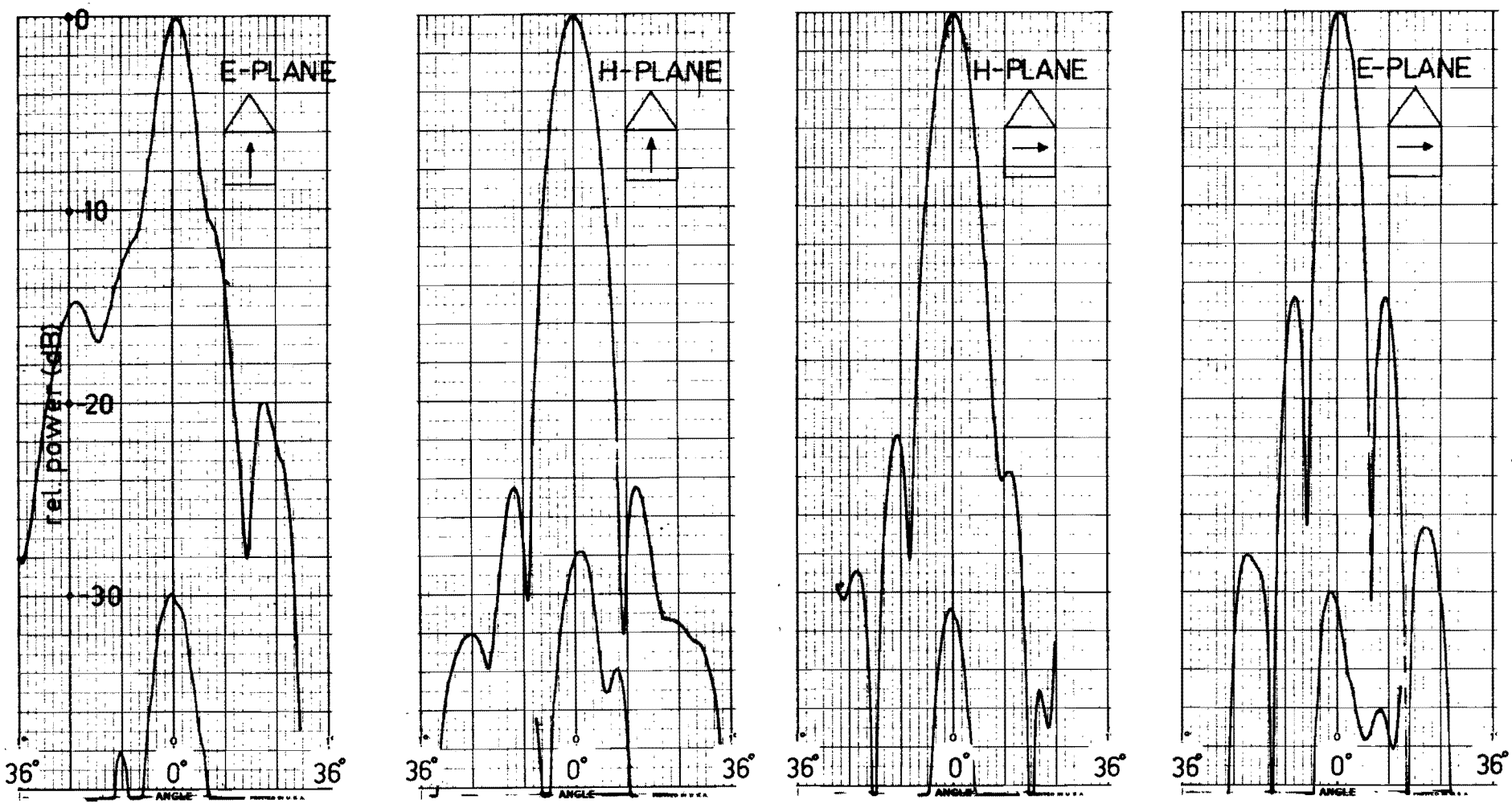

Fig. 5.16 A horn reflector with a very low cross-polarisation, radiation patterns of the far field.

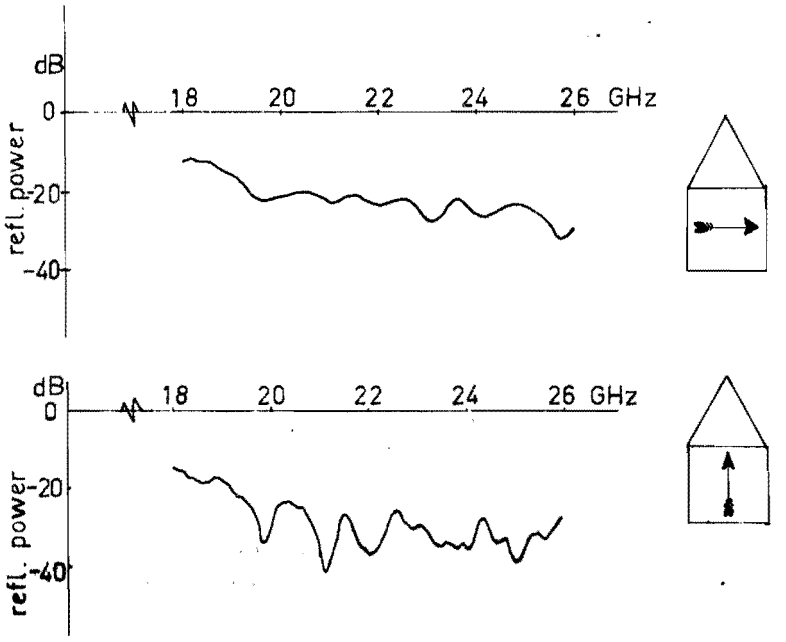

Fig. 5.17. Reflected power, single-mode operation.

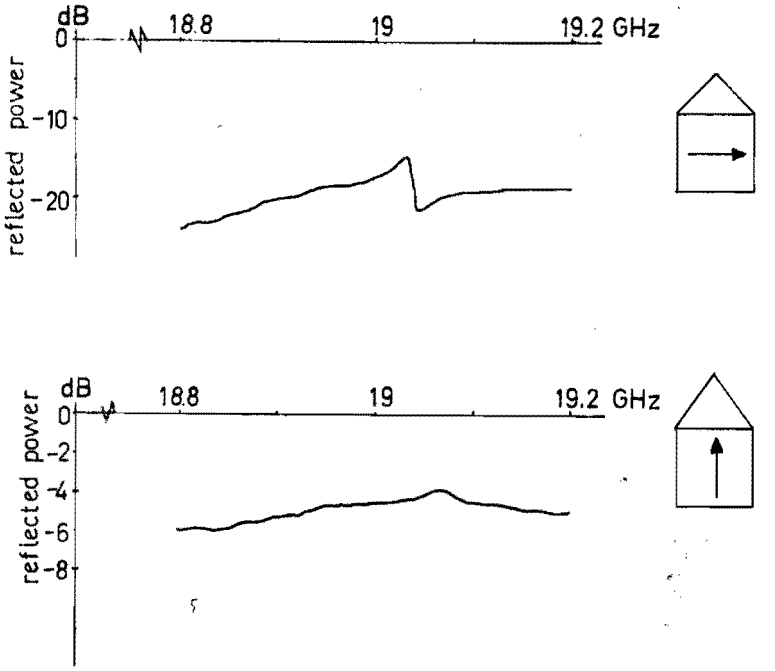

Fig. 5.18. Reflected power, dual-mode operation.

Chapter VI.

6. Conclusions, suggestions for future study.

We have investigated how the waveguide with a coax-segmental cross-section behaves as an off-set feed.
Since its far-field radiation is elliptically polarised, it is not suitable for eliminating the cross-polarisation of an off-set reflector if used in the classical way, that is with the reflector positioned in the far-field of the feed.

Bem [12] has calculated the field distribution in a plane which includes the focus of the paraboloid.
However, the possibility of matching the fields on a spherical surface with the focus as centre has not yet been investigated.
It might be worthwhile to use the BSH as feed, since its horn aperture is part of a sphere.

We have also investigated a system consisting of such a horn with the reflector positioned in the near-field region.
Again the aim has been the elimination of the cross-polarisation, which accounts for the BSHP design.

We have shown that such an antenna can be constructed without a cross-polarisation in one principal plane for both polarisations, while in the other plane the cross-polarisation can be kept below -30 dB.
Therefore we need a primary feed with an aperture field having only an E_φ-component for one polarisation or only an E_ϑ component for the orthogonal polarisation.

The experiments do confirm this theory for one polarisation, for the other polarisation, in single-mode operation the desired aperture field with only an E_ϑ-component cannot be realised with our model.
However, this can be approximated by choosing the boundary surfaces of the horn such that $(\nu - \nu_1)$ is small and α is large, or by adding a higher mode to the ground mode.
The latter solution has the disadvantage of being narrow-band.

The overall impression is that geometrical structures can be used to create a far field with such field characteristics that cross-polarisation generated elsewhere, for instance due to the transformation as in off-set reflectors, can be eliminated.

The great advantage of this method is that due to the single-mode operation and geometrical optics assumptions, the operating bandwidth is only limited by the coupling waveguides and structures of the system.

Acknowledgements.

The author appreciates the assistance of Mr. I. Ongers, who did a great part of the computer programming.
The antennas have been constructed by Mr. R. Atema.
The measurements have been carried out with the assistance of Mr. M. Knoben.

-. _ .-. _ .-. _ .-

Appendix A

Intersections of cones with a paraboloid of revolution are projected on the $x_s y_s$ plane perpendicular to the paraboloid axis. We shall derive the equations for these projections.

We distinguish two coordinate systems:
- the $(x_p y_p z_p)$ system in which the cone is described
- the $(x_s y_s z_s)$ system for the description of the paraboloid of revolution.

The y_p axis coincides with the y_s axis.
The angle between the z_s- and z_p axis is θ_0. (Fig. A.1)

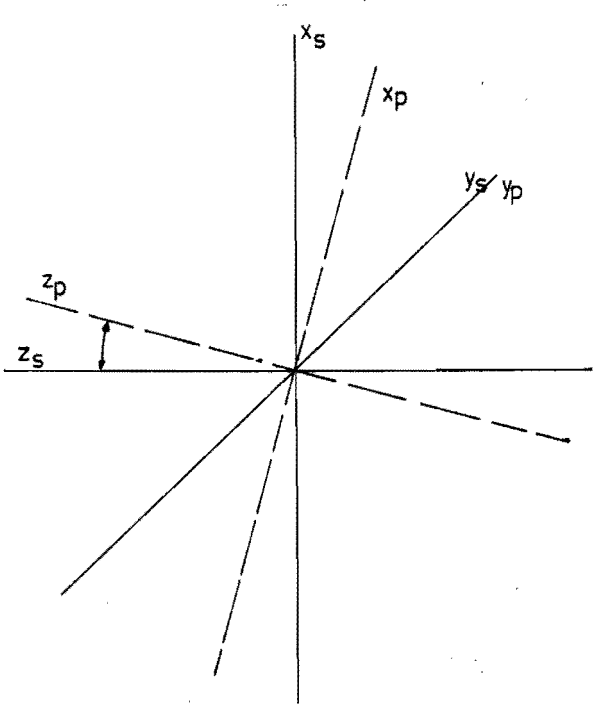

Fig. A.1. Coordinate systems for the cone and the paraboloid.

The transformation formulas are:

$$\left.\begin{aligned} x_p &= x_s \cos\vartheta_0 - z_s \sin\vartheta_0 \\ y_p &= y_s \\ z_p &= x_s \sin\vartheta_0 + z_s \cos\vartheta_0 \end{aligned}\right\} \qquad (A.1)$$

The paraboloid is given by: (apex in $z_s = f$)

$$x_s^2 + y_s^2 = 4f(f - z). \qquad (A.2)$$

Since

$$x_s^2 + y_s^2 + z_s^2 = (2f - z_s)^2 \quad , \qquad (A.3)$$

we get:

$$r_s = (2f - z_s) \, . \qquad (A.4)$$

The cone is given by: (flare angle $\theta_p = \theta_c$)

$$x_p^2 + y_p^2 = z_p^2 \tan^2 \vartheta_c \, . \qquad (A.5)$$

Since

$$x_p^2 + y_p^2 + z_p^2 = z_p^2 \frac{1}{\cos^2 \vartheta_c} \, , \qquad (A.6)$$

we get:

$$r_p = \frac{z_p}{\cos \vartheta_c} \, . \qquad (A.7)$$

The intersection of the cone with the paraboloid is given by $\theta_s = \theta_p$.
We obtain from (A.4) and (A.7), by applying the transformation (A.1):

$$\frac{z_p}{\cos \vartheta_c} = \frac{x_s \sin \vartheta_o + z_s \cos \vartheta_o}{\cos \vartheta_c} = 2f - z_s \, . \qquad (A.8)$$

After some calculation we get from (A.8):

$$z_s = \left[\frac{-\sin \vartheta_o}{\cos \vartheta_o + \cos \vartheta_c} \right] x_s + 2f \left[\frac{\cos \vartheta_c}{\cos \vartheta_o + \cos \vartheta_c} \right] , \qquad (A.9)$$

or in a shorter notation:

$$z_s = -a x_s + 2f \, b \, , \qquad (A.10)$$

where a and b are the coefficients given in (A.9).
This equation represents a plane parallel to the y_s-axis and with an angle with the x_s-axis given by

$$\gamma_s = -\arctan \left[\frac{\sin \vartheta_o}{\cos \vartheta_o + \cos \vartheta_c} \right] . \qquad (A.11)$$

Furthermore, (A.9) yields, if

$$\cos \vartheta_o = -\cos \vartheta_c \, , \qquad (A.12)$$

that

$$x_s = 2f \frac{\cos\vartheta_c}{\sin\vartheta_o}, \qquad (A.13)$$

which is a plane parallel to the $y_s z_s$ plane.

The projections of the intersections on the $x_s y_s$ plane are obtained by elimination of z_s from (A.2) and (A.10) as follows:

$$x_s^2 + y_s^2 = 4f(f + a x_s - 2fb), \qquad (A.14)$$

which yields after some calculation:

$$(x_s - 2fa)^2 + y_s^2 = 4f^2(1 + a^2 - 2b), \qquad (A.15)$$

or, after substitution of the expressions for a and b

$$\left(x_s - \frac{2f\sin\vartheta_o}{\cos\vartheta_c + \cos\vartheta_o}\right)^2 + y_s^2 = \left(\frac{2f.\sin\vartheta_c}{\cos\vartheta_c + \cos\vartheta_o}\right)^2 \qquad (A.16)$$

Expression (A.16) represents a circle, which degenerates to a straight line ($r = \infty$) for $\cos\theta_c = -\cos\theta_o$.

The intersections of planes, given by $\phi_p = \phi_c$, with the paraboloid of revolution are projected on the $x_s y_s$ plane. The equations of these projections are derived in the following:
The plane is given by:

$$y_p = \tan\varphi_c \, x_p, \qquad (A.17)$$

or in the primary system:

$$y_s = \tan\varphi_c \cos\vartheta_o \, x_s - \tan\varphi_c \sin\vartheta_o \, z_s. \qquad (A.18)$$

The paraboloid is given by:

$$x_s^2 + y_s^2 = 4f(f - z). \qquad (A.2)$$

Elimination of z_s from (A.2) and (A.18) yields the equation of the projection on the $x_s y_s$ plane.

From (A.18) we obtain:

$$z_s = \frac{\cos\vartheta_o}{\sin\vartheta_o} x_s - \frac{1}{\sin\vartheta_o \tan\varphi_c} y_s \qquad (A.19)$$

which gives with (A.2):

$$x_s^2 + y_s^2 = 4f\left(f - \frac{\cos\vartheta_o}{\sin\vartheta_o} x_s + \frac{1}{\sin\vartheta_o \tan\varphi_c} y_s\right), \qquad (A.20)$$

or, after some calculation:

$$\left[x_s + 2f\frac{\cos\vartheta_o}{\sin\vartheta_o}\right]^2 + \left[y_s - \frac{2f}{\sin\vartheta_o \tan\varphi_c}\right]^2 = 4f^2 \frac{1}{\sin^2\varphi_c \sin^2\vartheta_o}, \quad (A.21)$$

which is a circle in the $x_s y_s$ plane if $\phi_c \neq 0$.
For $\phi_c = 0$, the projection is the x_s axis.

Appendix B

We shall derive in this appendix the phase difference between the E_θ and E_ϕ component in the plane of asymmetry.

As shown by (4.39) and (4.40) for the one polarisation and by (4.41) and (4.42) for the other, this phase differerence is determined by the ϕ' integrals, denoted by Φ_1, and Φ_2 for E_ϑ and E_φ, respectively.

From (4.39) we have, with $\phi = \pi/2$ and $kr'\sin\theta = \zeta$:

$$\Phi_1 = \int_{-\alpha}^{\alpha} d\varphi' \cos\varphi' e^{j\zeta\sin\varphi'}, \qquad (B.1)$$

and from (4.40)

$$\Phi_2 = \int_{-\alpha}^{\alpha} d\varphi' \sin\varphi' e^{j\zeta\sin\varphi'} \qquad (B.2)$$

Elaboration of (B.1) yields

$$\Phi_1 = \frac{2\sin(\zeta\sin\alpha)}{\zeta}. \qquad (B.3)$$

This is a real function.

For (B.2), after evaluation with [29] we get

$$e^{\zeta/2(t-t^{-1})} = \sum_{n=-\infty}^{\infty} J_n(\zeta)\, t^n, \qquad (B.4)$$

with $t = e^{j\phi'}$

$$\Phi_2 = \int_{-\alpha}^{\alpha} d\varphi' \sin\varphi' \sum_{n=-\infty}^{\infty} J_n(\zeta) e^{jn\varphi'}. \qquad (B.5)$$

Thus

$$\Phi_2 = \sum_{n=-\infty}^{\infty} J_n(\zeta) \int_{-\alpha'}^{\alpha'} d\varphi' \left[\frac{e^{j(n+1)\varphi'} - e^{j(n-1)\varphi'}}{2j}\right] \qquad (B.6)$$

which, after some calculation gives

$$\Phi_2 = \sum_{n=-\infty}^{\infty} J_n(\zeta) \frac{e^{jn\varphi'}}{n^2-1}\left\{-jn\sin\varphi' + \cos\varphi'\right\}\Bigg]_{\varphi'=-\alpha}^{+\alpha}. \qquad (B.7)$$

Further elaboration yields

$$\Phi_2 = 2j \sum_{n=-\infty}^{\infty} \frac{J_n(\beta)}{n^2-1} \left\{ -n \sin\alpha \cos(n\alpha) + \cos\alpha \sin(n\alpha) \right\} \quad (B.8)$$

This expression is purely imaginar , which implies that the phase difference between Φ and Φ_2 is 90^0.
Thus the E_θ and E_ϕ componen.. given by (4.39) and (4.40) have a phase difference of 90° in the plane of asymmetry.

The proof that the E_θ and E_ϕ components given by (4.41) and (4.42) have a phase difference of 90^0 in the plane of asymmetry is somewhat laborious. As we are only interested in the phase, we neglect the identical functions before the integrals (4.41) and (4.42). Assuming that θ is small, for (4.41) and (4.42) with $\phi = 90^0$ and $kr'\sin\theta = \zeta$ we get:

$$= -\int_a^b dr' f(r') \int_{-\alpha}^{\alpha} d\varphi' \cos(\mu\varphi') \sin\varphi' e^{j\beta\sin\varphi'} + \int_a^b dr' g(r') \int_{-\alpha}^{\alpha} d\varphi' \sin(\mu\varphi') \cos\varphi' e^{j\beta\sin\varphi'}, \quad (B.9)$$

$$E_\varphi = \int_a^b dr' f(r') \int_{-\alpha}^{\alpha} d\varphi' \cos(\mu\varphi') \cos\varphi' e^{j\beta\sin\varphi'} + \int_a^b dr' g(r') \int_{-\alpha}^{\alpha} d\varphi' \sin(\mu\varphi') \sin\varphi' e^{j\beta\sin\varphi'} \quad (B.10)$$

For (B.9) we get:

$$E_\vartheta = -\int_a^b dr' f(r') \int_{-\alpha}^{\alpha} d\varphi' \left\{ \sin(\mu+1)\varphi' - \sin(\mu-1)\varphi' \right\} e^{j\beta\sin\varphi'} + \int_a^b dr' g(r') \int_{-\alpha}^{\alpha} d\varphi' \left\{ \sin(\mu-1)\varphi' + \sin(\mu+1)\varphi' \right\} e^{j\beta\sin\varphi'}, \quad (B.11)$$

and for (B.10):

$$E_\varphi = \int_a^b dr' f(r') \int_{-\alpha}^{\alpha} d\varphi' \left\{ \cos(\mu-1)\varphi' + \cos(\mu+1)\varphi' \right\} e^{j\beta \sin\varphi'} + \int_a^b dr' g(r') \int_{-\alpha}^{\alpha} d\varphi' \left\{ \cos(\mu-1)\varphi' - \cos(\mu+1)\varphi' \right\} e^{j\beta \sin\varphi'} \quad (B.12)$$

From (B.11) we have the ϕ^a- integrals

$$\Phi_a = \int_{-\alpha}^{\alpha} d\varphi' \sin\left[(\mu+1)\varphi'\right] e^{j\beta \sin\varphi'}, \quad (B.13)$$

$$\Phi_b = \int_{-\alpha}^{\alpha} d\varphi' \sin\left[(\mu-1)\varphi'\right] e^{j\beta \sin\varphi'}. \quad (B.14)$$

From (B.12) we have the ϕ^a integrals

$$\Phi_c = \int_{-\alpha}^{\alpha} d\varphi' \cos\left[(\mu+1)\varphi'\right] e^{j\beta \sin\varphi'}, \quad (B.15)$$

$$\Phi_d = \int_{-\alpha}^{\alpha} d\varphi' \cos\left[(\mu-1)\varphi'\right] e^{j\beta \sin\varphi'}. \quad (B.16)$$

Substitution of (B.4) in (B.13) gives:

$$\Phi_a = \int_{-\alpha}^{\alpha} d\varphi' \sin\left[(\mu+1)\varphi'\right] \sum_{n=-\infty}^{\infty} J_n(\beta) e^{jn\varphi'}, \quad (B.17)$$

$$\Phi_a = \sum_{n=-\infty}^{\infty} J_n(\beta) \int_{-\alpha}^{\alpha} d\varphi' \left\{ \frac{e^{j(n+\mu+1)\varphi'} - e^{j(n-\mu-1)\varphi'}}{2j} \right\}, \quad (B.18)$$

$$\Phi_a = \sum_{n=-\infty}^{\infty} J_n(\beta) \frac{e^{jn\varphi'}}{n^2-(\mu+1)^2} \left\{ -jn \sin\left[(\mu+1)\varphi'\right] + (\mu+1)\cos\left[(\mu+1)\varphi'\right] \right\} \Big|_{\varphi'=-\alpha}^{\alpha} \quad (B.19)$$

Substitution of the boundaries gives:

$$\Phi_a = 2j \sum_{n=-\infty}^{\infty} J_n(\beta) \frac{1}{n^2-(\mu+1)^2} \left\{ -n \sin(\mu+1)\alpha \cos(n\alpha) + (\mu+1)\cos(\mu+1)\alpha \sin(n\alpha) \right\}. \quad (B.20)$$

Replacing (μ+1) by (μ-1) gives:

$$\Phi_b = 2j \sum_{n=-\infty}^{\infty} J_n(\beta) \frac{1}{n^2-(\mu-1)^2} \left\{ -n \sin(\mu-1)\alpha \cos(n\alpha) + (\mu-1) \cos(\mu-1)\alpha \sin(n\alpha) \right\}. \tag{B.21}$$

Note that both expressions for Φ_a and Φ_b are purely imaginar .

Substitution of (B.4) in (B.15) gives:

$$\Phi_c = \int_{-\alpha}^{\alpha} d\varphi' \cos(\mu+1)\varphi' \sum_{n=-\infty}^{\infty} J_n(\beta)\, e^{jn\varphi'}, \tag{B.22}$$

$$\Phi_c = \sum_{n=-\infty}^{\infty} J_n(\beta) \int_{-\alpha}^{\alpha} d\varphi' \left\{ \frac{e^{j(n+\mu+1)\varphi'} + e^{j(n-\mu-1)\varphi'}}{2} \right\}, \tag{B.23}$$

$$\Phi_c = \sum_{n=-\infty}^{\infty} J_n(\beta) \frac{e^{jn\varphi'}}{n^2-(\mu+1)^2} \left\{ -jn \cos(\mu+1)\varphi' - (\mu+1) \sin(\mu+1)\varphi' \right\} \Bigg|_{\varphi'=-\alpha}^{\alpha}. \tag{B.24}$$

Substitution of the boundaries gives:

$$\Phi_c = 2 \sum_{n=-\infty}^{\infty} J_n(\beta) \frac{1}{n^2-(\mu+1)^2} \left\{ n \cos(\mu+1)\alpha \sin(n\alpha) - (\mu+1) \sin(\mu+1)\alpha \cos(n\alpha) \right\}. \tag{B.25}$$

Replacing (μ+1) by (μ-1) gives:

$$\Phi_d = 2 \sum_{n=-\infty}^{\infty} J_n(\beta) \frac{1}{n^2-(\mu-1)^2} \left\{ n \cos(\mu-1)\alpha \sin(n\alpha) - (\mu-1) \sin(\mu-1)\alpha \cos(n\alpha) \right\}. \tag{B.26}$$

Note that both expressions (B.25) and (B.26) are real.

For (B.11) and (B.12) we have:

$$E_\vartheta = -\int_a^b dr' f(r') \left\{ \Phi_a - \Phi_b \right\} + \int_a^b dr' g(r') \left\{ \Phi_a + \Phi_b \right\}, \tag{B.27}$$

$$E_\varphi = +\int_a^b dr' f(r') \left\{ \Phi_d + \Phi_c \right\} + \int_a^b dr' g(r') \left\{ \Phi_d - \Phi_c \right\}. \tag{B.28}$$

Note that $f(r')$ and $g(r')$ are real.
We have derived that $\tilde{\Phi}_a$ and $\tilde{\Phi}_b$ are purely imaginary and that $\tilde{\Phi}_c$ and $\tilde{\Phi}_d$ are real.
Then from (B.27) and (B.28) we may conclude that there is a phase difference of 90^0 between E_θ and E_ϕ.

Appendix C

The sphere of **Poincaré** is a very useful aid in representing polarisation states.
Here every position on the sphere is uniquely related to a polarisation state. Using geographical terminology, the north and south pole correspond respectively to left-handed and right-handed circular polarisations.
Points on the equator correspond to linearly polarised waves. Points lying between equator and north pole represent left-hand elliptically polarised waves and those between equator and south pole right-hand elliptically polarised waves.

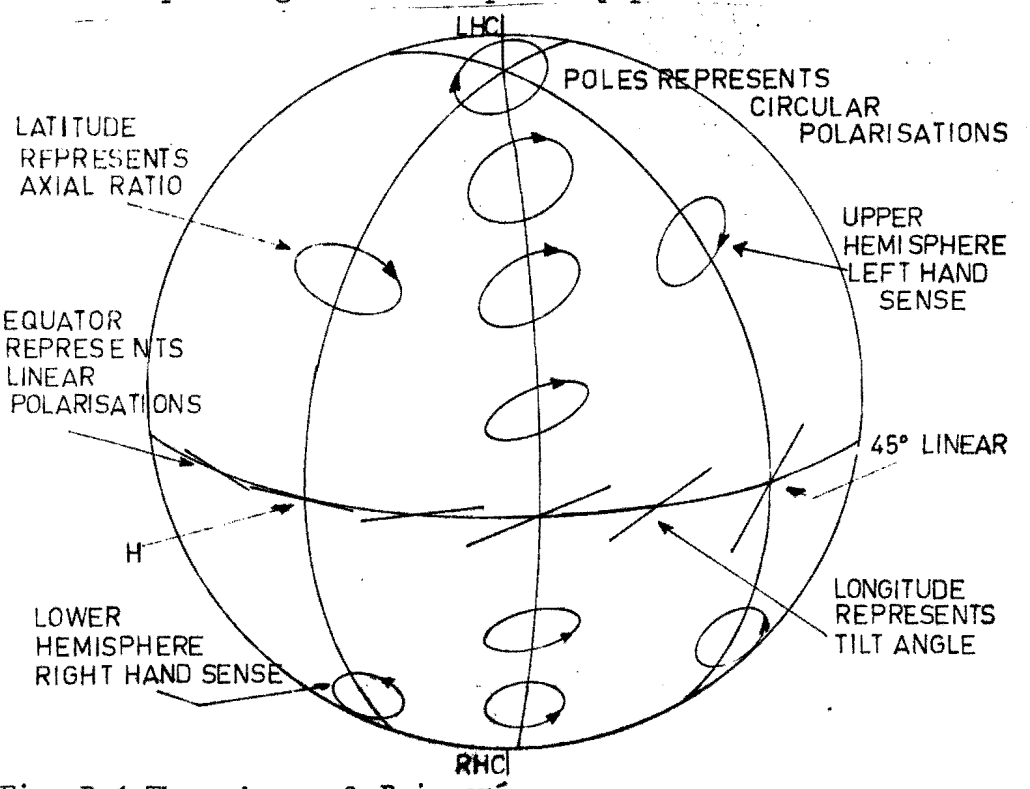

Fig. D.1 The sphere of **Poincaré**.

The longitude of a point is twice the orientation angle of the major axis of the polarisation ellipse, whereas the latitude corresponds to the axial ratio of the polarisation ellipse. Opposite points on the sphere represent orthogonal polarisation state. For example, the horizontally linear state lies diametrically opposite to vertically linear, left-handed and right-handed circular likewise.

Elliptically polarised waves with diametrically opposite polarisation states satisfy the conditions in (2.38) and (2.39). If, for example, one point represents the polarisation of a wave and another the polarisation of a receiving antenna, then the separation of the two points on the sphere is a measure of the efficiency with which the antenna will receive the wave. The wave will in fact not be received at all if the points are diametrically opposite [1], [2], [3].

References

[1] Harris, A.B. — Dual polarisation technology, Part I, POEEJ, Vol. 70, July 1977.

[2] Kummer, H. Gillespie, E.S. — Antenna measurements 1978, Proc. IEEE, Vol. 66, No. 4, April 1978.

[3] Hollis, J.S. Lyon, T.J. Clayton, L. — Microwave antenna measurements, Scientific Atlanta, July 1970.

[4] — IEEE, Standard definitions of terms for antennas. TAP, Vol. AP-17, No 3, May 1969.

[5] Ludwig, A.C. — The definition of cross-polarisation, IEEE, TAP, Vol. AP-21, Jan 1973.

[6] Frijters, H.A. — A reflector antenna with a shaped beam using a dual-mode corrugated feed, Ir. Thesis, 1978.

[7] Ta Shing Chu Turrin, R.H. — Depolarisation properties of offset reflector antennas, IEEE, TAP, Vol. AP-21, May 1973.

[8] — Final acts of the world administrative radio conference for the planning of the broadcasting-satellite service, Geneva 1977.

[9] Cook, J.S. Elam, E.M. Zucker, H. — The open cassegrain antenna Part I, electromagnetic design and analysis, Bell Systems Technical Journal Sept. 1965

[10] Rudge, A.W. Adatia, N.A. — New class of primary-feed antennas for use with offset parabolic-reflector antennas. Electronic Letters, Vol. II, No. 24, Nov. 1975.

[11] Rudge, A.W. — Multiple beam antennas, offset reflectors with offset feeds, IEEE, TAP, Vol. AP-23, No. 3, May 1975.

[12] Bem, D.J. — Electric field distribution in the focal region of an offset paraboloid, Proc. IEE, Vol. 116, No. 5, May 1969.

[13] Ghobrial, S.I. Cross polarisation in satellite and and earth-station antennas, Proc. IEEE, Vol. 65, No. 3, March 1977.

[14] Jacobsen, J. On the cross-polarisation of asymmetric reflector antennas for satellite applications, IEEE, TAP, Vol. AP-25, March 1977.

[15] Knittel, G.H. Comments on the definition of cross-polarisation, IEEE, TAP, Jan. 1973.

[16] Vokurka, V. Feeds and reflector antennas for shaped beams. Dr. thesis, Eindhoven 1977.

[17] Collin, R.E. Zucker, F.J. Antenna Theory Part I, Antenna Theory Part II, Mc Graw-Hill, 1969.

[18] Silver, S. Microwave antenna theory and design, Mc Graw-Hill, 1949.

[19] Harrington, R.F. Time harmonic electromagnetic fields, Mc Graw-Hill, 1961.

[20] Marcuvitz, N. Waveguide handbook, Mc Graw-Hill, 1951.

[21] Haan de, H.G. Een belichter voor een offset reflector, Stage Report 1977, TH Eindhoven.

[22] Jeuken, M.E.J. Corrugated horn antennas. Lecture notes, TH Eindhoven.

[23] Jeuken, M.E.J. Electromagnetische golven en antennes I, Lecture notes, TH Eindhoven.

[24] Hines, J.N. Tingye, Li Turrin, R.H. The electrical characteristics of the conical horn-reflector antenna, Bell Systems Technical Journal, July 1963.

[25] Crawford, A.B. Hogg, D.C. Hunt, L.H. A horn reflector antenna for space communication, Bell Systems Technical Journal, July 1961.

[26] Koffman, I. Feed polarisation for parallel currents in reflector generated by conic sections, IEEE, TAP, Vol. AP-14, No. 1 1966.

[27] CC IR XIIIth Plenary Assembly, Gener. "Fixed Service Using Radio-Relay System, (Study Group 9)", Vol. IX, I.T.V., Geneva, 1975.

[28] Gans, M.J.
Semplak, R.A. Some far-field studies of an offset-launcher. B.S.T.J., Vol. 54, No. 7, 1975.

[29] Bouwkamp, C.J. Toegepaste analyse I, Lecture notes, TH Eindhoven.